Neural Plasticity

Visual Plasticity in Adults

Lead Guest Editor: Jiawei Zhou
Guest Editors: Zili Liu, Simon Clavagnier, Alexandre Reynaud, and Fang Hou

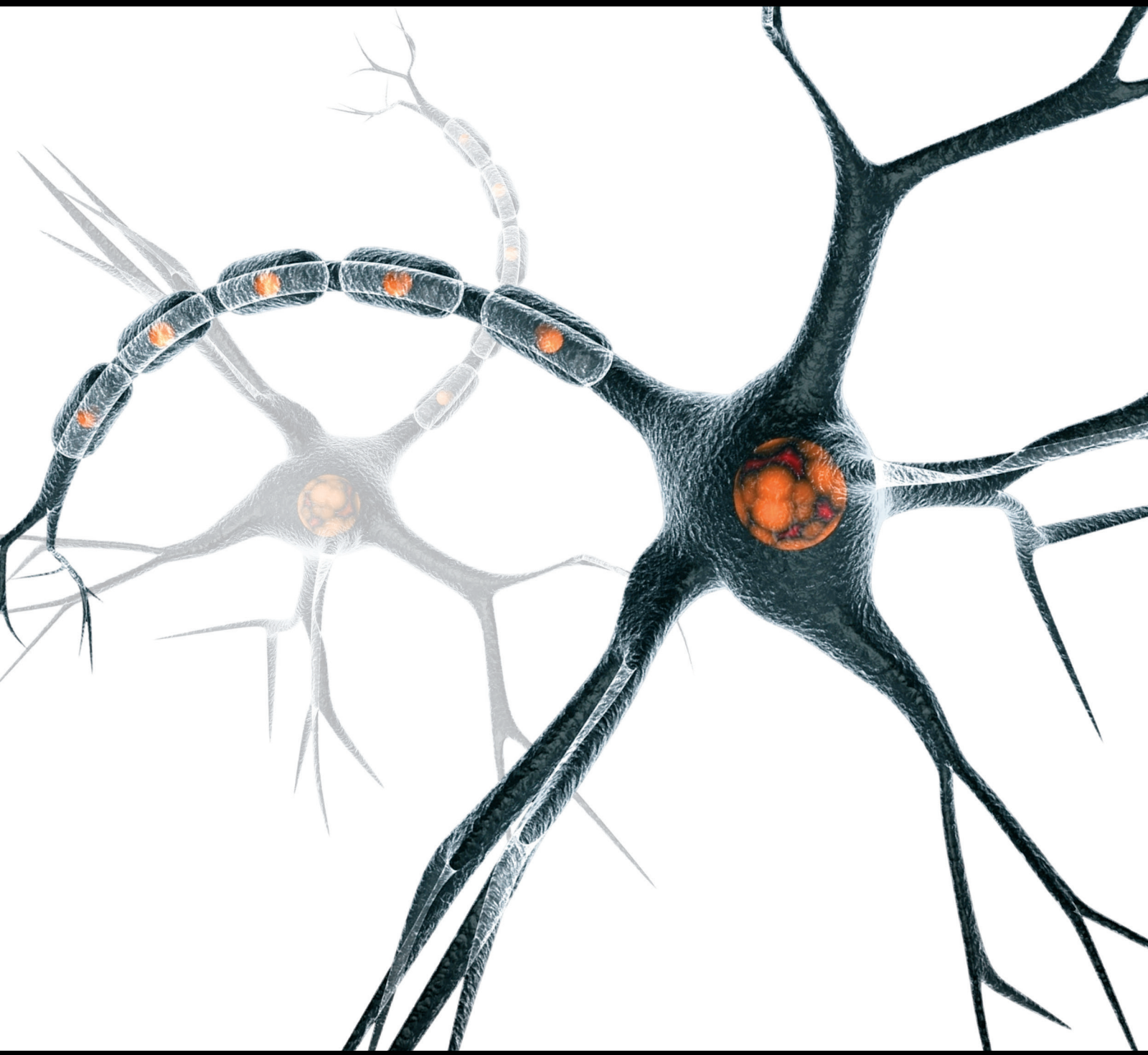

Visual Plasticity in Adults

Neural Plasticity

Visual Plasticity in Adults

Lead Guest Editor: Jiawei Zhou
Guest Editors: Zili Liu, Simon Clavagnier, Alexandre Reynaud, and Fang Hou

Editorial Board

Contents

Hindawi
Neural Plasticity
Volume 2017, Article ID 8469580, 2 pages
https://doi.org/10.1155/2017/8469580

Editorial

Visual Plasticity in Adults

Jiawei Zhou,[1] Zili Liu,[2] Simon Clavagnier,[3] Alexandre Reynaud,[3] and Fang Hou[1]

[1]*School of Ophthalmology and Optometry and Eye Hospital, Wenzhou Medical University, Wenzhou, Zhejiang, China*
[2]*Department of Psychology, University of California Los Angeles, Los Angeles, CA, USA*
[3]*McGill Vision Research, Department of Ophthalmology, McGill University, Montreal, QC, Canada*

Correspondence should be addressed to Jiawei Zhou; zhoujw@mail.eye.ac.cn

Received 14 May 2017; Accepted 14 May 2017; Published 4 June 2017

The pioneering work of Hubel and Wiesel established the concept of a critical period for visual development early in life. During this period, cortical development is most susceptible to the alteration of sensory experience by the environment or other factors. Although this is a well-accepted concept in neurobiology, it is also now recognized that there is some limited plasticity remains after a critical period well into adulthood. A range of visual functions in adult subjects can be modified as a result of perceptual learning, brain stimulation, or adaptation, some with effects that can last very long, up to several months [1].

Perceptual learning can be achieved through intensive training during which a subject repeats a perceptual detection or discrimination task over and over again [2]. Noninvasive brain stimulation techniques such as transcranial magnetic stimulation (TMS) and transcranial direct current stimulation (tDCS) have also been shown to induce functional change in the adult brain [3, 4]. Finally, plastic changes can also be induced by visual adaptation and deprivation [5, 6]. These procedures seem very promising in the perspective of developing new clinical therapies, such as the treatment of adult amblyopia [7]. Hence, this special issue aims to provide a kaleidoscope that presents novel findings in adult visual plasticity from whole brain network to human behavior.

Two studies tackled directly with clinical cases. The first one focused on the plastic changes occurring in congenital and late blindness. With tractography based on diffusion-weighted magnetic resonance imaging and diffusion tensor imaging, N. H. Reislev et al. observed plastic microstructural changes in thalamocortical connectivity of blind people that could not be captured at the network level. The other one assessed the sensory eye dominance in treated anisometropic amblyopes. Y. Chen et al. showed that the treated anisometropic amblyopes, even those with a normal range of visual acuity, exhibited abnormal binocular processing. Their results thus suggest that there is potential for improvement in treated anisometropic amblyopes that may further enhance their binocular visual functioning.

Then, two other studies examined how short-term changes can be driven by exogenous stimuli. Y. Chen et al. tested the effect of different types of ambient illumination during 3D TV viewing on ocular status. They observed that, in general, 3D TV viewing modifies the ocular status of adults. A front illumination has less impact on the accommodative response and microfluctuation, suggesting that this type of illumination is the most appropriate mode for 3D TV viewing. On the other hand, M.A. De Niear et al. investigated the impact of feedback in multisensory temporal recalibration. They concluded that feedback signals promote and sustain audiovisual recalibration over the course of cumulative learning and enhance rapid trial-to-trial learning.

Lastly, it has recently been shown by Lunghi et al. [6] that short-term monocular deprivation alters binocular balance. In this special issue, P. Binda and C. Lunghi extended their previous work and illustrated how plastic effects due to monocular deprivation can be assessed physiologically. They demonstrated that slow pupil oscillation amplitude increased after monocular deprivation, with larger changes correlated with larger ocular dominance changes measured by binocular rivalry. Their findings suggest that there might be a common mechanism shared by the slow pupil oscillation and ocular balance. Instead of using binocular rivalry as used

in the other study [8], J. Zhou et al. investigated the effect of aerobic exercise on the monocular deprivation effect using a binocular fusion task. They found no additional effect of exercise after short-term monocular occlusion and argued that the enhancement of ocular dominance plasticity from exercise could not be generalized to all visual functions.

Altogether, these studies will contribute to a better understanding of how plastic changes can occur or can be induced in our visual system. These could potentially contribute to the new clinical therapies for developmental visual disorders such as amblyopia.

Acknowledgments

We would like to thank all the reviewers that have contributed their time and insight to this special issue.

Jiawei Zhou
Zili Liu
Simon Clavagnier
Alexandre Reynaud
Fang Hou

References

[1] K. Ball and R. Sekuler, "Direction-specific improvement in motion discrimination," *Vision Research*, vol. 27, no. 6, pp. 953–965, 1987.

[2] Z. Liu and D. Weinshall, "Mechanisms of generalization in perceptual learning," *Vision Research*, vol. 40, no. 1, pp. 97–109, 2000.

[3] D. P. Spiegel, W. D. Byblow, R. F. Hess, and B. Thompson, "Anodal transcranial direct current stimulation transiently improves contrast sensitivity and normalizes visual cortex activation in individuals with amblyopia," *Neurorehabilitation and Neural Repair*, vol. 27, no. 8, pp. 760–769, 2013.

[4] B. Thompson, B. Mansouri, L. Koski, and R. F. Hess, "Brain plasticity in the adult: modulation of function in amblyopia with rTMS," *Current Biology*, vol. 18, no. 14, pp. 1067–1071, 2008.

[5] K. V. Haak, E. Fast, M. Bao, M. Lee, and S. A. Engel, "Four days of visual contrast deprivation reveals limits of neuronal adaptation," *Current Biology*, vol. 24, no. 21, pp. 2575–2579, 2014.

[6] C. Lunghi, D. C. Burr, and C. Morrone, "Brief periods of monocular deprivation disrupt ocular balance in human adult visual cortex," *Current Biology*, vol. 21, no. 14, pp. R538–R539, 2011.

[7] J. Li, B. Thompson, D. Deng, L. Y. Chan, M. Yu, and R. F. Hess, "Dichoptic training enables the adult amblyopic brain to learn," *Current Biology*, vol. 23, no. 8, pp. R308–R309, 2013.

[8] C. Lunghi and A. Sale, "A cycling lane for brain rewiring," *Current Biology*, vol. 25, no. 23, pp. R1122–R1123, 2015.

Hindawi
Neural Plasticity
Volume 2017, Article ID 9438072, 7 pages
https://doi.org/10.1155/2017/9438072

Research Article

Sensory Eye Dominance in Treated Anisometropic Amblyopia

Yao Chen,[1] Jiafeng Wang,[1] Hongmei Shi,[1] Xiaoxiao Wang,[2] and Lixia Feng[1]

[1]*Department of Ophthalmology, The First Affiliated Hospital of Anhui Medical University, Hefei, Anhui, China*
[2]*Centers for Biomedical Engineering, University of Science and Technology of China, Hefei, Anhui, China*

Correspondence should be addressed to Lixia Feng; lixiafeng@163.com

Received 29 October 2016; Revised 27 February 2017; Accepted 11 April 2017; Published 10 May 2017

Academic Editor: J. Michael Wyss

Amblyopia results from inadequate visual experience during the critical period of visual development. Abnormal binocular interactions are believed to play a critical role in amblyopia. These binocular deficits can often be resolved, owing to the residual visual plasticity in amblyopes. In this study, we quantitatively measured the sensory eye dominance in treated anisometropic amblyopes to determine whether they had fully recovered. Fourteen treated anisometropic amblyopes with normal or corrected to normal visual acuity participated, and their sensory eye dominance was assessed by using a binocular phase combination paradigm. We found that the two eyes were unequal in binocular combination in most (11 out of 14) of our treated anisometropic amblyopes, but none of the controls. We concluded that the treated anisometropic amblyopes, even those with a normal range of visual acuity, exhibited abnormal binocular processing. Our results thus suggest that there is potential for improvement in treated anisometropic amblyopes that may further enhance their binocular visual functioning.

1. Introduction

Amblyopia is a common visual disorder that affects 1.6% to 3.5% of the population [1]. Patients with amblyopia normally exhibit abnormal visual processing without any discoverable organic pathological ocular abnormalities, and this abnormality cannot be corrected by glasses [2]. Asymmetric refractive errors between the eyes (i.e., anisometropia) during the critical period of visual maturation (i.e., at ages less than 8 years old) is a widely known cause of anisometropic amblyopia [3]. Patients with anisometropic amblyopia tend to have abnormal monocular visual functions in the amblyopic eye [4], abnormal interocular suppression (i.e., the inhibitory influence of the fixing eye on the amblyopic eye under binocular viewing), as reflected by an abnormal sensory eye dominance, and poor stereopsis [5].

In clinical practice, amblyopia is usually treated with patching therapy, to force the patients' brain to learn to see through the amblyopic eye [6]. This therapy, which is efficient in recovering the monocular visual acuity of the amblyopic eye [7], prevents the two eyes from working together. Because amblyopia is a neurodevelopmental disorder [8] that affects both monocular and binocular visual processing, it is unclear whether the binocular visual deficits recover in clinically treated amblyopes. If not, then neural plasticity targeted at those remaining deficits may be required to recover visual functions.

We set to provide a definitive answer to this question by using a binocular phase combination paradigm [9, 10] to quantitatively assess the sensory eye dominance of treated anisometropic amblyopes, who had normal or corrected-to-normal visual acuity in both eyes, to determine whether their binocular visual systems had fully recovered. Specifically, we ask one question: whether the treated anisometropic amblyopes still have abnormal sensory eye dominance. The binocular phase combination paradigm was developed by Ding and Sperling [9] and has recently been adapted to measure the sensory eye dominance in amblyopia by Huang et al. [10].

To answer this question, we measured the sensory eye dominance of each patient to determine the interocular contrast difference necessary for individuals to achieve balanced binocular viewing in binocular phase combination. Any existing abnormal sensory eye dominance suggests a potential for improvement in treated amblyopes. Most (11 out of 14) of our treated anisometropic amblyopes still exhibited

binocular imbalance (our measure of "suppression"), whereas none of the controls were binocularly imbalanced.

2. Materials and Methods

2.1. Participants. Fourteen treated anisometropic amblyopes, between the ages of 6 and 11 years, (average age: 8.50 ± 1.16 years old), were recruited. The participants had normal or corrected to normal visual acuity in both the previously amblyopic eye and the fellow eye. They were diagnosed with anisometropic amblyopia before treatment, and the detailed clinical information of the treated anisometropia amblyopes, including the refractive errors and visual acuity before and after the treatment, are shown in Table 1. The participants were screened at the ophthalmology practice of the corresponding author LF at the First Affiliated Hospital of Anhui Medical University of China. Another fifteen age-matched (between the ages of 7 and 11 years old) normal subjects were enrolled as the controls. All participants have normal or corrected-to-normal visual acuity, an absence of any ocular or oculomotor abnormalities, and no previous eye surgery. All participants were naïve to the purpose of the experiment.

The study was approved by the Institutional Review Board of Anhui Medical University in China. All observations were performed in accordance with the Declaration of Helsinki before the experiment.

2.2. Design and Procedure

2.2.1. Stereopsis Measurement. Stereopsis was tested at a viewing distance of 40 cm in a bright room, using Randot stereotest (Baoshijia, Zhengzhou, China). Red-green glasses were worn over subjects' full refractive correction during the test.

2.2.2. Balance Point Measurement. We used the same set up used by Feng et al. [11] to measure the sensory eye dominance. The experimental procedures were conducted with a PC computer running Matlab (MathWorks Inc., Natick, MA, USA) with Psych Tool Box 3.0.9 extensions. The stimuli were generated by a gamma-corrected LG D2342PY 3D LED screen (LG Life Science, Korea; 1920×1080 resolution; refresh rate 60 Hz). The observers were asked to sit at a distance of 1.36 m from the screen and viewed the display dichoptically with their full refractive correction spectacles underneath polarized glasses in a silent and dimly lit space. The luminance of the screen background was 46.2 cd/m^2 and 18.8 cd/m^2 through the polar glasses. A chin-forehead rest was provided to minimize head movement.

During the test, two horizontal sine-wave gratings (2 degrees × 2 degrees; 1 cycle/deg) with equal and opposite phase-shifts of 22.5° (relative to the center of the screen) were dichoptically presented to observers through the polarized glasses; the perceived phase of the cyclopean percept was measured as a function of the interocular contrast ratio; the contrast of the grating in the nondominant eye was fixed at 100%, and the following interocular contrast ratios were used: 0, 0.1, 0.2, 0.4, 0.8, and 1. We fitted the perceived phases versus interocular contrast ratio (PvR; phase versus ratio curve) curve, and by which, we derived a balance point when the perceived phase was 0°, which represents the interocular contrast ratio when the contributions of each eye are equal (Figure 1(a)). To avoid any potential positional bias, we used two different stimuli compositions in the measurement for each interocular contrast ratio (Figure 1(b)); in one configuration, the phase-shift was +22.5° in the previously amblyopic eye and −22.5° in the fellow eye; similarly, the phase-shift was −22.5° in the previously amblyopic eye and +22.5° in the fellow eye. The perceived phase of the cyclopean grating at each interocular contrast ratio (δ) was quantified as half of the difference between the measured perceived phases in these two configurations. Different interocular contrast ratios and configurations were randomized in each trial. We calculated the cyclopean phase and the standard error on the basis of 8 measurement repetitions.

The observers were asked to practice before the experiment to ensure that they understood the task. In each trial, subjects were asked to finish two tasks: eye alignment and phase adjustment. In the line alignment task, they were instructed to move the stimuli (binocular fixation crosses, the high contrast frames, and the monocular fixation dots) in the amblyopic eye to align with the stimuli in the fellow eye. The corresponding coordinate between two eyes was then used in the following phase measurement. The subjects were asked to press the "space" bar on the computer keyboard when they achieved stable vergence. This was followed by a 500 ms presentation of the frames, and then the presentation of two sine-wave gratings in the two eyes, and the observers were asked to finish the phase adjustment task. They were asked to adjust the position of a sided reference line to indicate the perceived phase of the cyclopean grating that they perceived after binocular combination, which was defined as the location of the center of the dark stripe of the grating. The initial position of the reference line was randomly (−9 to 10 pixels) assigned relative to the center of the frame in each trial. The reference line was moved with a fixed step size of 1 pixel, which corresponds to the 4-degree phase angle of the sine-wave grating. The stimuli were presented continually until the subjects finished the phase adjustment task. The observers were asked to press the "space" bar again after they finished the phase adjustment task. The next trial would be started after a 1 sec blank display.

2.2.3. Curve Fits. The perceived phases versus interocular contrast ratio (PvR) curves for different observers were fitted with a modified contrast-gain control model from Huang et al. [10] and Zhou et al. [12]. The fits were conducted in Matlab (MathWorks, Natick, MA) using the nonlinear least squares method.

2.3. Statistical Analysis. Two-tailed independent samples t-test was used for comparisons between groups. Repeated-measures within-subject ANOVA was used to analyze the relationship between the perceived phase and the interocular contrast ratio. The power and sample size program (version 3.0.43) was used to do the power analysis.

Table 1: Clinical data of the treated anisometropic amblyopes.

Patient	Age/sex	Best corrected VA (OD/OS)		Stereopsis (arc sec)	Refractive errors (OD/OS)		History
		Before	After		Before	After	
S1	8/F	20/32	20/20	40	+4.75DS/0.75DC*90	+2.25DS/0.50DC*80	Detected at 3 years old, glasses, normal at 6 years old
		20/32	20/20		+2.50DS/1.250DC*105	+1.75DS/1.50DC*100	
S2	8/M	20/80	20/20	60	+5.50DS/1.25DC*100	+3.75DS/1.25DC*100	Detected at 3 years old, glasses, patching, normal at 7 years old
		20/80	20/16		+4.00DS/1.50DC*80	+3.75DS/1.75DC*80	
S3	9/M	20/100	20/20	40	+3.50DS/2.00 DC*90	+1.25DS/2.00 DC*95	Detected at 7 years old, glasses, patching, normal at 8 years old
		20/20	20/16		+1.50DS/1.00DC*90	+1.00DS/1.00DC*85	
S4	8/F	20/32	20/20	100	Plano	Plano	Detected at 3 years old, glasses, patching, normal at 7 years old
		20/40	20/20		+3.00DS	+2.00DS	
S5	8/F	20/80	20/20	100	−4.00DC*180	−4.00DC*180	Detected at 5 years old, glasses, patching, bead-threading, normal at 7 years old
		20/100	20/20		−2.50 DC*180	−3.75 DC*5	
S6	8/M	20/40	20/20	40	+5.25DS	+5.00DS	Detected at 7 years old, glasses, patching, normal at 7 years old
		20/16	20/16		+2.00DS	+1.50DS	
S7	9/F	20/32	20/20	40	+4.50DS/1.00DC*70	+4.25DS/1.00DC*70	Detected at 7 years old, glasses, patching, bead-threading, normal at 8 years old
		20/32	20/20		+7.25DS	+4.50DS	
S8	9/F	20/50	20/20	100	+6.50DS/1.00DC*90	+5.50DS/1.00DC*90	Detected at 5 years old, glasses, bead-threading, normal at 8 years old
		20/46	20/20		+5.25DS/1.25DC*85	+5.00DS/0.75 DC*80	
S9	8/F	20/50	20/25	400	+1.00DS/2.25DC*100	−0.25DS/2.00DC*90	Detected at 6 years old, glasses, patching, bead-threading, normal at 6 years old
		20/32	20/25		1.00DC*100	−0.50DS/0.75DC*90	
S10	9/F	20/40	20/20	100	+4.25DS/0.75 DC*85	+3.00DS/1.00 DC*85	Detected at 5 years old, glasses, patching, normal at 8 years old
		20/32	20/20		+3.00DS/1.00DC*100	+2.75DS/1.00DC*95	
S11	11/M	20/50	20/25	40	+4.25 DC*85	+4.00 DC*95	Detected at 10 years old, glasses, patching, normal at 11 years old
		20/20	20/25		Plano	Plano	
S12	6/M	20/25	20/20	40	+1.00DS/3.50DC*100	+2.50DC*105	Detected at 3 years old, glasses, patching, bead-threading, normal at 5 years old
		20/40	20/20		2.00DC*105	+2.00DC*95	
S13	10/M	20/32	20/16	60	+7.50DS/0.50DC*85	+6.75DS/0.37DC*5	Detected at 6 years old, glasses, patching, normal at 8 years old
		20/40	20/20		+9.00DS/0.50DC*60	+7.00DS/0.37DC*175	
S14	8/M	20/32	20/20	60	+3.75DS/1.00DC*105	+2.50DS/0.75DC*95	Detected at 5 years old, glasses, patching, bead-threading, normal at 6 years old
		20/63	20/20		+2.25DS/1.00DC*90	+2.00DS/1.00DC*85	

VA: visual acuity; OD: right eye; OS: left eye. (i) Visual acuity was measured on the basis of the Snellen visual acuity chart; (ii) all subjects accepted treatment immediately after diagnosis; * represents the axial astigmatism.

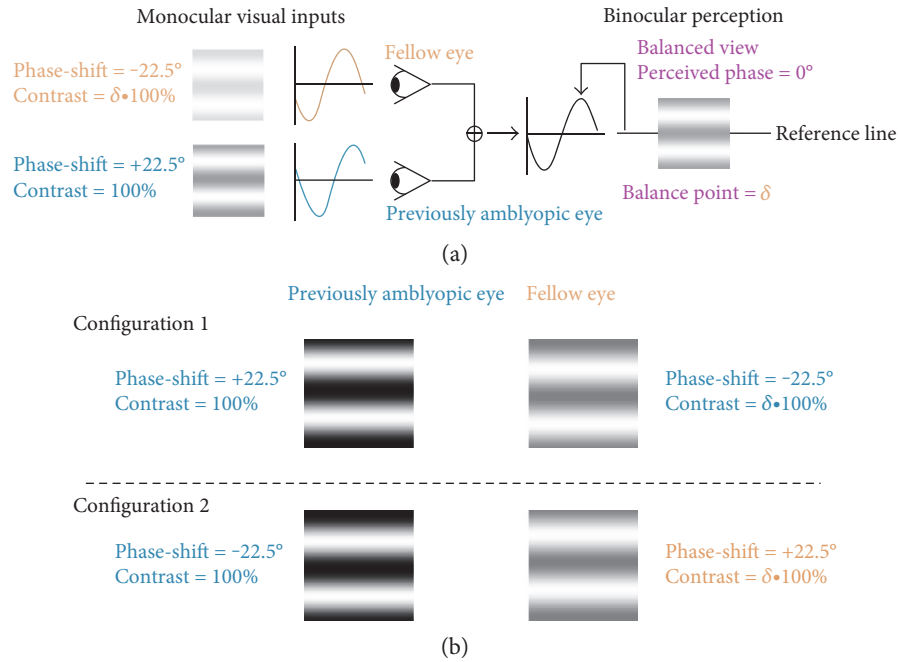

Figure 1: An illustration of the binocular phase combination paradigm for measuring sensory eye dominance. (a) Two horizontal sine-wave gratings with equal and opposite phase-shifts of 22.5° (relative to the center of the screen) were dichoptically presented to observers through polarized glasses; the perceived phase of the cyclopean percept was measured as a function of the interocular contrast ratio; we derived a balance point when the perceive phase was 0°, which represents the interocular contrast ratio at which the contributions of each eye are equal. (b) The phase-shift was +22.5° in the previously amblyopic eye and −22.5° in the fellow eye; similarly, the phase-shift was −22.5° in the previously amblyopic eye and +22.5° in the fellow eye. The perceived phase of the cyclopean grating at each interocular contrast ratio (δ) was quantified by half of the difference between the measured perceived phases in these two configurations.

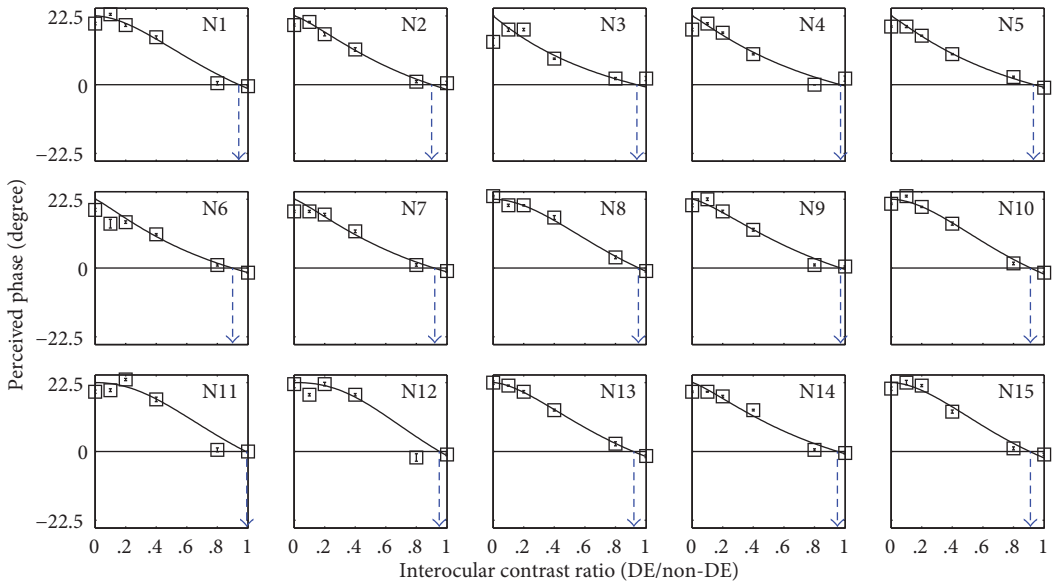

Figure 2: Binocular combination of the normal controls. The relationship between the perceived phase and interocular contrast ratio (dominant eye/nondominant eye) is plotted for 15 normal controls (N1–N15). The crossing of blue dotted line and the horizontal black line represents the balance point at which the two eyes are equally effective. The error bars represent standard errors.

3. Results

The PvR functions for the normal controls are plotted in Figure 2. The results are consistent with results from previous studies assessing binocular functions in normal controls with the same method [10, 12, 13]. A repeated measures ANOVA indicated that the perceived phase significantly depended on the interocular contrast ratios: $F(5, 70) = 374.80$, $p < 0.05$.

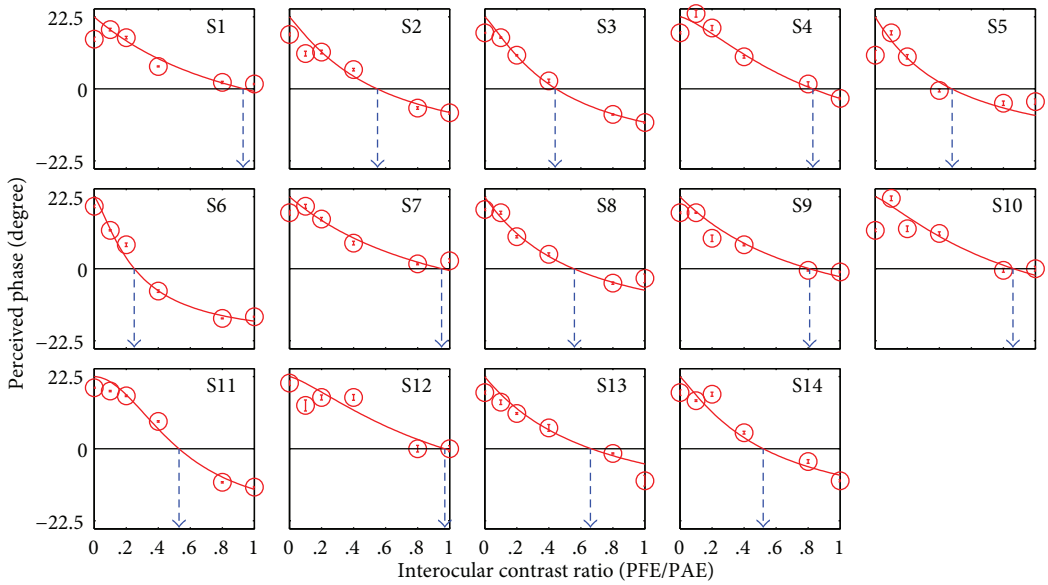

Figure 3: Binocular combination of treated anisometropic amblyopes. The relationship of perceived phase against interocular contrast ratio (previous fellow eye/previously amblyopic eye) is plotted for 14 treated anisometropic amblyopes (S1–S14). The figure is organized in the same manner as Figure 2.

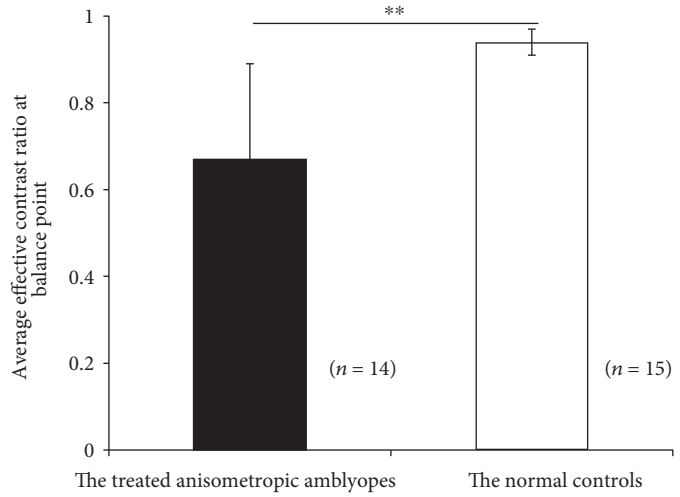

Figure 4: Different sensory eye dominance in treated anisometropia amblyopes and normal controls. The two eyes of the treated anisometropic amblyopes are significantly imbalanced compared with those of normal subjects. "**" represents the result of two-tailed t-test for two samples, $p < 0.05$. Error bars represent standard deviation.

The derived balance point from the fitted PvRs (i.e., the interocular contrast ratio where the binocular perceived phase was zero degrees) are marked as triangle symbols in Figure 2, and all the normal observers' balance points were close to 1 (the average balance point of the normal subjects was 0.94 ± 0.03; mean $\pm$ SD), thus indicating balanced eyes in the normal controls.

The PvR functions for the treated anisometropic amblyopes are plotted in Figure 3. Similarly, the perceived phase also significantly depended on the interocular contrast ratios: $F(5, 65) = 112.13$, $p < 0.05$. The derived balance points were close to unity in some observers (i.e., S1, S7, and S12). However, most of our treated patients had a relatively small balance point, thus indicating the existence of strong sensory eye imbalance. The average balance point of these treated amblyopes was 0.67 ± 0.22 (mean $\pm$ SD), which was significantly different from that of the normal subjects $t\ (27) = -4.63$, $p < 0.05$, the effect size (using Cohen's d) $= 1.75$, 2-tailed independent samples t-test (Figure 4). There was no significant correlation between the degree of anisometropia and the balance point in our treated patients ($p = 0.12$). We also did not find any significant correlation between the balance point and the age at first treatment ($p = 0.13$). In Figure 5, the average PvR curves of the treated amblyopes and the controls are plotted and were found to be consistent with the average balance point shown in Figure 4.

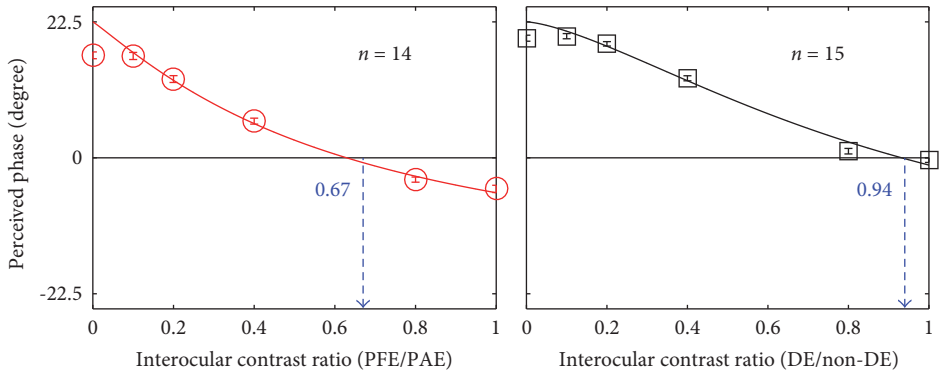

Figure 5: The average PvR curves of treated amblyopia and the controls.

The relationship of average perceived phase against interocular contrast ratio is plotted for the two groups. The figure is organized in the same manner as Figure 2.

4. Discussion

In our investigation, we used the binocular phase combination paradigm to quantitatively measure the sensory eye dominance of treated anisometropic amblyopes and found that the contribution of the two eyes were still unequal in most of the treated patients, even though they had normal visual acuity after successful treatments. Only 3 of 14 treated patients showed the balanced pattern seen in normal controls.

Some observers remained different degrees of anisometropia after successful treatment. Recently, Zhou et al. [14] showed that the two eyes are imbalanced in anisometropes without amblyopia, which was not significantly correlated with the degree of anisometropia. In the present study, we also did not find any significant correlation between the degree of anisometropia and the balance point in our treated patients ($p = 0.12$). We suspect that similar mechanisms may account for the abnormal sensory eye dominance in the treated anisometropic amblyopes and the anisometropes without amblyopia.

Using similar methods to those used in this study, we have recently shown that surgically corrected intermittent exotropes also have abnormal sensory eye dominance [11]. Here, we focused on anisometropic amblyopes, whose visual deficits are mechanistically different from amblyopes with strabismus [15, 16]. To the best of our knowledge, this is the first work that shows abnormal sensory eye dominance in treated anisometropic amblyopia. Even abnormal sensory eye dominance has been found in both anisometropic amblyopia and strabismic amblyopia [13], and we do not know whether the abnormal sensory eye dominance we reported here resulted from the same mechanism as that of the surgically corrected intermittent exotropes that we previously reported on [11]. This issue would need to be addressed in future work by using the binocular phase and contrast combination paradigm and the multipathway contrast gain control model [17].

Our study is not the first to show that there is still some degree of visual deficits in treated amblyopes. For example, Huang et al. [18] have also found that treated amblyopes with normal visual acuity remain deficient in contrast sensitivity functions, and the deficits are significant only at high frequencies (i.e., 8 cycle/degree or above). Because our measurements were conducted at a relatively low spatial frequency (i.e., 1 cycle/deg), in which the previously amblyopic eye's contrast sensitivity is normal [18], our results cannot account for the monocular contrast sensitivity deficit of the amblyopic eye. In addition, the contrast of the stimuli in the amblyopic eye was fixed at 100%, which was far above the contrast threshold. Previous reports have found that the amblyopic eye's perception is intact at suprathreshold contrast level [19, 20]. Therefore, the abnormal sensory eye dominance observed herein reflects the learning potential in the binocular processing in treated amblyopes, rather than the monocular contrast sensitivity deficit of the previously amblyopic eye.

Our study provides additional insight into binocular function in treated anisometropic amblyopes. The abnormal sensory eye dominance reported here suggests that the current patching therapy, which can restore the visual acuity of the amblyopic eye, is not sufficient in rebalancing the two eyes in binocular processing. However, our data cannot confirm whether the residual difference in eye dominance has any functional significance, because most of our subjects had normal to near-normal stereopsis. This issue must be addressed in future work. Nevertheless, our results together with those previous reports [18] indicate that the learning (or improving) potential is still present in treated amblyopes, who have normal monocular visual acuity and that additional treatment [21] might be necessary to elicit a "fully" treated status.

Disclosure

Chen Yao and Jiafeng Wang are co-first authors.

Conflicts of Interest

The authors declare that there are no conflicts of interest regarding the publication of this paper.

Authors' Contributions

Lixia Feng conceived the experiments. Yao Chen, Jiafeng Wang, and Hongmei Shi performed the experiments. Yao Chen and Lixia Feng interpreted the data and wrote the manuscript. Yao Chen, Jiafeng Wang, and Lixia Feng modified the manuscript. Xiaoxiao Wang drew the PvR curves. All authors reviewed the manuscript.

Acknowledgments

The authors thank Dr. Jiawei Zhou and Dr. Robert F. Hess for providing some of the programs. This work was supported by a National Natural Science Foundation of China grant (NSFC81300796) to Lixia Feng. The authors are grateful to all study participants.

References

[1] K. Attebo, P. Mitchell, R. Cumming, W. Smith, N. Jolly, and R. Sparkes, "Prevalence and causes of amblyopia in an adult population," *Ophthalmology*, vol. 105, no. 1, pp. 154–159, 1998.

[2] J. M. Holmes and M. P. Clarke, "Amblyopia," *Lancet*, vol. 367, no. 9519, pp. 1343–1351, 2006.

[3] P. J. Kutschke, W. E. Scott, and R. V. Keech, "Anisometropic amblyopia," *Ophthalmology*, vol. 98, no. 2, pp. 258–263, 1991.

[4] R. Agrawal, I. P. Conner, J. V. Odom, T. L. Schwartz, and J. D. Mendola, "Relating binocular and monocular vision in strabismic and anisometropic amblyopia," *Archives of Ophthalmology*, vol. 124, no. 6, pp. 844–850, 2006.

[5] I. C. Wood, J. A. Fox, and M. G. Stephenson, "Contrast threshold of random dot stereograms in anisometropic amblyopia: a clinical investigation," *British Journal of Ophthalmology*, vol. 62, no. 1, pp. 34–38, 1978.

[6] Y. F. Choong, H. Lukman, S. Martin, and D. E. Laws, "Childhood amblyopia treatment: psychosocial implications for patients and primary carers," *Eye (London, England)*, vol. 18, no. 4, pp. 369–375, 2004.

[7] M. X. Repka, S. A. Cotter, R. W. Beck et al., "A randomized trial of atropine regimens for treatment of moderate amblyopia in children," *Ophthalmology*, vol. 111, no. 11, pp. 2076–2085, 2004.

[8] G. R. Barnes, R. F. Hess, S. O. Dumoulin, R. L. Achtman, and G. B. Pike, "The cortical deficit in humans with strabismic amblyopia," *The Journal of Physiology*, vol. 533, no. 1, pp. 281–297, 2001.

[9] J. Ding and G. Sperling, "A gain-control theory of binocular combination," *Proceedings of the National Academy of Sciences of the United States of America*, vol. 103, no. 4, pp. 1141–1146, 2006.

[10] C. B. Huang, J. Zhou, Z. L. Lu, L. Feng, and Y. Zhou, "Binocular combination in anisometropic amblyopia," *Journal of Vision*, vol. 9, no. 3, p. 17, 2009, 11-16.

[11] L. Feng, J. Zhou, L. Chen, and R. F. Hess, "Sensory eye balance in surgically corrected intermittent exotropes with normal stereopsis," *Scientific Reports*, vol. 5, pp. 1–8, 2015.

[12] J. Zhou, R. Liu, Y. Zhou, and R. F. Hess, "Binocular combination of second-order stimuli," *PloS One*, vol. 9, no. 1, pp. 1–7, 2014.

[13] J. Zhou, P. C. Huang, and R. F. Hess, "Interocular suppression in amblyopia for global orientation processing," *Journal of Vision*, vol. 13, no. 5, pp. 1–14, 2013.

[14] J. Zhou, L. Feng, H. Lin, and R. F. Hess, "On the maintenance of normal ocular dominance and a possible mechanism underlying refractive adaptation," *Investigative Ophthalmology & Vision Science*, vol. 57, no. 13, pp. 5181–5185, 2016.

[15] R. F. Hess, A. Bradley, and L. Piotrowski, "Contrast-coding in amblyopia. I. Differences in the neural basis of human amblyopia," *Proceedings of the Royal Society of London B: Biological Sciences*, vol. 217, no. 1208, pp. 309–330, 1983.

[16] S. P. McKee, D. M. Levi, and J. A. Movshon, "The pattern of visual deficits in amblyopia," *Journal of Vision*, vol. 3, no. 5, pp. 380–405, 2003.

[17] C. B. Huang, J. Zhou, Z. L. Lu, and Y. Zhou, "Deficient binocular combination reveals mechanisms of anisometropic amblyopia: signal attenuation and interocular inhibition," *Journal of Vision*, vol. 11, no. 6, pp. 1–17, 2011.

[18] C. Huang, L. Tao, Y. Zhou, and Z. L. Lu, "Treated amblyopes remain deficient in spatial vision: a contrast sensitivity and external noise study," *Vision Research*, vol. 47, no. 1, pp. 22–34, 2007.

[19] D. S. Loshin and D. M. Levi, "Suprathreshold contrast perception in functional amblyopia," *Documenta Ophthalmologica*, vol. 55, no. 3, pp. 213–236, 1983.

[20] R. F. Hess and A. Bradley, "Contrast perception above threshold is only minimally impaired in human amblyopia," *Nature*, vol. 287, no. 5781, pp. 463–464, 1980.

[21] A. L. Webber, J. M. Wood, and B. Thompson, "Fine motor skills of children with amblyopia improve following binocular treatment," *Investigative Ophthalmology & Vision Science*, vol. 57, no. 11, pp. 4713–4720, 2016.

Hindawi
Neural Plasticity
Volume 2017, Article ID 9807512, 11 pages
https://doi.org/10.1155/2017/9807512

Research Article

Thalamocortical Connectivity and Microstructural Changes in Congenital and Late Blindness

N. H. Reislev,[1] T. B. Dyrby,[1,2] H. R. Siebner,[1,3] H. Lundell,[1] M. Ptito,[4,5] and R. Kupers[5,6,7]

[1]*Danish Research Centre for Magnetic Resonance, Centre for Functional and Diagnostic Imaging and Research, Copenhagen University Hospital Hvidovre, Hvidovre, Denmark*
[2]*Department of Applied Mathematics and Computer Science, Technical University of Denmark, Kongens Lyngby, Denmark*
[3]*Department of Neurology, Copenhagen University Hospital Bispebjerg, Copenhagen, Denmark*
[4]*Laboratory of Neuropsychiatry, Psychiatric Centre Copenhagen, Copenhagen, Denmark*
[5]*School of Optometry, Université de Montréal, Montréal, QC, Canada*
[6]*BRAINlab, Danish Centre for Sleep Medicine, Rigshospitalet, Department of Clinical Neurophysiology, University of Copenhagen, Copenhagen, Denmark*
[7]*Department of Radiology & Biomedical Imaging, Yale University, 300 Cedar Street, New Haven, CT 06520, USA*

Correspondence should be addressed to N. H. Reislev; ninar@drcmr.dk

Received 24 November 2016; Revised 2 February 2017; Accepted 19 February 2017; Published 13 March 2017

Academic Editor: Jiawei Zhou

There is ample evidence that the occipital cortex of congenitally blind individuals processes nonvisual information. It remains a debate whether the cross-modal activation of the occipital cortex is mediated through the modulation of preexisting corticocortical projections or the reorganisation of thalamocortical connectivity. Current knowledge on this topic largely stems from anatomical studies in animal models. The aim of this study was to test whether purported changes in thalamocortical connectivity in blindness can be revealed by tractography based on diffusion-weighted magnetic resonance imaging. To assess the thalamocortical network, we used a clustering method based on the thalamic white matter projections towards predefined cortical regions. Five thalamic clusters were obtained in each group representing their cortical projections. Although we did not find differences in the thalamocortical network between congenitally blind individuals, late blind individuals, and normal sighted controls, diffusion tensor imaging (DTI) indices revealed significant microstructural changes within thalamic clusters of both blind groups. Furthermore, we find a significant decrease in fractional anisotropy (FA) in occipital and temporal thalamocortical projections in both blind groups that were not captured at the network level. This suggests that plastic microstructural changes have taken place, but not in a degree to be reflected in the tractography-based thalamocortical network.

1. Introduction

There is strong evidence that the occipital cortex in visually deprived humans undergoes massive cross-modal reorganisation and processes sensory information from other modalities than vision (for review, see [1]). However, there is no consensus as to whether these cross-modal responses are mediated by structural alterations in corticocortical or thalamocortical connectivity [2, 3], or a combination of both [4].

The thalamus forms an important relay between sensory input and the cerebral cortex for all sensory modalities, with the exception of olfaction. Specialised nuclei within the thalamus receive and process specific sensory input which is further sent to specialised cortical areas via thalamocortical projections [5, 6]. In the normal healthy human brain, visual information is relayed from the lateral geniculate nucleus (LGN) to the primary visual cortex via the optic radiations (for review, see Metzger et al. [7]).

In blind individuals, cross-modal responses in the occipital cortex could potentially be mediated through rerouting of information from auditory and somatosensory thalamic nuclei to the occipital cortex via the LGN. Although both the LGN and the optic radiations are reduced in size in congenital blindness [8], nonvisual information might be relayed to the visual cortex through the optic radiations [9–12]. This would

imply the formation of novel ectopic connections between the thalamic somatosensory nucleus and the LGN, as has been shown in animal models of blindness [13, 14]. Alternatively, nonvisual occipital activation could also be mediated by strengthening of existing corticocortical connections [15]. To the best of our knowledge, no studies have reported on the contribution of the thalamus to the transfer of nonvisual information to the visual cortex in human blind subjects. Therefore, purported alterations in thalamocortical connectivity in the human blind brain remain to be proven.

The aim of this study is therefore to map thalamocortical structural connectivity in vivo using tractography based on diffusion-weighted imaging (DWI). A second aim was to test whether changes in the intrinsic regional microstructure of the thalamic nuclei can be demonstrated by diffusion tensor imaging (DTI). Adopting the method of Behrens et al. [16], we segmented the thalamus into clusters based on their thalamocortical connectivity as revealed by DWI-based tractography and compared the structural thalamocortical connectivity patterns among age-matched groups of congenitally blind (CB), late blind (LB), and normal sighted (NS) control subjects. We reasoned that between-group changes in thalamocortical white matter projections would be reflected by altered thalamic segmentation patterns and that these alterations would depend on the onset of blindness.

2. Materials and Methods

2.1. Subjects and Data Acquisition. A total of 12 CB (mean age 42 ± 13 years), 15 LB (mean age 52 ± 15 years, mean onset of blindness 16.6 ± 8.9 years), and 15 NS (mean age 46 ± 13 years) individuals were included in the study. The cause of blindness was restricted to be of peripheral origin and subjects with residual vision were excluded. The Danish ethics committee for Copenhagen and Frederiksberg (KF 01 328 723) approved the study and all participants gave oral and written informed consent.

Magnetic resonance images (MRI) of the brain were acquired using a 3.0 Tesla Siemens Verio scanner with a 32-channel head coil (Siemens, Erlangen, Germany). Data from the same study cohort have been used in two related publications [17, 18] and will therefore be only shortly summarised. Two DWI data sets of the whole brain (61 axial slices with an isotropic voxel resolution of 2.3 mm) were consecutively acquired using a twice-refocused spin-echo sequence [19]. Sequence settings were as follows: TE = 89 ms, TR = 11440 ms, Grappa factor = 2, with 24 reference lines and 61 uniformly distributed directions with $b = 1500\,\text{s/mm}^2$, and 10 non-diffusion-weighted images. For postprocessing purposes, a set of non-diffusion-weighted reversed phase-encoding images was acquired with the same imaging parameters. High-resolution T1-weighted structural image volumes were acquired for anatomical information (TE = 2.32 ms, TR = 1900 ms, and flip angle = 9°) with an isotropic voxel resolution of 0.9 mm.

2.2. Data Preprocessing. We used MATLAB R2012a (MathWorks, Inc., Natick, Massachusetts, USA) and FSL [20–22] for image processing. Susceptibility artefacts in the raw DWIs were minimised with the application of a voxel displacement map (VDM). The two reversed phase-encoding $b = 0\,\text{s/mm}^2$ images were used for estimating the voxel shifts for the VDM, as implemented in FSL's topup tool [20, 23]. We applied the VDM and a full affine transformation to correct for movement and eddy currents in the DWIs using FSL's eddy tool [24], by reslicing to original image resolution using spline interpolation. Finally, the 61 directions were reoriented similarly to the orientation introduced by the applied transformations [25]. The T1-weighted images were corrected for gradient nonlinearities [26].

2.3. Defining Seed and Target Masks of Thalamus and Cortex. To examine the thalamocortical connectivity pattern, seed and target masks for tractography were defined. The target masks were obtained through a subject-based cortical segmentation with FreeSurfer software v. 5.3.0 [27, 28] based on the averaged T1-weighted volumes [29]. The cortical segmentation from FreeSurfer was used to define anatomical regions of interest using the Desikan-Killiany atlas [30]. We created five cortical target masks, which were used for tractography, including the occipital, temporal, somatosensory/parietal-postcentral, motor/precentral, and frontal cortical areas. Table 1 shows the expected relation in terms of brain connectivity in the normal healthy human brain between the five cortical target masks and thalamic regions. The seed mask for tractography included all voxels within the thalamus region. This region also included the LGN and MGN as defined in the AAL atlas [31]. The seed mask was then transformed from MNI space into each individual subject's diffusion space for tractography. This was done using nonlinear registration from the MNI template to the structural T1-weighted image space and then using linear registration from the T1-weighted to the non-diffusion-weighted image. For each subject, the thalamic seed mask was manually edited to ensure proper coverage of the anatomical area of the thalamus. The cortical target masks were transformed from each individual subject in FreeSurfer space through the structural T1-weighted images to each individual subject's diffusion space through the FA image. The transformations were done using FreeSurfer and FSL v. 5.0 registration tools [20–22, 32, 33].

2.4. Tractography-Based Thalamocortical Segmentation. Based on the preprocessed DWIs, we used FSL's bedpostx tool to estimate the multifibre directions within each voxel of the brain using the ball-and-two-sticks model [34, 35] as the fibre orientation distribution function for subsequent tractography. For tractography-based thalamic segmentation, we used the tractography and clustering procedure available in FSL and standard settings [16]. First and in native space, probabilistic tractography was performed for each voxel in the thalamic seed mask (5000 streamlines per voxel) and to each of the five cortical target masks. Tractography was run separately in each hemisphere, and a midsagittal exclusion mask ensured exclusion of transhemispheric connections. Then, FSL "find-the-biggest" hard clustering approach was applied to

Table 1: Overview of the cortical target masks and the corresponding thalamic nuclei.

Target mask	Cortical labels	Corresponding thalamic nuclei
Occipital	Pericalcarine Cuneus Lateral occipital Lingual	Pulvinar LGN MGN Lateral nucleus
Temporal	Middle temporal Inferior temporal Superior temporal Transverse temporal Fusiform Temporal pole Banks of superior temporal sulcus Entorhinal Parahippocampal	Pulvinar MGN
Somatosensory/parietal-postcentral	Postcentral Supramarginal Superior parietal Inferior parietal Precuneus Isthmus cingulate Posterior cingulate	Lateral nucleus Ventrolateral nucleus Ventroposterior nucleus
Motor/precentral	Precentral Caudal middle frontal Paracentral	Ventrolateral nucleus Ventroanterior nucleus
Frontal	Superior frontal Frontal pole Medial orbitofrontal Lateral orbitofrontal Rostral middle frontal Rostral anterior cingulate Pars opercularis Pars orbitalis Pars triangularis	Anterior nucleus Mediodorsal nucleus

Cortical target masks defined by combining labels given by the Desikan-Killiany atlas. The last column shows the thalamic nuclei, corresponding to the respective cortical projection sites as defined from an anatomical atlas based on the normal healthy human brain [5]. LGN: lateral geniculate nuclei; MGN: medial geniculate nuclei.

the tractography results to segment the thalamus into five clusters, corresponding to the tractography connectivity pattern to each of the five cortical target masks. For each individual, seeds-to-target information on the connectivity from the seed to each individual target mask was obtained from the tractography. Based on this information, the find-the-biggest clustering assigns each voxel within the thalamus to the class with the highest connectivity count. We additionally used the seeds-to-target information as a marker of connection strength between the thalamus and each cortical target mask represented by the connectivity count within each voxel of the thalamus normalised with total number of streamlines. Lastly, to extract a region of interest within the individual thalamocortical white matter projections between the thalamus and each cortical target mask, tractography was run from the thalamus to each individual target mask, using the remaining cortical masks as exclusion masks.

2.5. Volume and DTI-Derived Indices of Whole Thalamus and Thalamic Clusters. The overall thalamic volume was assessed in native space based on the T1-weighted images. The volume of each cluster was evaluated in native diffusion image space based on the five cluster segmentations. The volume of each cluster was normalised with the total thalamic volume. Applying a diffusion tensor model to the preprocessed DWIs, the DTI-derived indices fractional anisotropy (FA) and mean diffusivity (MD) were extracted for each voxel and the mean value was calculated for the whole thalamus and each individual cluster.

2.6. Microstructural Features of Thalamocortical White Matter Projections. Regions of interest within the white matter projections from the thalamus to each cortical target mask were extracted from the tractography by thresholding. A threshold of 40% of the highest number of streamlines connecting the thalamus and the target was set to focus on the core tract area,

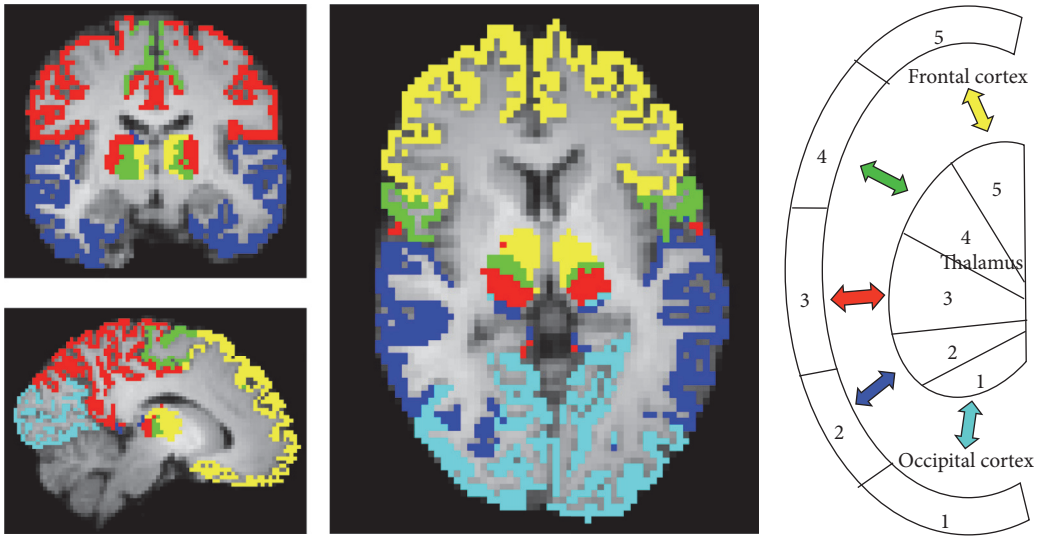

Figure 1: Find-the-biggest segmentation of the thalamus into five clusters and their corresponding cortical target masks in a NS subject ($x = 52$, $y = 48$, $z = 28$). Occipital cluster 1 (light blue), temporal cluster 2 (dark blue), somatosensory postcentral cluster 3 (red), motor precentral cluster 4 (green), and frontal cluster 5 (yellow). The right part of the figure shows a color-coded schematic illustration of the thalamocortical connectivity.

that is, typically situated in the midline of the tract, removing spurious streamlines. Furthermore, we ensured that there was no overlap between white matter projections by keeping only the streamlines within the tract that had the highest connection strength. MD and FA were extracted to calculate the mean of each voxel within this core tract region of interest of each white matter projection.

2.7. Statistical Analyses. Based on our previous report on thalamic volume reductions in congenitally blind subjects [8], we applied a one-tailed t-test under the assumption of unequal variance between groups to test for between-group differences in overall thalamic volume at a significance level of $p < 0.05$. A one-way ANOVA was applied to test for differences in individual cluster volume, correcting for multiple comparisons using the Bonferroni method.

We used a similar one-way ANOVA for testing the overall group differences of the DTI-derived microstructural indices within the whole thalamus and thalamic clusters at a significance level of $p < 0.05$. Group and cluster were main effects, whereas "group × cluster" was the interaction of interest. Post hoc two-sample t-tests were used to assess differences between each group and cluster, adjusting for multiple testing. The same procedure was applied to test for statistical differences in MD and FA in the five white matter projections from each thalamic cluster. For all variables, Levene's test was used to check for homogeneity of the variance prior to application of the ANOVA.

3. Results

3.1. Connectivity-Based Segmentation of the Thalamus. Connectivity-based segmentation of the thalamus resulted in five clusters. Figure 1 shows the thalamic segmentation pattern and the corresponding cortical target masks in a normal sighted control. The occipital cluster (light blue) comprised mainly the LGN that projects to the primary visual cortex. The temporal thalamic cluster (dark blue) included mainly the MGN but also the pulvinar, which projects to occipital, parietal, and temporal areas. We wish to point out that because of the close anatomical proximity of the LGN and MGN in the metathalamus and overlapping thalamic projections, the clustering method is not likely to separate these small structures completely. The sensory thalamic cluster (red) included the lateral nucleus and the ventral posterior and the ventral lateral thalamic nuclei projecting to posterior parietal and postcentral cortical areas. The motor cluster (green) covered the ventral anterior nucleus projecting to precentral but also superior frontal cortices. The frontal cluster (yellow) included the anterior nucleus and the mediodorsal nucleus, which project to superior frontal and prefrontal areas.

Segmentation of the thalamus based on structural thalamocortical connectivity resulted in similar clusters in all groups (Figure 2). Figure 2(a) shows an example of the thalamic segmentation pattern for a CB, LB, and NS subject, whereas Figure 2(b) shows a bar plot of the marker of connection strength, represented as the normalised seed to target, for each of the thalamocortical projections. There was no significant group difference in the connection strength. Hence, we could not confirm our hypothesis that blindness would be associated with differences in thalamocortical connectivity relative to normally sighted controls. Specifically, we found no increase in connectivity strength between occipital cortex and somatosensory and auditory projection nuclei. For all groups, the occipital cluster was very small, and the connection strength was much lower compared to that of the other clusters (Figure 2(b)). In several cases, the occipital cluster was overruled by the larger projections from nearby regions, which lead to no occipital cluster using the

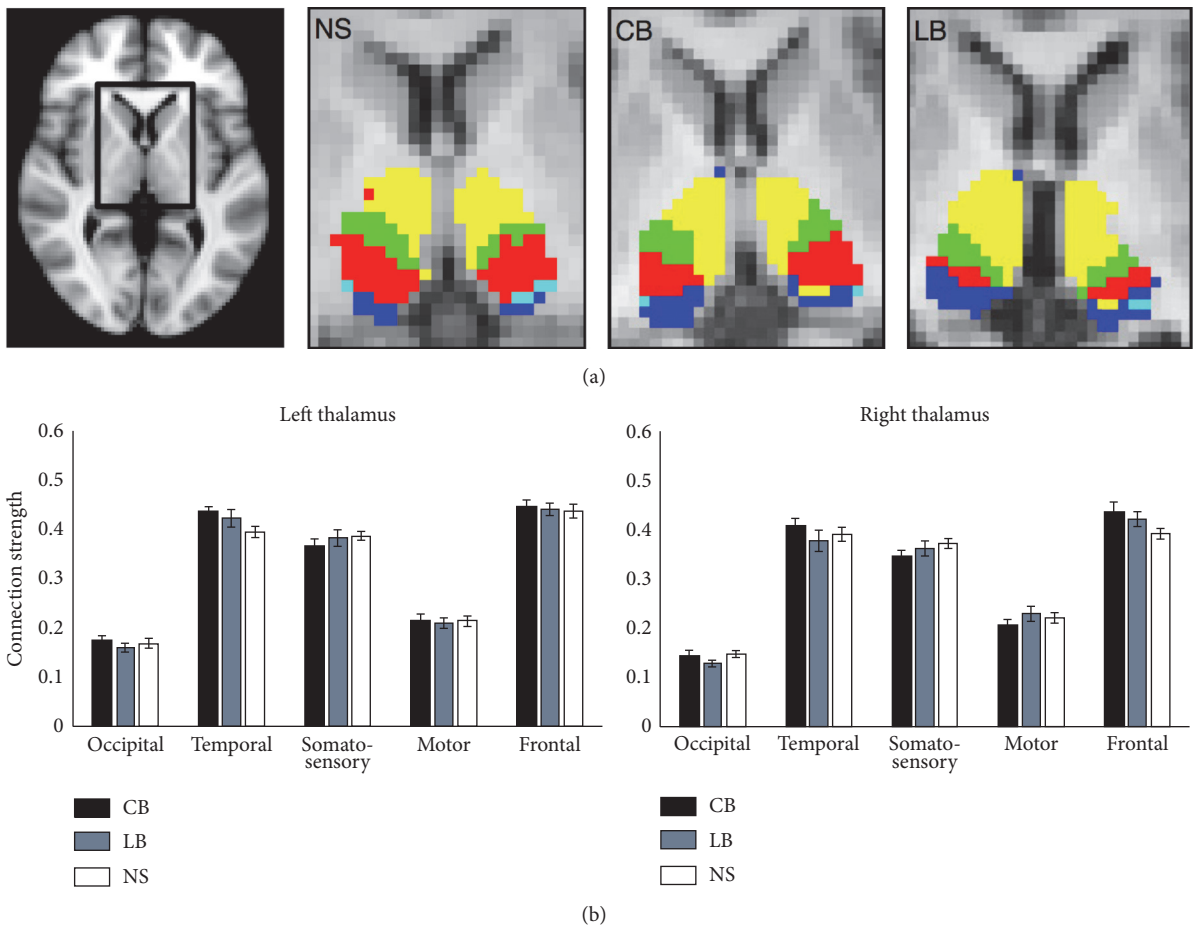

FIGURE 2: (a) Find-the-biggest segmentation within thalamus in a CB, LB, and NS participant. (b) Bar plot of the thalamocortical connectivity strength for the left and right thalamus for all CB, LB, and NS subjects. The y-axis represents the marker of connection strength between the thalamus and each cortical target mask, as measured by the seed to target connectivity count normalised with the total number of streamlines. Error bars indicate the standard error of the mean.

find-the-biggest segmentation (number of instances of presence of an occipital cluster for each group: CB: left 5/12, right 3/12 subjects; LB: left 8/15, right 2/15 subjects; NS: left 9/12, right 9/15 subjects).

3.2. Thalamic Volume and Microstructure. Overall thalamic volumes, corrected for intracranial brain volume, were significantly lower in congenitally blind (left/right: 6206 ± 702 mm^3/6460 ± 763 mm^3, $p = 0.033$ and 0.027, resp.) and late blind (left/right: 6059 ± 578 mm^3/6419 ± 659 mm^3, $p = 0.002$ and 0.008, resp.) individuals compared to sighted controls (left/right: NS: 6661 ± 439 mm^3/7014 ± 603 mm^3). Analysis of the MD and FA within the total thalamus mask (including all five clustered regions) showed a significant group difference in FA for the left ($F = 10.69$, $p < 0.0005$) and right ($F = 12.17$, $p < 0.0005$) thalamus. Post hoc tests revealed that reduced FA in CB (left and right: $p_{corr.} < 0.0005$) and LB (left: $p_{corr.} < 0.02$; right: $p_{corr.} < 0.03$) caused the difference. Analysis of each thalamic cluster showed that the reduced FA was located in the temporal, sensory, and frontal cluster (Table 2). No differences were found in MD within the total thalamus mask or in any of the clusters.

3.3. Microstructural Properties within Thalamocortical Projections. Figure 3 shows that the five thalamocortical white matter projections appeared visually similar across all three groups and also that the optic radiations remained present in the CB and LB groups, despite the absence of visual input (Figure 3, first column). MD and FA indices extracted within each of the five white matter projection regions of interest showed a significant group difference in FA for the occipital (left: $F = 14.47$, $p < 0.0001$; right: $F = 25.19$, $p < 0.0001$) and temporal (left: $F = 7.58$, $p < 0.05$; right: $F = 7.19$, $p < 0.05$) thalamocortical projections. Post hoc tests revealed reduced FA in CB and LB relative to the NS group (occipital left/right: $p_{corr.} < 0.0001$; temporal left/right: $p_{corr.} < 0.05$). A between-group difference was also found in MD for the occipital (left: $F = 3.88$, $p < 0.05$; right: $F = 4.54$, $p < 0.05$) and temporal (left: $F = 3.65$, $p < 0.05$; right: $F = 3.66$, $p < 0.05$) thalamic white matter projections. Post hoc tests revealed that this between-group difference was driven by an increased MD, but only in the LB group relative to the NS group (visual left/right: $p_{corr.} < 0.05$; temporal left/right: $p_{corr.} < 0.05$). No difference in MD was found in the CB group as compared to the NS group. FA and

Table 2: Mean and standard deviations of FA within the whole thalamus mask and the five segmented clusters.

		Thalamus			Occipital			Temporal			Sensory			Motor			Frontal		
		CB	LB	NS	CB	LB	NS	CB	LB	NS	CB	LB	NS	CB	LB	NS	CB	LB	NS
FA Mean (SD)	L	0.28^{**}	0.29^{*}	0.31	0.31	0.29	0.30	0.26^{**}	0.27	0.29	0.30^{*}	0.32	0.33	0.34	0.35	0.38	0.26^{**}	0.27^{*}	0.29
		(0.02)	(0.02)	(0.02)	(0.07)	(0.05)	(0.03)	(0.03)	(0.02)	(0.02)	(0.03)	(0.03)	(0.02)	(0.05)	(0.06)	(0.01)	(0.02)	(0.02)	(0.02)
	R	0.28^{**}	0.30^{*}	0.32	0.28	0.28	0.31	0.24^{**}	0.26^{*}	0.29	0.31^{*}	0.33	0.35	0.36	0.36	0.38	0.26^{**}	0.28	0.29
		(0.03)	(0.02)	(0.02)	(0.07)	(0.10)	(0.06)	(0.03)	(0.03)	(0.02)	(0.04)	(0.03)	(0.02)	(0.05)	(0.04)	(0.04)	(0.03)	(0.02)	(0.02)

Significantly reduced FA in CB and LB compared to NS at $^{**}p < 0.001$ or $^{*}p < 0.05$, Bonferroni corrected. CB: congenitally blind; LB: late blind; NS: normal sighted controls; L: left; R: right; FA: fractional anisotropy; SD: standard deviation.

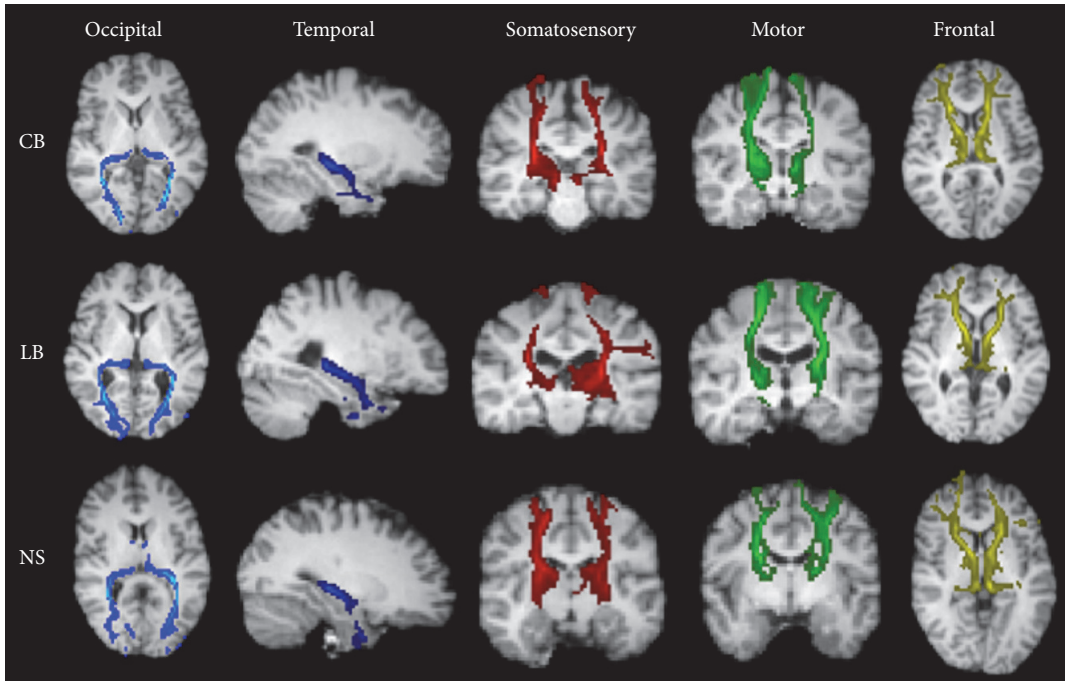

Figure 3: Examples of cortical white matter projections from each of the five thalamic clusters to the cortical target masks in a CB, LB, and NS participant. The cortical target masks are defined from the Desikan-Killiany atlas provided with FreeSurfer, as described in Table 1. The tracts are overlaid on each subject's T1-weighted image and presented in a slice of the most representative view, axial or coronal.

MD values within each white matter projection are shown in Table 3.

4. Discussion

We here present a connectivity-based clustering of the thalamus based on a hard segmentation between predefined cortical areas and the thalamus in blind and sighted individuals. We did not find evidence for changes in thalamocortical connectivity, as was shown with histological tracing techniques in animal studies (see [14]). Since DWI-based in vivo tractography maps larger fibre bundles and lacks specificity and sensitivity towards subtle axon bundles, these results do not rule out the possibility that there are subtle thalamocortical rearrangements related to blindness. However, analysis of DTI-derived microstructural indices revealed regional alterations in thalamic microstructure. Both blind groups showed reduced regional FA values relative to normal sighted controls in thalamic clusters that were connected to temporal, somatosensory, and frontal cortex. This indicates that blindness is associated with structural alterations within the thalamus and suggests a possible reorganisation of a thalamocortical connectivity pattern that was not captured with tractography. We also found a decrease in FA in the thalamooccipital and thalamotemporal projections. Furthermore, late blind, but not congenitally blind, participants additionally showed increased MD in these tracts compared to normal controls. However, these microstructural changes were not sufficiently large to be reflected in the tractography-based thalamocortical connectivity results. We suggest that changes in the microstructural environment are not a direct indicator of thalamic reorganisation but rather reflect a neuroplastic effect of the thalamic projections responding to a functional change. However, specific functional studies are needed to support this structural-functional relation in the blind.

4.1. How Does Nonvisual Information Reach the Visual Cortex? The functional reorganisation of the visually deprived human brain could be supported either by unmasking of already existing thalamic projections or by the development of new connections. Changes in thalamocortical connectivity might be related to connections from nonvisual thalamic nuclei that send out new axon collaterals conveying nonvisual information flow to the visual cortex. Despite a complete lack of afferent visual input, the geniculocalcarine pathway remains relatively spared [11, 12, 36, 37]. Data from the present study confirm that the connectivity between the thalamus and the occipital cortex in the human is preserved in congenitally blind individuals, as testified by the absence of group differences in posterior thalamic clusters and normal looking optic radiations on visual inspection. Since congenitally blind individuals have never had any visual experience, it seems plausible that the geniculocalcarine tract is kept alive by the relay of nonvisual sensory information to the occipital cortex, a contention that is now generally accepted (see [38] for review). For instance, Bridge et al. [12] reported a decrease in FA of the optic radiations but suggested normal connectivity, assessed through the number of tractography streamlines (i.e., strength of connectivity) from the thalamus to the primary visual cortex in six anophthalmic subjects. Using anatomical connectivity mapping (ACM) and DTI,

Table 3: Mean and standard deviations of FA and MD within the five thalamic white matter projections.

		Occipital			Temporal			Sensory			Motor			Frontal		
		CB	LB	NS	CB	LB	NS	CB	LB	NS	CB	LB	NS	CB	LB	NS
FA Mean (SD)	L	0.46**	0.45**	0.53	0.36*	0.35*	0.40	0.45	0.44	0.45	0.47	0.43	0.44	0.41	0.41	0.41
		(0.05)	(0.05)	(0.03)	(0.05)	(0.04)	(0.02)	(0.05)	(0.03)	(0.04)	(0.04)	(0.05)	(0.05)	(0.05)	(0.03)	(0.04)
	R	0.43**	0.42**	0.51	0.35*	0.34*	0.39	0.44	0.44	0.44	0.46	0.44	0.46	0.40	0.38	0.40
		(0.05)	(0.04)	(0.03)	(0.04)	(0.04)	(0.03)	(0.04)	(0.03)	(0.04)	(0.03)	(0.03)	(0.04)	(0.04)	(0.03)	(0.03)
MD Mean (SD)	L	0.67	0.72*	0.65	0.71	0.72*	0.67	0.64	0.64	0.64	0.63	0.65	0.65	0.62	0.62	0.62
		(0.04)	(0.09)	(0.04)	(0.04)	(0.07)	(0.04)	(0.04)	(0.05)	(0.06)	(0.06)	(0.08)	(0.09)	(0.04)	(0.05)	(0.03)
	R	0.70	0.71*	0.64	0.71	0.72*	0.67	0.62	0.62	0.62	0.61	0.62	0.61	0.64	0.65	0.64
		(0.05)	(0.09)	(0.03)	(0.04)	(0.06)	(0.04)	(0.03)	(0.04)	(0.04)	(0.04)	(0.05)	(0.04)	(0.04)	(0.05)	(0.02)

Significantly reduced FA in CB and LB and increased MD in LB compared to NS at $^{**}p < 0.001$ or $^{*}p < 0.05$, Bonferroni corrected. CB: congenitally blind; LB: late blind; NS: normal sighted controls; L: left; R: right; FA: fractional anisotropy; MD: mean diffusivity, values $\times 10^{-3}$; SD: standard deviation.

we also previously reported decreased FA within the optic radiations in the same blind groups, whereas ACM was mainly decreased within the splenium and midbody of the corpus callosum [18]. A retrograde tracer injection study in the primary visual cortex of early bilaterally enucleated opossums reported preservation of normal connectivity, but also new corticocortical and thalamocortical connections [14]. The authors suggested that the visually deprived occipital cortex receives inputs from various nonvisual thalamic nuclei related to somatosensory, auditory (see also [39]), and motor functions. Hamsters and ferrets, in which the occipital cortex has been ablated at birth, leaving the eyes and the optic tract intact, show a rearrangement of the thalamic intrinsic connectivity patterns [40]. Anatomical tracer studies in these animals have shown that the MGN becomes invaded by retinal projections and that neurons within the auditory cortex now also respond to visual stimuli. Importantly, rewired animals can use their auditory cortex to perform visual tasks (for review, see [38, 41]). Such thalamic rearrangements might result in a subtle shift in the border between thalamic nuclei projecting to auditory and visual areas, whereby projections from the MGN invade the LGN or the pulvinar nucleus, thereby rerouting auditory information to the visual cortex. Other studies have also reported a similar mechanism when the somatosensory thalamic nucleus (VB) receives projections from the retina [41]. VB neurons in rewired animals project to the somatosensory cortex and become responsive to visual stimulation [41].

Using tractography-based thalamic network analysis, we did not find evidence for a shift in the borders of the thalamic clusters, nor for a change in thalamocortical connectivity per se. However, our findings of decreased FA within several clusters of the thalamus suggest a change in the microstructural distribution of fibre connections within the thalamus, possibly related to a change in the internal connectivity between the clusters. We previously reported an overall volumetric reduction of the thalamus as well as several of its atlas-based subdivisions in congenitally blind subjects [8, 11, 41]. The present data confirm and extend these findings by showing that similar volumetric reductions take place in late blind individuals.

The reduction in the size of the thalamus, and particularly that of the LGN, parallels animal models of early visual deprivation, enucleation, or cortical lesions. For example, the early cortical ablation of all visual cortical areas in the monkey leads to a largely reduced dLGN that is still layered and metabolically active [42, 43].

4.2. The Link between Functional and Structural Reorganisation: Methodological Limitations. The animal and human literature on visual deprivation provides key elements that subcortical mechanisms play an important role in the reorganisation of the thalamofugal projections [38, 41]. In animal models, subcortical rearrangements lead to rerouting of the auditory and somatosensory inputs to the dLGN [13, 14, 41]. Using dynamic causal modelling analysis of human fMRI data, Klinge et al. [44] argue in favour of increased corticocortical connectivity, supporting the hypothesis of increased functional connectivity between the primary auditory and primary visual cortex, as opposed to increased thalamocortical connectivity. There is also evidence for increased corticocortical connectivity between primary somatosensory and occipital cortex in congenital blindness of humans, as demonstrated by transcranial magnetic stimulation (TMS) [15], combined TMS and positron emission tomography [45], and magnetoencephalography studies [4]. Behavioral and imaging studies using a sensory substitution device that translates visual information into electrotactile stimulation also showed increased corticocortical connectivity between the primary somatosensory and primary visual cortex [3, 15]. However, the strengthening of corticocortical connectivity does not preclude the possibility that changes also may take place in thalamocortical connectivity, and the two types of connectivity changes may exist together. Interestingly, we did observe microstructural changes along some thalamocortical connections, suggesting that connectivity-related changes have taken place, but not at a level reflected in the thalamocortical connectivity revealed by tractography.

We found a difference in mean FA within the occipital and temporal white matter projections in both groups of blind subjects. Even though we restricted the region of interest to the core part of the tracts for voxel-wise analysis, differences in mean FA can be caused by the modulation of macroscopic effects, such as bending, crossing, and fanning axons [46]. Macrostructural effects as tract shape and volume may blur true differences in microscopic anisotropy [47] in blind individuals.

We selected a constrained thalamocortical segmentation method, based on five predefined cortical areas that are connected with different thalamic nuclei. Although the five-cluster segmentation gave robust thalamic clusters, it grouped several thalamic nuclei into one common cluster, making it difficult to distinguish visual, auditory, and somatosensory connectivity. Furthermore, the find-the-biggest approach is a hard clustering approach not taking into account less probable connections in the final segmentation. However, the find-the-biggest approach is based on the "seeds-to-target" analysis, in which each voxel is given a number according to the probability of that voxel to be assigned to a certain cortical mask. This hard clustering approach does not allow an examination of potential reorganisations within the cortex. Modulation of the thalamocortical projections might also be reflected at the cortical level through internal corticocortical connectivity changes. Alternatively, an unconstrained clustering method, such as k-means clustering, could be used. Our exploratory results using this unconstrained method (data not shown) demonstrate that five clusters is a good choice, supporting the constrained method used [16, 48, 49]. However, unconstrained clustering provides noisy results, challenging a robust definition of thalamic clusters. Different sources can contribute to the noisy clustering results, for instance, seeding streamlines within grey matter voxels. Since subcortical grey matter areas as the thalamus have low anisotropy, this introduces fluctuations in tractography streamlining until they reach the surface of thalamus and enter the white matter tracts. These fluctuations can introduce false positives as well as false negatives of especially the finer detailed tracts and therefore mainly the gross tract systems

are reliably estimated with tractography [50, 51]. When using constrained clustering with fixed cortical regions, we reduce the noise but at the cost of losing finer connectivity details. However, to support the robustness of finer tracking details, that is, white matter tracts consisting of fewer numbers of streamlines, the data must be supplemented by results of tracer studies in animals and translated to human in combination with Klingler dissection [52, 53].

5. Conclusion

We here presented a connectivity-based segmentation of the thalamus into five clusters and showed differences in DTI indices within the thalamus in congenital and late-onset blindness. These results indicate overall preservation of the structural thalamocortical connectivity but suggest that a reorganisation has taken place at the level of the thalamic nuclei. However, changes in DTI indices did appear in some of the thalamocortical projections, but they did not impact the overall structural thalamocortical network as revealed by tractography. The absence of macrostructural changes might be explained by a combination of how the tractography works and image quality (i.e., signal-to-noise and image resolution). The use of high-field MRI at 7 teslas might furnish a more appropriate tool for the detailed investigation of the connectivity pattern within the thalamus and cortex in sensory deprivation.

Competing Interests

The authors declare that there are no competing interests regarding the publication of this paper.

Acknowledgments

This work was supported by the Lundbeck Foundation (Grant no. 3156-50-28667 to R. Kupers and Grant no. R59 A5399 [Grant of Excellence on Mapping, Modulation & Modelling the Control of Actions] to H. R. Siebner) and the Danish Council for Independent Research, Medical Sciences (Grant no. 09-063392, 0602-01340B to M. Ptito).

References

[1] R. Kupers and M. Ptito, "Insights from darkness: what the study of blindness has taught us about brain structure and function," *Progress in Brain Research*, vol. 192, pp. 17–31, 2011.

[2] D. Bavelier and H. J. Neville, "Cross-modal plasticity: where and how?" *Nature Reviews Neuroscience*, vol. 3, no. 6, pp. 443–452, 2002.

[3] M. Ptito, S. M. Moesgaard, A. Gjedde, and R. Kupers, "Cross-modal plasticity revealed by electrotactile stimulation of the tongue in the congenitally blind," *Brain*, vol. 128, no. 3, pp. 606–614, 2005.

[4] A. A. Ioannides, L. Liu, V. Poghosyan et al., "MEG reveals a fast pathway from somatosensory cortex to occipital areas via posterior parietal cortex in a blind subject," *Frontiers in Human Neuroscience*, 2013.

[5] R. Nieuwenhuys, J. Voogd, and C. van Huijzen, *The Human Central Nervous System*, Springer, Berlin, Germany, 3rd edition, 1988.

[6] D. G. Amaral, "The functional organisation of perception and movement," in *Principles of Neural Science*, E. R. Kandel, J. H. Schwartz, T. M. Jessel, S. A. Siegelbaum, and A. J. Hudspeth, Eds., pp. 356–369, McGraw-Hill Medical, 5th edition, 2013.

[7] C. D. Metzger, Y. D. Van der Werf, and M. Walter, "Functional mapping of thalamic nuclei and their integration into cortico-striatal-thalamo-cortical loops via ultra-high resolution imaging—*from animal anatomy to in vivo imaging in humans*," *Frontiers in Neuroscience*, vol. 7, article 24, 2013.

[8] L. Cecchetti, E. Ricciardi, G. Handjaras, R. Kupers, M. Ptito, and P. Pietrini, "Congenital blindness affects diencephalic but not mesencephalic structures in the human brain," *Brain Structure and Function*, vol. 221, no. 3, pp. 1465–1480, 2016.

[9] U. Noppeney, K. J. Friston, J. Ashburner, R. Frackowiak, and C. J. Price, "Early visual deprivation induces structural plasticity in gray and white matter," *Current Biology*, vol. 15, no. 13, pp. R488–R490, 2005.

[10] W.-J. Pan, G. Wu, C.-X. Li, F. Lin, J. Sun, and H. Lei, "Progressive atrophy in the optic pathway and visual cortex of early blind Chinese adults: a voxel-based morphometry magnetic resonance imaging study," *NeuroImage*, vol. 37, no. 1, pp. 212–220, 2007.

[11] M. Ptito, F. C. G. Schneider, O. B. Paulson, and R. Kupers, "Alterations of the visual pathways in congenital blindness," *Experimental Brain Research*, vol. 187, no. 1, pp. 41–49, 2008.

[12] H. Bridge, A. Cowey, N. Ragge, and K. Watkins, "Imaging studies in congenital anophthalmia reveal preservation of brain architecture in 'visual' cortex," *Brain*, vol. 132, no. 12, pp. 3467–3480, 2009.

[13] J. Hyvärinen, L. Hyvärinen, and I. Linnankoski, "Modification of parietal association cortex and functional blindness after binocular deprivation in young monkeys," *Experimental Brain Research*, vol. 42, no. 1, pp. 1–8, 1981.

[14] S. J. Karlen, D. M. Kahn, and L. Krubitzer, "Early blindness results in abnormal corticocortical and thalamocortical connections," *Neuroscience*, vol. 142, no. 3, pp. 843–858, 2006.

[15] R. Kupers, A. Fumal, A. M. De Noordhout, A. Gjedde, J. Schoenen, and M. Ptito, "Transcranial magnetic stimulation of the visual cortex induces somatotopically organized qualia in blind subjects," *Proceedings of the National Academy of Sciences of the United States of America*, vol. 103, no. 35, pp. 13256–13260, 2006.

[16] T. E. J. Behrens, H. Johansen-Berg, M. W. Woolrich et al., "Non-invasive mapping of connections between human thalamus and cortex using diffusion imaging," *Nature Neuroscience*, vol. 6, no. 7, pp. 750–757, 2003.

[17] N. L. Reislev, R. Kupers, H. R. Siebner, M. Ptito, and T. B. Dyrby, "Blindness alters the microstructure of the ventral but not the dorsal visual stream," *Brain Structure and Function*, vol. 221, no. 6, pp. 2891–2903, 2016.

[18] N. L. Reislev, T. B. Dyrby, H. R. Siebner, R. Kupers, and M. Ptito, "Simultaneous assessment of white matter changes in microstructure and connectedness in the blind brain," *Neural Plasticity*, vol. 2016, Article ID 6029241, 12 pages, 2016.

[19] T. G. Reese, O. Heid, R. M. Weisskoff, and V. J. Wedeen, "Reduction of eddy-current-induced distortion in diffusion MRI using a twice-refocused spin echo," *Magnetic Resonance in Medicine*, vol. 49, no. 1, pp. 177–182, 2003.

[20] S. M. Smith, M. Jenkinson, M. W. Woolrich et al., "Advances in functional and structural MR image analysis and implementation as FSL," *NeuroImage*, vol. 23, no. 1, pp. S208–S219, 2004.

[21] M. W. Woolrich, S. Jbabdi, B. Patenaude et al., "Bayesian analysis of neuroimaging data in FSL," *NeuroImage*, vol. 45, no. 1, pp. S173–S186, 2009.

[22] M. Jenkinson, C. F. Beckmann, T. E. J. Behrens, M. W. Woolrich, and S. M. Smith, "FSL," *NeuroImage*, vol. 62, no. 2, pp. 782–790, 2012.

[23] J. L. R. Andersson, S. Skare, and J. Ashburner, "How to correct susceptibility distortions in spin-echo echo-planar images: application to diffusion tensor imaging," *NeuroImage*, vol. 20, no. 2, pp. 870–888, 2003.

[24] J. L. R. Andersson and S. N. Sotiropoulos, "An integrated approach to correction for off-resonance effects and subject movement in diffusion MR imaging," *NeuroImage*, vol. 125, pp. 1063–1078, 2015.

[25] D. C. Alexander, C. Pierpaoli, P. J. Basser, and J. C. Gee, "Spatial transformations of diffusion tensor magnetic resonance images," *IEEE Transactions on Medical Imaging*, vol. 20, no. 11, pp. 1131–1139, 2001.

[26] J. Jovicich, S. Czanner, D. Greve et al., "Reliability in multi-site structural MRI studies: effects of gradient non-linearity correction on phantom and human data," *NeuroImage*, vol. 30, no. 2, pp. 436–443, 2006.

[27] A. M. Dale, B. Fischl, and M. I. Sereno, "Cortical surface-based analysis: I. Segmentation and surface reconstruction," *NeuroImage*, vol. 9, no. 2, pp. 179–194, 1999.

[28] B. Fischl, M. I. Sereno, and A. M. Dale, "Cortical surface-based analysis: II. Inflation, flattening, and a surface-based coordinate system," *NeuroImage*, vol. 9, no. 2, pp. 195–207, 1999.

[29] M. Reuter, H. D. Rosas, and B. Fischl, "Highly accurate inverse consistent registration: a robust approach," *NeuroImage*, vol. 53, no. 4, pp. 1181–1196, 2010.

[30] R. S. Desikan, F. Ségonne, B. Fischl et al., "An automated labeling system for subdividing the human cerebral cortex on MRI scans into gyral based regions of interest," *NeuroImage*, vol. 31, no. 3, pp. 968–980, 2006.

[31] N. Tzourio-Mazoyer, B. Landeau, D. Papathanassiou et al., "Automated anatomical labeling of activations in SPM using a macroscopic anatomical parcellation of the MNI MRI single-subject brain," *NeuroImage*, vol. 15, no. 1, pp. 273–289, 2002.

[32] M. Jenkinson and S. Smith, "A global optimisation method for robust affine registration of brain images," *Medical Image Analysis*, vol. 5, no. 2, pp. 143–156, 2001.

[33] M. Jenkinson, P. Bannister, M. Brady, and S. Smith, "Improved optimization for the robust and accurate linear registration and motion correction of brain images," *NeuroImage*, vol. 17, no. 2, pp. 825–841, 2002.

[34] T. E. J. Behrens, M. W. Woolrich, M. Jenkinson et al., "Characterization and propagation of uncertainty in diffusion-weighted MR imaging," *Magnetic Resonance in Medicine*, vol. 50, no. 5, pp. 1077–1088, 2003.

[35] T. E. J. Behrens, H. J. Berg, S. Jbabdi, M. F. S. Rushworth, and M. W. Woolrich, "Probabilistic diffusion tractography with multiple fibre orientations: what can we gain?" *NeuroImage*, vol. 34, no. 1, pp. 144–155, 2007.

[36] N. Shu, Y. Liu, J. Li, Y. Li, C. Yu, and T. Jiang, "Altered anatomical network in early blindness revealed by diffusion tensor tractography," *PLoS ONE*, vol. 4, no. 9, Article ID e7228, 2009.

[37] D. Wang, W. Qin, Y. Liu, Y. Zhang, T. Jiang, and C. Yu, "Altered white matter integrity in the congenital and late blind people," *Neural Plasticity*, vol. 2013, Article ID 128236, 8 pages, 2013.

[38] R. Kupers and M. Ptito, "Compensatory plasticity and cross-modal reorganization following early visual deprivation," *Neuroscience and Biobehavioral Reviews*, vol. 41, pp. 36–52, 2014.

[39] L. K. Laemle, N. L. Strominger, and D. O. Carpenter, "Cross-modal innervation of primary visual cortex by auditory fibers in congenitally anophthalmic mice," *Neuroscience Letters*, vol. 396, no. 2, pp. 108–112, 2006.

[40] M. Ptito, J.-F. Giguère, D. Boire, D. O. Frost, and C. Casanova, "When the auditory cortex turns visual," *Progress in Brain Research*, vol. 134, pp. 447–458, 2001.

[41] S. Desgent and M. Ptito, "Cortical GABAergic interneurons in cross-modal plasticity following early blindness," *Neural Plasticity*, vol. 2012, Article ID 590725, 20 pages, 2012.

[42] D. Boire, H. Théoret, and M. Ptito, "Visual pathways following cerebral hemispherectomy," *Progress in Brain Research*, vol. 134, pp. 379–397, 2001.

[43] M. Ptito, M. Herbin, D. Boire, and A. Ptito, "Neural bases of residual vision in hemicorticectomized monkeys," *Progress in Brain Research*, vol. 112, pp. 385–404, 1996.

[44] C. Klinge, F. Eippert, B. Röder, and C. Büchel, "Corticocortical connections mediate primary visual cortex responses to auditory stimulation in the blind," *Journal of Neuroscience*, vol. 30, no. 38, pp. 12798–12805, 2010.

[45] G. F. Wittenberg, K. J. Werhahn, E. M. Wassermann, P. Herscovitch, and L. G. Cohen, "Functional connectivity between somatosensory and visual cortex in early blind humans," *European Journal of Neuroscience*, vol. 20, no. 7, pp. 1923–1927, 2004.

[46] S. N. Jespersen, H. Lundell, C. K. Sønderby, and T. B. Dyrby, "Orientationally invariant metrics of apparent compartment eccentricity from double pulsed field gradient diffusion experiments," *NMR in Biomedicine*, vol. 26, no. 12, pp. 1647–1662, 2013.

[47] S. B. Vos, D. K. Jones, B. Jeurissen, M. A. Viergever, and A. Leemans, "The influence of complex white matter architecture on the mean diffusivity in diffusion tensor MRI of the human brain," *NeuroImage*, vol. 59, no. 3, pp. 2208–2216, 2012.

[48] H. Johansen-Berg, T. E. J. Behrens, E. Sillery et al., "Functional-anatomical validation and individual variation of diffusion tractography-based segmentation of the human thalamus," *Cerebral Cortex*, vol. 15, no. 1, pp. 31–39, 2005.

[49] D. Zhang, A. Z. Snyder, J. S. Shimony, M. D. Fox, and M. E. Raichle, "Noninvasive functional and structural connectivity mapping of the human thalamocortical system," *Cerebral Cortex*, vol. 20, no. 5, pp. 1187–1194, 2010.

[50] T. B. Dyrby, L. V. Søgaard, G. J. Parker et al., "Validation of in vitro probabilistic tractography," *NeuroImage*, vol. 37, no. 4, pp. 1267–1277, 2007.

[51] C. Thomas, F. Q. Ye, M. O. Irfanoglu et al., "Anatomical accuracy of brain connections derived from diffusion MRI tractography is inherently limited," *Proceedings of the National Academy of Sciences of the United States of America*, vol. 111, no. 46, pp. 16574–16579, 2014.

[52] G. M. Innocenti, T. B. Dyrby, K. W. Andersen, E. M. Rouiller, and R. Caminiti, "The crossed projection to the striatum in two species of monkey and in humans: behavioral and evolutionary significance," *Cerebral Cortex*, 2016.

[53] J. Hau, S. Sarubbo, J. C. Houde et al., "Revisiting the human uncinate fasciculus, its subcomponents and asymmetries with stem-based tractography and microdissection validation," *Brain Structure and Function*, 2016.

Hindawi
Neural Plasticity
Volume 2017, Article ID 4780876, 7 pages
https://doi.org/10.1155/2017/4780876

Research Article

Aerobic Exercise Effects on Ocular Dominance Plasticity with a Phase Combination Task in Human Adults

Jiawei Zhou,[1,2] Alexandre Reynaud,[2] and Robert F. Hess[2]

[1]*School of Ophthalmology and Optometry and Eye Hospital, Wenzhou Medical University, Wenzhou, Zhejiang 325003, China*
[2]*McGill Vision Research, Department of Ophthalmology, McGill University, Montreal, QC, Canada H3A 1A1*

Correspondence should be addressed to Jiawei Zhou; zhoujw@mail.eye.ac.cn

Received 22 September 2016; Revised 24 January 2017; Accepted 7 February 2017; Published 5 March 2017

Academic Editor: Clive R. Bramham

Several studies have shown that short-term monocular patching can induce ocular dominance plasticity in normal adults, in which the patched eye becomes stronger in binocular viewing. There is a recent study showing that exercise enhances this plasticity effect when assessed with binocular rivalry. We address one question, is this enhancement from exercise a general effect such that it is seen for measures of binocular processing other than that revealed using binocular rivalry? Using a binocular phase combination task in which we directly measure each eye's contribution to the binocularly fused percept, we show no additional effect of exercise after short-term monocular occlusion and argue that the enhancement of ocular dominance plasticity from exercise could not be demonstrated with our approach.

1. Introduction

There is ample evidence that the adult brain retains a degree of neural plasticity [1, 2]. In terms of the visual cortex this has been shown in studies on perceptual learning [3–6], noninvasive brain stimulation [7–9], and short-term monocular deprivation [10–14]. Since residual plasticity could be harnessed for therapeutic benefit, it is of interest to know how best to enhance it. A number of rodent models have shown enhancement effects from pharmacological and environmental manipulations. These include the role of donepezil, a centrally acting reversible acetylcholinesterase inhibitor [15], and fluoxetine, a selective serotonin-reuptake inhibitor [16]. Also "environmental enrichment" has been identified as an important factor [17, 18]. This encompasses enhanced motor, sensory, and social activity, of which the motor activity has been assumed to be primal [19]. This is consistent with the finding that visual cortical sensitivity in rodents can be enhanced during motor activity [20] and therefore it has been argued that such enhancement might lead to stronger activity-dependent plasticity [19]. The relationship between visual plasticity and physical activity in rodents is concordant with the generally accepted view that physical activity is beneficial to human adult brain function in general, particularly prefrontal and hippocampal regions [21]. However, it is unclear whether physical activity promotes plasticity in the human visual cortex and in particular the striate cortex, the focus of the present study.

One interesting index of brain plasticity in adult humans is short-term ocular dominance plasticity. This involves the short-term changes that occur in ocular dominance during 2.5 hours of monocular deprivation [10]. This deprivation can be initiated by an opaque patch, a translucent patch [10, 12], or a spatially filtered dichoptic movie [22]. The resultant change in ocular dominance, which is seen in the cellular changes within ocular dominance columns in striate cortex using intrinsic optical imaging [23], is such that the contribution of the previously patched eye to the binocular percept is strengthened while the contribution of the unpatched eye is weakened. Since these neuroplastic effects are reflected through the use of either fusible stimuli, by examining the relative left/right eye contribution to the binocular percept [12, 22, 24], or nonfusible stimuli, by examining the relative left/right eye contributions to binocular rivalry [10, 11, 25], it has been argued that the underlying mechanisms may involve inhibitory interactions at a site before binocular combination

[26]. Pertinent to the current debate as to whether physical activity can promote visual cortical plasticity in human adults, a recent study [27] reported that intermittent periods of cycling exercise undertaken during a 2-hour period of monocular patching result in a greater change in ocular dominance, reflecting activity-dependent neuroplasticity. Since this is the first indication that physical activity modulates visual plasticity in the human adult, we wanted to see whether the effects could be generalized to other tasks that would be expected to reflect the same neuroplastic modulation of ocular dominance.

The demonstration [27] of enhanced plasticity as a result of physical activity was shown using a binocular rivalry paradigm, which is one of the two methods that have been used in recent years to quantify ocular dominance plasticity in adult humans. The other approach [12, 22, 24] has involved the use of fusible stimuli by measuring the contribution that each eye makes to the binocularly fused percept and how this eye balance is perturbed by short-term monocular deprivation. Here we use this latter approach to assess what contribution physical activity makes to the neuroplastic modulation of ocular dominance. We use a comparable protocol to that previously reported by Lunghi and Sale [27], in terms of the type of exercise and how it is administered during the 2 hours of monocular occlusion. We assess neuroplastic effects for two levels of exercise in an attempt to define a dose-dependent response. We show no beneficial effect of exercise on ocular dominance plasticity using our binocular combination paradigm for either level of aerobic exercise.

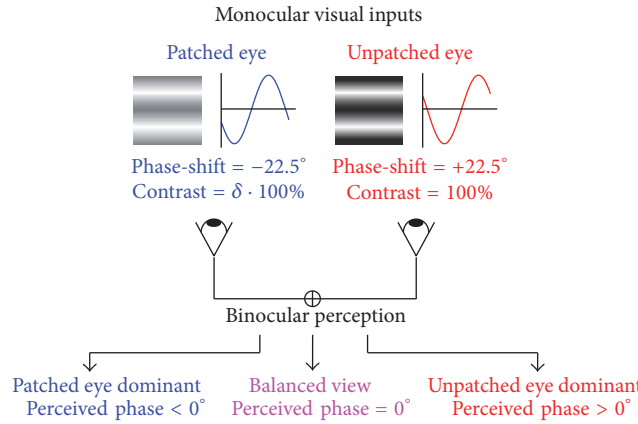

Figure 1: The binocular phase combination paradigm. As illustrated in the figure, two horizontal sine-wave gratings with equal and opposite phase-shift of 22.5° relative to the centre screen were dichoptically presented to the two eyes, and the binocular perceived phase would be 0° when the two eyes are balanced. In our study, we set the phase-shift of the grating to −22.5° in the patched eye and to 22.5° in the unpatched eye. After patching, if the patched eye became stronger, the binocularly perceived phase would be more minus; otherwise, if the patched eye became weaker, the binocularly perceived phase would be more positive.

2. Methods

2.1. Participants. Ten normal adults (mean age: 30.2 ± 1.6 years old; 3 females) with normal or corrected to normal vision participated in this study. Except the first and second authors, all subjects were naive to the purpose of this study. Observers wore their normal optical correction if required. A written informed consent was obtained from each of them before the start of the test. This study complied with the Declaration of Helsinki and was approved by the Institutional Review Boards of Wenzhou Medical University and McGill University. The methods were carried out in accordance with the approved guidelines.

2.2. Apparatus. Interocular sensory balance measurements were conducted on a Mac computer using Matlab and PsychToolBox 3.0.9 extensions. The stimuli were dichoptically presented by head mount goggles (eMagin Z800 pro, OLED), with a refresh rate of 60 Hz and a resolution of 800 × 600 in each eye. The mean luminance of OLED goggles was 160 cd/m^2.

Heartbeat was measured with a Polar H7 heart rate sensor, monitored online, and recorded with the Polar Beat 1.5.2 application running on an Apple iPod Touch G6.

2.3. Design. For each observer, the dominant eye was chosen for short-term deprivation. In particular, the dominant eye was deprived by covering with a translucent patch, which transmits light with 80% light transmission but no pattern transmission. The effects of 2-hour monocular patching were accessed by measuring observers' sensory eye dominance before and after the patching period. Three 2-hour patching conditions were studied, which were as follows: (1) resting condition: while the dominant eye was patched, observers were asked to sit quietly to watch a movie; (2) moderate cycling condition: while the dominant eye was patched, observers were asked to watch a movie and do 10 minutes of cycling every 20 minutes. During each 10-minute cycling period, participants were asked to adjust their cycling efforts in order to reach a target heart rate of 60% of their estimated maximum age-related heart rate, calculated as 220 minus the age of the participants, in beats per minute [28]; and (3) hard cycling condition: it is the same as the moderate cycling condition, but with a higher target heart rate (80% of their estimated maximum age-related heart rate).

These three conditions were conducted in a randomized order between subjects on three different days. For each day, observers' ocular dominance was tested before the patching and at 0′, 5′, 10′, 15′, 30′, and 45′ after the completion of the 2 hours of patching. Each test session lasted about 3 minutes.

2.4. Procedures. The change of sensory eye dominance was quantified by a binocular phase combination task, identical to that used previously [12, 24], in which the binocular perceived phase was measured and used as an index of sensory eye dominance. As shown in Figure 1, two horizontal sine-wave gratings (0.3 cycle/°, 6.6° × 6.6°) with equal and opposite phase-shift of 22.5° relative to the centre screen were dichoptically presented to the two eyes; if the patched eye

became stronger, the binocularly perceived phase would be more minus; otherwise, if the patched eye became weaker, the binocularly perceived phase would be more positive. For each subject, the contrast of stimuli of their nondominant eye was set as 100% and the contrast of stimuli of their dominant eye was set so that there was equal contribution from each eye to the binocularly fused image (binocularly perceived phase = zero) before the patching. The procedure for measuring perceived phase was similar to that reported in previous studies [29], in which observers were asked to adjust the vertical position of a 1-pixel reference line to indicate the perceived phase of the binocularly perceived horizontal grating, defined by the location of the centre of the dark bar of the grating.

3. Results and Discussion

In Figure 2, the results of moderate exercise on the effects of short-term ocular dominance plasticity are summarized. Ocular dominance is measured using our binocular phase combination task as explained in Methods. Changes in dominance are plotted relative to baseline measurements; a shift in the negative direction indicates that the previously patched eye is more dominant. The at-rest results (Figure 2(c)) for a group of healthy young observers (age 30.20 ± 1.55 years) are displayed in black with open circles. The plasticity of ocular dominance is seen to last for about 30 minutes after removal of the monocular occluder; this is consistent with all our previous studies [12, 22]. The exercise involved cycling on an exercise bike for 10-minute periods every 20 minutes during the deprivation period. Subjects watched a movie of their choice for the 2-hour period during which they were monocularly deprived. The exercise was designed to increase the heart rate by around 60% of its estimated maximum age-related heart rate. The heart rate was monitored and the average heart rates before and after exercise are shown in Figure 2(b). Subjects found this degree of exercise significant but manageable. The results showing the effect of exercise on ocular dominance plasticity are plotted in blue with open square symbols. No significant effect of exercise was found compared to the at-rest baseline. A repeated-measures within-subject Analysis of Variance (ANOVA) also showed that the perceived phase change was significantly varied by time ($F(5, 45) = 10.16$, $p < 0.001$), but not significantly different between the exercise and no exercise conditions ($F(1, 9) = 0.21$, $p = 0.66$); the interaction of these two factors was also not significant ($F(5, 45) = 0.39$, $p = 0.85$). In Figure 2(d), the computed areal change (degrees × minutes) is compared for each subject at rest and after exercise. The average ratio between the areal change at the moderate condition and that at the rest condition was 0.981 ± 0.856 (mean ± SD), which was not significantly different with 1: $t(9) = -0.07$, $p = 0.95$ (2-tailed one sample t-test).

In Figure 3, results are shown for the same protocol repeated but where the exercise was more strenuous. Now the exercise was increased so that the heart rate was increased by around 80% of its estimated maximum age-related heart rate (Figure 3(b)). Subjects considered this a demanding exercise routine. Ocular dominance plasticity measured before and after this heavier exercise is shown in Figure 3(c) as black lines/open circles and red lines/filled squares, respectively. No influence of exercise on ocular dominance plasticity was observed. A repeated-measures within-subject ANOVA also showed that the perceived phase change was significantly varied by time ($F(5, 45) = 8.01$, $p < 0.001$), but not significantly different between the exercise and no exercise conditions ($F(1, 9) = 0.21$, $p = 0.66$); the interaction of these two factors was also not significant ($F(5, 45) = 0.71$, $p = 0.62$). In Figure 3(d), the computed areal change (degrees × minutes) is compared for each subject at rest and after exercise. The average ratio between the areal change at the hard condition and that at the rest condition was 1.383 ± 1.144 (mean ± SD), which was not significantly different with 1: $t(9) = 1.06$, $p = 0.32$ (2-tailed one sample t-test).

When one eye is deprived of spatial contrast for a period of around 2 hours, there is an observable change in ocular dominance that lasts for about 30 minutes. The previously deprived eye becomes more dominant and the nondeprived eye becomes less dominant. Originally this was demonstrated using binocular rivalry as an index of ocular dominance [10] and later shown using fusible stimuli, by determining the relative left/right eye contribution to the binocularly fused percept [12, 22].

The recent report that exercise enhances this plasticity effect when assessed with binocular rivalry [27] is not generalized to the use of fusible stimuli used in the present study. It is unclear why such an exercise enhancement would not be reflected in our measurements. There are two obvious possibilities; the first is that the approach we use lacks sensitivity, and the second is that our sample size is too small. Concerning the first issue, the approach we use has been shown to be sensitive in that it can reveal much smaller changes in dominance produced by much subtler forms of deprivation that achieved by translucent occlusion. These subtle changes in dominance are the result of monocular spatial filtering of dichoptically presented videos [22]. It is unlikely to be due to ceiling effects (i.e., saturation), as we have previously shown [24], using the same technique, that both the magnitude and the duration of the dominance change can be larger in some humans with amblyopia. Concerning the sample size, it should be pointed out that any trends we find from exercise are in the opposite direction, so we would have to assume that all our subjects were outliers to entertain an explanation based on sample size. Another way of addressing this issue is to calculate, from the effect size previously reported by Lunghi and Sale [27] using binocular rivalry, given our measurement variance, how many subjects we should need to achieve a power greater than 80%. The areal analysis shown in panel (d) of Figures 2 and 3 allows a comparison with Lunghi and Sale's [27] results (see Supplemental Information for full analysis in Supplementary Material available online at https://doi.org/10.1155/2017/4780876). For our moderate exercise conditions we calculate that only the results from 2 subjects should be sufficient and for the hard exercise condition only 3 subjects are necessary. The 10 subjects we tested should certainly have been sufficient. A remaining possibility is that these two methods (binocular rivalry and binocular combination) reflect very different neural

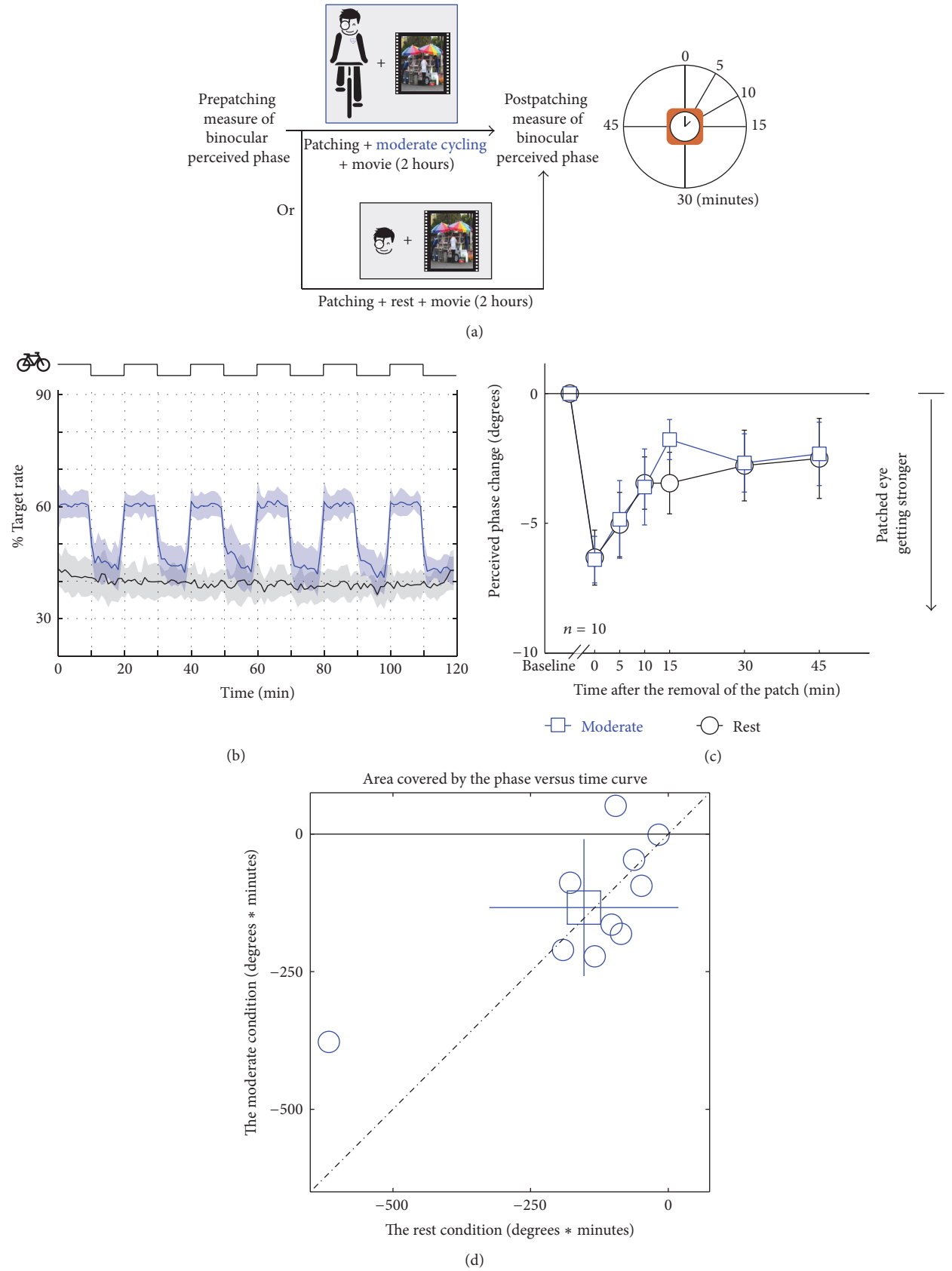

Figure 2: Illustration of the protocol for assessing the effect of moderate exercise on ocular dominance plasticity as a result of short-term monocular deprivation. Subjects ($n = 10$) are monocularly patched while cycling (10 min cycling, 10 min rest) and watching a movie for 2 hours (a). The exercise was intended to raise the heat rate by around 60% of its estimated maximum age-related heart rate (b). The change in ocular dominance as a result of the monocular deprivation is compared for the baseline (resting condition: black lines and open circles) and the exercise condition (blue lines and open squares) (c). The computed areal change (degrees × minutes) is compared for each subject at rest and after exercise; the open square symbol is the group mean ± SD (d).

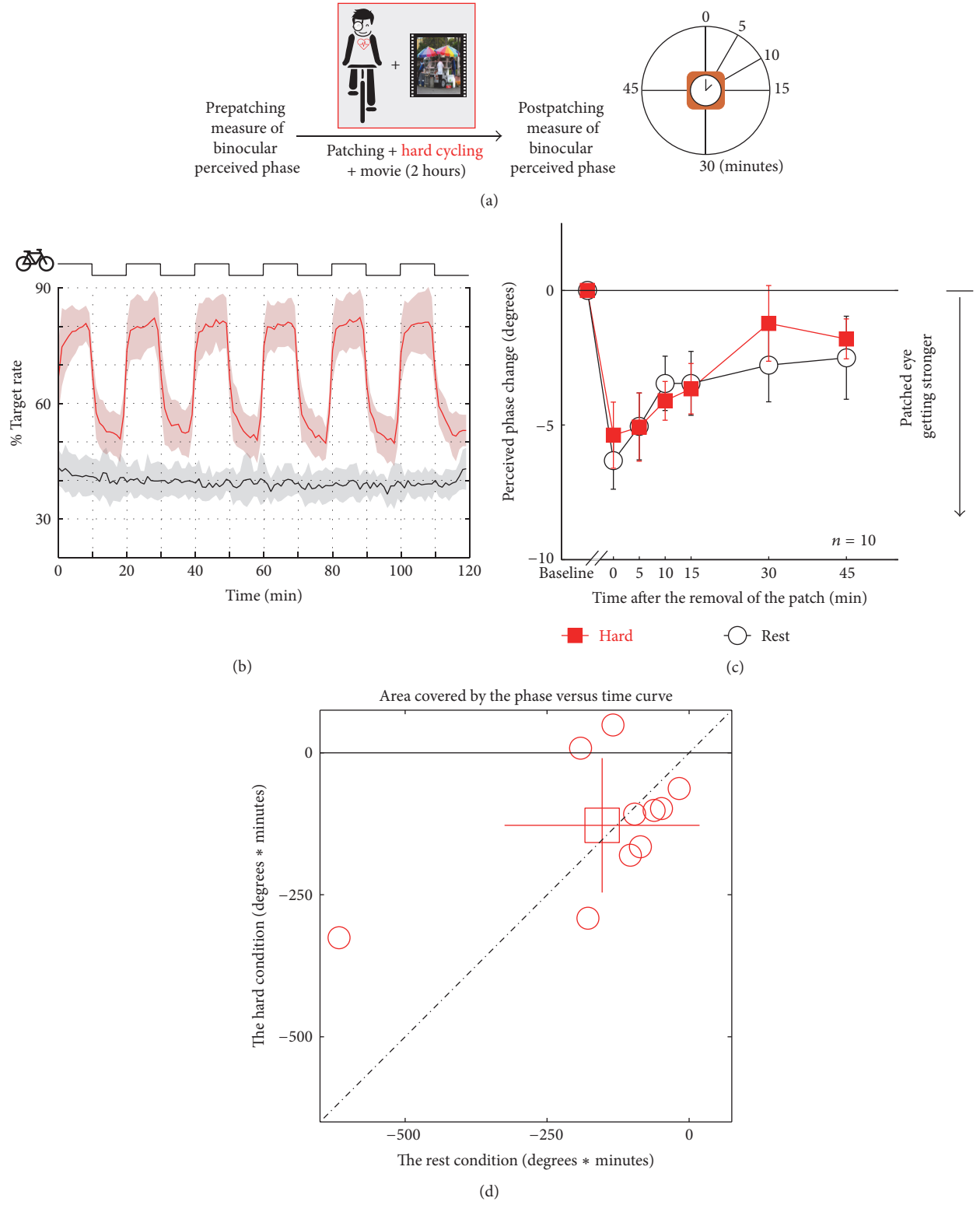

FIGURE 3: Illustration of the protocol for assessing the effect of severe exercise on ocular dominance plasticity as a result of short-term monocular deprivation. Subjects ($n = 10$) are monocularly patched while cycling (10 min cycling, 10 min rest) and watching a movie for 2 hours (a). The exercise raises the heat rate by around 80% of its estimated maximum age-related heart rate (b). The change in ocular dominance as a result of the monocular deprivation is compared for the baseline (resting condition: black lines/open circles) and exercise condition (red lines/filled squares) (c). The computed areal change (degrees × minutes) is compared for each subject at rest and after exercise; the open square symbol is the group mean ± SD (d).

processes. The approach that we have taken involves the direct estimation of each eye's contribution to the binocularly fused percept. It can be modeled in terms of the standard contrast-gain control model [30] that describes the excitatory and inhibitory interactions that are limited to the striate cortex/LGN circuit [31, 32]. Binocular rivalry arises from the competition between neurons in the LGN and in V1 [33–36] and reflects amongst other things the contralateral inhibitory interactions that are known to occur prior to binocular combination. Its neural circuitry extends well beyond the striate visual cortex as it is contour dependent and potentially involves neural competition at multiple levels of the visual pathways beyond the striate cortex [25, 37, 38]. Neural correlates of the perceptual fluctuations have been found in the parietal cortex and the frontal cortex [38, 39], which explains the high susceptibility of binocular rivalry to attention [40]. It is possible, based on the known effects of exercise on prefrontal and hippocampal regions [21], that the exercise-dependent effects for binocular rivalry could involve a top-down influence of a more general, nonvisual nature [41]. All that we can say at the moment is that the enhancement of dominance plasticity due to excise is not reflected in all measures.

4. Conclusions

We conclude that any effects of exercise on ocular dominance plasticity are not revealed using our binocular combination approach.

Competing Interests

The authors declare that there is no conflict of interests regarding the publication of this paper.

Authors' Contributions

Jiawei Zhou and Alexandre Reynaud equally contributed.

Acknowledgments

This work was supported by the National Natural Science Foundation of China Grant NSFC 81500754 and the Wenzhou Medical University Grant QTJ16005 to Jiawei Zhou and the Canadian Institutes of Health Research Grants MOP-53346, CCI-125686, and MT-10818, an ERA-NET NEURON Grant (JTC 2015), and FRQS Vision Health Research Network of Quebec Networking Grant to Robert F. Hess.

References

[1] H.-Y. He, B. Ray, K. Dennis, and E. M. Quinlan, "Experience-dependent recovery of vision following chronic deprivation amblyopia," *Nature Neuroscience*, vol. 10, no. 9, pp. 1134–1136, 2007.

[2] A. Harauzov, M. Spolidoro, G. DiCristo et al., "Reducing intracortical inhibition in the adult visual cortex promotes ocular dominance plasticity," *Journal of Neuroscience*, vol. 30, no. 1, pp. 361–371, 2010.

[3] R. W. Li, C. Ngo, J. Nguyen, and D. M. Levi, "Video-game play induces plasticity in the visual system of adults with amblyopia," *PLoS Biology*, vol. 9, no. 8, Article ID e1001135, 2011.

[4] J. Zhou, Y. Zhang, Y. Dai et al., "The eye limits the brain's learning potential," *Scientific Reports*, vol. 2, 2012.

[5] J. Li, B. Thompson, D. Deng, L. Y. L. Chan, M. Yu, and R. F. Hess, "Dichoptic training enables the adult amblyopic brain to learn," *Current Biology*, vol. 23, no. 8, pp. R308–R309, 2013.

[6] Z. Ren, J. Zhou, Z. Yao et al., "Neuronal basis of perceptual learning in striate cortex," *Scientific Reports*, vol. 6, 2016.

[7] B. Thompson, B. Mansouri, L. Koski, and R. F. Hess, "Brain plasticity in the adult: modulation of function in amblyopia with rTMS," *Current Biology*, vol. 18, no. 14, pp. 1067–1071, 2008.

[8] S. Clavagnier, B. Thompson, and R. F. Hess, "Long lasting effects of daily theta burst rTMS sessions in the human amblyopic cortex," *Brain Stimulation*, vol. 6, no. 6, pp. 860–867, 2013.

[9] D. P. Spiegel, W. D. Byblow, R. F. Hess, and B. Thompson, "Anodal transcranial direct current stimulation transiently improves contrast sensitivity and normalizes visual cortex activation in individuals with amblyopia," *Neurorehabilitation and Neural Repair*, vol. 27, no. 8, pp. 760–769, 2013.

[10] C. Lunghi, D. C. Burr, and C. Morrone, "Brief periods of monocular deprivation disrupt ocular balance in human adult visual cortex," *Current Biology*, vol. 21, no. 14, pp. R538–R539, 2011.

[11] C. Lunghi, D. C. Burr, and M. C. Morrone, "Long-term effects of monocular deprivation revealed with binocular rivalry gratings modulated in luminance and in color," *Journal of Vision*, vol. 13, no. 6, article 1, 2013.

[12] J. Zhou, S. Clavagnier, and R. F. Hess, "Short-term monocular deprivation strengthens the patched eye's contribution to binocular combination," *Journal of Vision*, vol. 13, no. 5, article 12, 2013.

[13] C. Lunghi, M. Berchicci, M. C. Morrone, and F. Di Russo, "Short-term monocular deprivation alters early components of visual evoked potentials," *Journal of Physiology*, vol. 593, no. 19, pp. 4361–4372, 2015.

[14] J. Zhou, D. H. Baker, M. Simard, D. Saint-Amour, and R. F. Hess, "Short-term monocular patching boosts the patched eye's response in visual cortex," *Restorative Neurology and Neuroscience*, vol. 33, no. 3, pp. 381–387, 2015.

[15] J. I. Kang, F. Huppé-Gourgues, and E. Vaucher, "Boosting visual cortex function and plasticity with acetylcholine to enhance visual perception," *Frontiers in Systems Neuroscience*, vol. 8, article 172, 2014.

[16] J. F. Maya Vetencourt, A. Sale, A. Viegi et al., "The antidepressant fluoxetine restores plasticity in the adult visual cortex," *Science*, vol. 320, no. 5874, pp. 385–388, 2008.

[17] A. Sale, J. F. Maya Vetencourt, P. Medini et al., "Environmental enrichment in adulthood promotes amblyopia recovery through a reduction of intracortical inhibition," *Nature Neuroscience*, vol. 10, no. 6, pp. 679–681, 2007.

[18] L. Baroncelli, J. Bonaccorsi, M. Milanese et al., "Enriched experience and recovery from amblyopia in adult rats: impact of motor, social and sensory components," *Neuropharmacology*, vol. 62, no. 7, pp. 2388–2397, 2012.

[19] A. Sale, N. Berardi, and L. Maffei, "Environment and brain plasticity: towards an endogenous pharmacotherapy," *Physiological Reviews*, vol. 94, no. 1, pp. 189–234, 2014.

[20] M. Kaneko and M. P. Stryker, "Sensory experience during locomotion promotes recovery of function in adult visual cortex," *eLife*, vol. 3, Article ID e02798, 2014.

[21] K. I. Erickson, A. G. Gildengers, and M. A. Butters, "Physical activity and brain plasticity in late adulthood," *Dialogues in Clinical Neuroscience*, vol. 15, no. 1, pp. 99–108, 2013.

[22] J. Zhou, A. Reynaud, and R. F. Hess, "Real-time modulation of perceptual eye dominance in humans," *Proceedings of the Royal Society B: Biological Sciences*, vol. 281, no. 1795, Article ID 20141717, 2014.

[23] D. Y. Ts'o, M. Begum, and B. T. Backus, *Short-Term Monocular Deprivation Disrupts Interocular Balance in Adult Macaque Visual Cortex*, Society for Neuroscience, Chicago, Ill, USA, 2014.

[24] J. Zhou, B. Thompson, and R. F. Hess, "A new form of rapid binocular plasticity in adult with amblyopia," *Scientific Reports*, vol. 3, Article ID 2638, 2013.

[25] C. Lunghi, U. E. Emir, M. C. Morrone, and H. Bridge, "Short-Term monocular deprivation alters GABA in the adult human visual cortex," *Current Biology*, vol. 25, no. 11, pp. 1496–1501, 2015.

[26] E. Chadnova, A. Reynaud, S. Clavagnier, S. Baillet, and R. Hess, "Short-term ocular dominance changes in human V1," *Journal of Vision*, vol. 15, no. 12, p. 378, 2015.

[27] C. Lunghi and A. Sale, "A cycling lane for brain rewiring," *Current Biology*, vol. 25, no. 23, pp. R1122–R1123, 2015.

[28] S. M. Fox III, J. P. Naughton, and W. L. Haskell, "Physical activity and the prevention of coronary heart disease," *Annals of Clinical Research*, vol. 3, no. 6, pp. 404–432, 1971.

[29] J. Zhou, P.-C. Huang, and R. F. Hess, "Interocular suppression in amblyopia for global orientation processing," *Journal of Vision*, vol. 13, no. 5, article 19, 2013.

[30] J. Ding and G. Sperling, "A gain-control theory of binocular combination," *Proceedings of the National Academy of Sciences of the United States of America*, vol. 103, no. 4, pp. 1141–1146, 2006.

[31] A. M. Truchard, I. Ohzawa, and R. D. Freeman, "Contrast gain control in the visual cortex: monocular versus binocular mechanisms," *The Journal of Neuroscience*, vol. 20, no. 8, pp. 3017–3032, 2000.

[32] C.-B. Huang, J. Zhou, Y. Zhou, and Z.-L. Lu, "Contrast and phase combination in binocular vision," *PLoS ONE*, vol. 5, no. 12, Article ID e15075, 2010.

[33] F. Sengpiel, C. Blakemore, and R. Harrad, "Interocular suppression in the primary visual cortex: a possible neural basis of binocular rivalry," *Vision Research*, vol. 35, no. 2, pp. 179–195, 1995.

[34] A. Polonsky, R. Blake, J. Braun, and D. J. Heeger, "Neuronal activity in human primary visual cortex correlates with perception during binocular rivalry," *Nature Neuroscience*, vol. 3, no. 11, pp. 1153–1159, 2000.

[35] J.-D. Haynes, R. Deichmann, and G. Rees, "Eye-specific effects of binocular rivalry in the human lateral geniculate nucleus," *Nature*, vol. 438, no. 7067, pp. 496–499, 2005.

[36] J.-D. Haynes and G. Rees, "Predicting the stream of consciousness from activity in human visual cortex," *Current Biology*, vol. 15, no. 14, pp. 1301–1307, 2005.

[37] D. A. Leopold and N. K. Logothetis, "Activity changes in early visual cortex reflect monkeys' percepts during binocular rivalry," *Nature*, vol. 379, no. 6565, pp. 549–553, 1996.

[38] E. D. Lumer, K. J. Friston, and G. Rees, "Neural correlates of perceptual rivalry in the human brain," *Science*, vol. 280, no. 5371, pp. 1930–1934, 1998.

[39] E. D. Lumer and G. Rees, "Covariation of activity in visual and prefrontal cortex associated with subjective visual perception," *Proceedings of the National Academy of Sciences of the United States of America*, vol. 96, no. 4, pp. 1669–1673, 1999.

[40] S.-H. Lee, R. Blake, and D. J. Heeger, "Hierarchy of cortical responses underlying binocular rivalry," *Nature Neuroscience*, vol. 10, no. 8, pp. 1048–1054, 2007.

[41] C. D. Gilbert and M. Sigman, "Brain states: top-down influences in sensory processing," *Neuron*, vol. 54, no. 5, pp. 677–696, 2007.

Hindawi
Neural Plasticity
Volume 2017, Article ID 1432037, 9 pages
https://doi.org/10.1155/2017/1432037

Research Article

Effect of Illumination on Ocular Status Modifications Induced by Short-Term 3D TV Viewing

Yuanyuan Chen, Yuwen Wang, Xinping Yu, Aiqin Xu, Jian Jiang, and Hao Chen

The Affiliated Eye Hospital of Wenzhou Medical University, Wenzhou, Zhejiang 325000, China

Correspondence should be addressed to Hao Chen; chenhao@mail.eye.ac.cn

Received 24 October 2016; Revised 22 December 2016; Accepted 29 January 2017; Published 27 February 2017

Academic Editor: Alexandre Reynaud

Objectives. This study aimed to compare changes in ocular status after 3D TV viewing under three modes of illumination and thereby identify optimal illumination for 3D TV viewing. *Methods.* The following measures of ocular status were assessed: the accommodative response, accommodative microfluctuation, accommodative facility, relative accommodation, gradient accommodative convergence/accommodation (AC/A) ratio, phoria, and fusional vergence. The observers watched 3D television for 90 minutes through 3D shutter glasses under three illumination modes: A, complete darkness; B, back illumination (50 lx); and C, front illumination (130 lx). The ocular status of the observers was assessed both before and after the viewing. *Results.* After 3D TV viewing, the accommodative response and accommodative microfluctuation were significantly changed under illumination Modes A and B. The near positive fusional vergence decreased significantly after the 90-minute 3D viewing session under each illumination mode, and this effect was not significantly different among the three modes. *Conclusions.* Short-term 3D viewing modified the ocular status of adults. The least amount of such change occurred with front illumination, suggesting that this type of illumination is an appropriate mode for 3D shutter TV viewing.

1. Introduction

3D TV and stereo video games have become increasingly popular in recent years. When viewing 3D TV, slightly different images with different extents of offset are dichoptically presented to both eyes and fused into one single image with depth perception.

Despite improvements in modern 3D viewing techniques, several studies have shown that prolonged exposure to 3D TV can temporally modify ocular status [1], including the conflict between accommodation and convergence while viewing stereo displays [2], a reduction in accommodation velocity [3], transient myopia [4], a reduction in pupillary movement in the near reflex [5], and microfluctuation in human adults [6], indicating some degree of visual plasticity in adults. Such ocular modifications induced by 3D TV have been suspected as a primary cause of visual discomfort [2, 7, 8].

Alternatively, there is evidence that inappropriate illumination may also cause ocular discomfort [9–11]. Appropriate illumination and image brightness of visual display terminals (VDT) may decrease discomfort from the flicker of the display [12]. However, it is unclear which commonly used illumination mode leads to the least amount of ocular status modulation when watching a 3D display in a living room. To answer this question, we assessed ocular status before and after a short-term (90 minutes) 3D viewing session with shutter glasses under three commonly used illumination modes [13, 14]: (A) complete darkness; (B) back illumination (50 lx); and (C) front illumination (130 lx). We show that a part of ocular status was significantly affected under all three illumination modes. Overall, the lowest degree of ocular modulation occurred with front illumination.

2. Materials and Methods

2.1. Participants. Thirty-two normal adults (16 females and 16 males; mean age: 23.63 ± 1.58 years) participated in the study. All the viewing observers had no history of ocular disease and had normal or corrected-to-normal visual acuity (see Table 1 for a summary of their characteristics). Informed consent was obtained from all the observers after an explanation of the

Table 1: Summary of the ocular status of observers before 3D TV viewing.

Number	Age (years)	Phoria (Δ)* (near)	Phoria (Δ)* (distance)	Refraction (spherical equivalent; diopter)
32	23.63 ± 1.58	−2.60 ± 5.05	−0.47 ± 2.21	−2.81 ± 1.43

*A positive phoria is "eso" and a negative phoria is "exo."

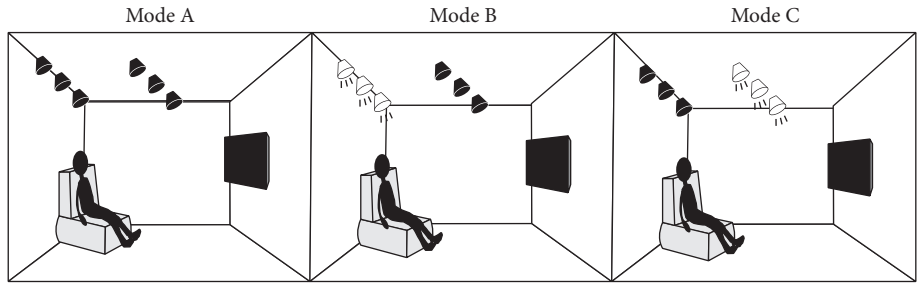

Figure 1: Illustration of our experimental environment for three illumination modes.

nature and possible risks of the study. The study followed the tenets of the Declaration of Helsinki and was approved by the Ethics Committee of the Eye Hospital of Wenzhou Medical University.

2.2. Illumination Mode. The study was conducted in an ordinary living room with white painted walls (7.5 × 3.3 m and 2.7 m high; see Figure 1 for an illustration). Observers were instructed to sit on a sofa that was located 2.5 m away from the television and watch a 3D movie using shutter glasses. Six 15-watt fluorescent lamps were mounted onto the ceiling. Each lamp could be controlled separately. Three commonly used illumination modes were studied in this experiment: *Mode A*, *Complete Darkness*, in which observers watched 3D television in complete darkness, without any source of illumination other than the television; *Mode B*, *Back Illumination*, in which only the three fluorescent lamps mounted onto the ceiling behind the viewers were turned on, and the luminance measured at the viewer's position was 50 lx; and *Mode C*, *Front Illumination*, in which only the three fluorescent lamps mounted onto the middle of the ceiling were turned on, and the luminance measured at the viewer's position was 130 lx.

2.3. Display. All visual stimuli were presented on a Samsung 3D television (Model number UA46D6000SJ, South Korea). The viewers looked at the screen through commercially available active shutter glasses, which were provided by Samsung for 3D viewing. The television had a screen size of 46 in, a screen resolution of 1920 × 1080 pixels, and a refresh rate of 200 HZ. The default settings of the television were as follows: back light 20, contrast gradient 100, brightness 100 lumens, clarity 59, chromaticity 50, and tone green 50/red 50, which resulted in a luminance of 750 cd/m^2 on the screen and 23 cd/m^2 on the glasses at a distance of 2.5 m.

2.4. Measurements. Ocular statuses, including accommodative response, accommodative microfluctuation, accommodative facility, positive and negative relative accommodation, gradient accommodative convergence/accommodation (AC/A), distant and near phoria, and positive and negative fusional vergence, were measured. These binocular visual function parameters were focused on in this study because these parameters have been widely used in previous studies of 3D TV viewing-induced visual discomfort [6, 15, 16].

The accommodative response and accommodative microfluctuation are sensitive indicators of the accommodation function. Accommodative microfluctuation represents the viability of the accommodative response and is the average amount of fluctuation in diopters around the mean accommodative response for a specified period [17]. These parameters were measured at 25 cm, 40 cm, and 6 m with an infrared autorefractor (Grand Seiko WAM-5500 autorefractor, Grand Seiko, Co., Japan) at a rate of 5 times per second [18–20].

Positive and negative relative accommodation, AC/A, and positive and negative fusional vergence were measured using a phoropter (Topcon Model IS-600, Japan). Phoria was measured at 33 cm and 6 m using the von Graefe test (with a 3-measurement average). Accommodative facility was measured with a ±2.00 diopter flipper.

2.5. Procedure. To save time and reduce the potential discomfort from ocular examinations of the observers, we assessed all the ocular status measures prior to the start of the experiment, except for the accommodative response and accommodative microfluctuation. We set these measures as previewing baselines for all three illumination modes. This arrangement also made sense according to our pilot study, in which we asked five normal healthy adults to view 3D TV on different days and assessed their ocular status before 3D viewing for each day; we found that all of the above-mentioned measures of ocular status, except for the accommodative response and accommodative microfluctuation, were stable across different time points. Since the accommodative response and accommodative microfluctuation were different with each previewing test, we measured these parameters both before and after the 3D viewing with the three illumination modes.

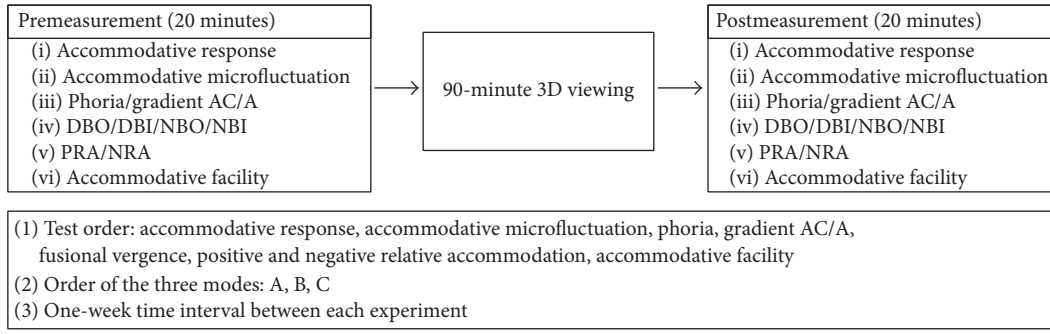

Figure 2: Illustration of our experimental sequence.

For each illumination mode session, we conducted the study in the following sequence: a premeasurement of the accommodative response and accommodative microfluctuation of the observers; a 20-minute break; a 90-minute 3D TV viewing session; and postmeasurement of the ocular status of each observer (including the accommodative response and accommodative microfluctuation as well as all the other measures mentioned above), which were measured immediately after the observers finished the 3D TV viewing session. The postmeasurement session was completed within 20 minutes for each individual. We assessed the different measures of ocular status in a fixed order in each session as follows: the accommodative response, accommodative microfluctuation, phoria, gradient AC/A, fusional vergence, relative accommodation, and then accommodative facility (Figure 2).

Three 3D movie VCDs were randomly selected for each observer, who was instructed to view the three movies under the three different illumination modes over three weeks. During the entire experiment, the TV was used with the same default settings, including brightness, contrast, color saturation, and clarity. Any other 3D display viewing was forbidden during this 3-week experimental period.

2.6. Statistical Analysis. Pre- and post-3D viewing measures were compared using a 2-tailed paired-samples t-test for each mode. The results from the three different illumination modes were compared using a three-way repeated measures ANOVA or one-way repeated measures ANOVA ($\alpha = 0.05$). All the statistical analyses were performed using the IBM SPSS version 19.0 software, SPSS (Chicago, IL, USA).

3. Results

3.1. Accommodative Response. The accommodative responses at measuring distances of 25 cm, 40 cm, and 6 m before and after 3D viewing are plotted in Figure 3 for the three illumination modes. According to Figure 3, a 90-minute 3D viewing session did not appear to greatly alter the accommodative response for the conditions we measured. A repeated measures ANOVA for each illumination mode, with the measuring distance (i.e., 25 cm, 40 cm and 6 m) and test session (pre- and post-3D viewing) as within observers factors, indicated that the accommodative response was significantly changed after 3D viewing under Mode A ($F(1,31) = 11.029$, $p = 0.002$) but not under Mode B ($F(1,31) = 0.661$, $p = 0.422$) or Mode C ($F(1,31) = 0.044$, $p = 0.836$). A further 3-way ANOVA combining the results of Mode B and Mode C revealed that the effect of 3D viewing on the accommodative response was not significantly different between Mode B and Mode C; the joint effects of test session and mode were not significant, $F(1,31) = 0.136$, $p = 0.715$. These results indicate that, regarding the accommodative response, Mode B and Mode C are superior to Mode A.

3.2. Accommodative Microfluctuation. In Figure 4, the accommodative microfluctuation at measuring distances of 25 cm, 40 cm, and 6 m before and after 3D viewing is plotted for the three illumination modes. A repeated measures ANOVA for each illumination mode, with measuring distance (i.e., 25 cm, 40 cm, and 6 m) and test session (pre- and post-3D viewing) as within observers factors, showed that the accommodative microfluctuation was significantly changed after 3D viewing under Mode A ($F(1,31) = 5.237$, $p = 0.011$) and Mode B ($F(1,31) = 4.233$, $p = 0.048$) but not under Mode C ($F(1,31) = 1.028$, $p = 0.360$). The accommodative microfluctuation displayed a trend toward an increase after 90 minutes of 3D viewing under Mode A and under Mode B at a near distance. These results indicated that the accommodative microfluctuation was most stable under Mode C.

3.3. Other Accommodative Statuses

3.3.1. Accommodative Facility. A two-tailed paired-samples t-test was conducted for the different illumination modes, which indicated no significant change in accommodative facility ($p > 0.05$) with any of the three modes. A one-way ANOVA also showed that there was no significant difference among the three modes ($F(2,93) = 0.166$, $p = 0.847$; Figure 5(a)).

3.3.2. Positive Relative Accommodation (PRA). The positive relative accommodation of the observers increased slightly after 3D viewing; however, this increase was not significant (2-tailed paired-samples t-test, $p > 0.05$). The results of the three modes were also not significantly different ($F(2,93) = 0.416$, $p = 0.661$; Figure 5(b)).

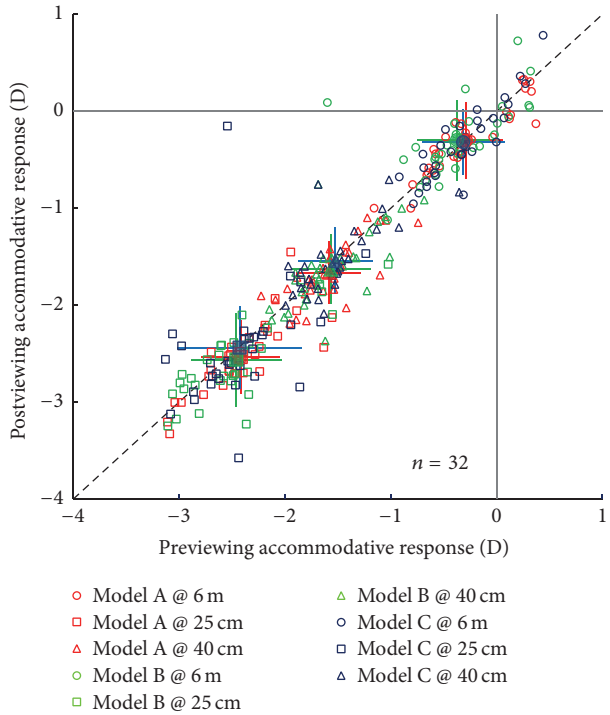

Figure 3: The effect of a 90-minute 3D viewing session on accommodative response. The postviewing accommodative responses of individuals are plotted as open points as a function of their previewing accommodative responses for the three illumination modes, which were measured at distances of 25 cm, 40 cm, and 6 m. The average values of the accommodative responses are plotted as solid points (the mean ± SD). The dashed line is the identity line ($X = Y$).

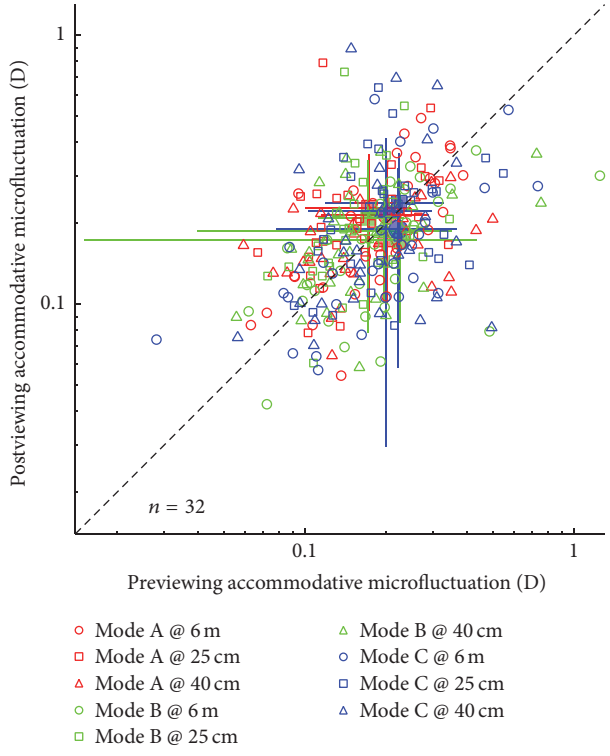

Figure 4: The effect of a 90-minute 3D viewing session on accommodative microfluctuation. The postviewing accommodative microfluctuations of individuals are plotted as open points as a function of their previewing accommodative microfluctuation measurements for the three illumination modes, which were measured at distances of 25 cm, 40 cm, and 6 m. The average values of the accommodative responses are plotted as solid points (the mean ± SD). The dashed line is the identity line ($X = Y$).

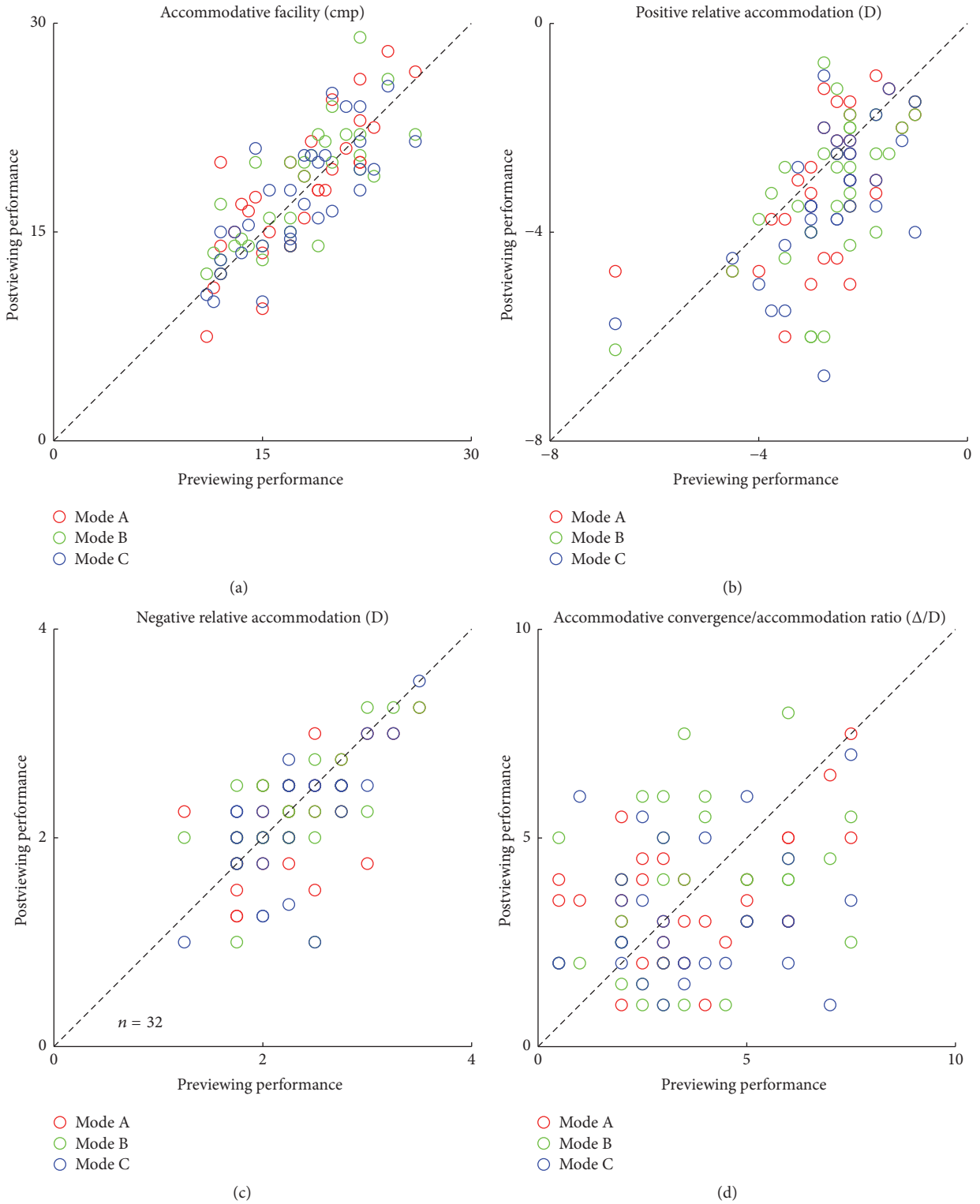

Figure 5: The effect of a 90-minute 3D viewing session on other accommodative statuses. The effect of a 90-minute 3D viewing session on accommodative facility (a), positive relative accommodation (b), negative relative accommodation (c), and the accommodative convergence/accommodation (AC/A) ratio (d). An identity line ($X = Y$) is plotted in each panel.

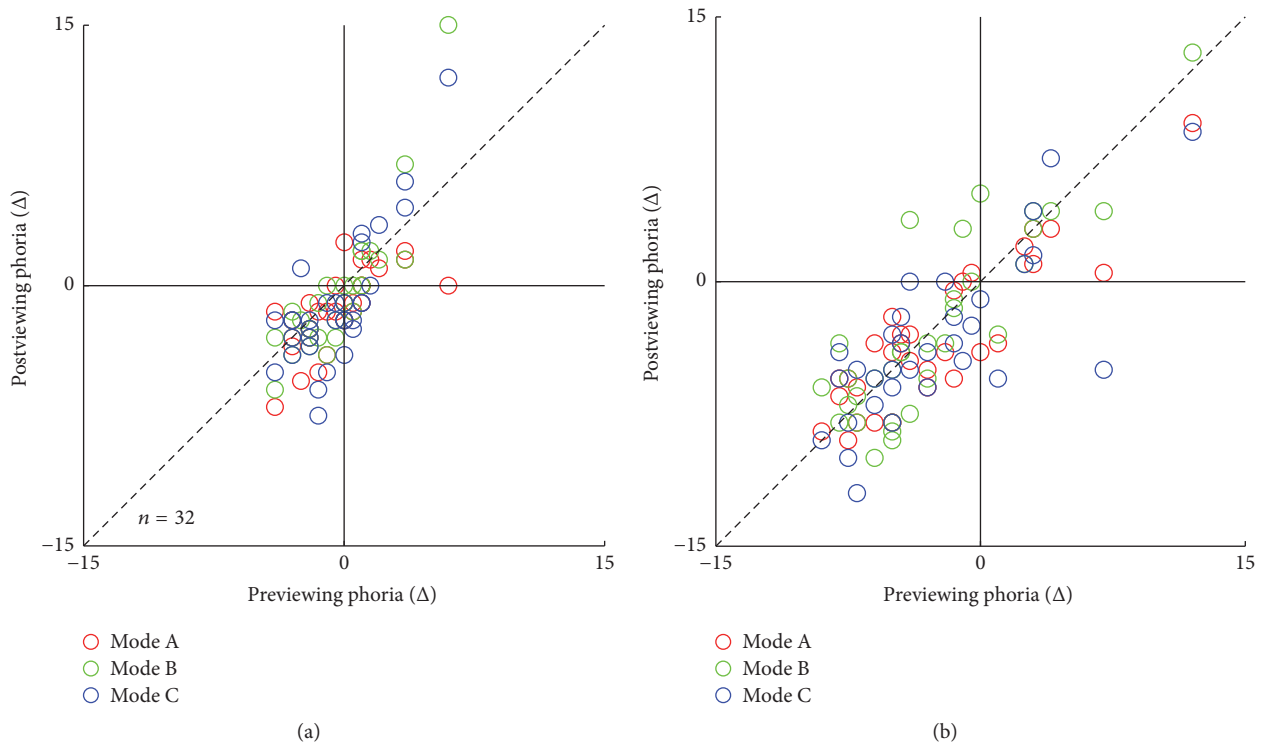

Figure 6: The effect of a 90-minute 3D viewing session on phoria. The effects of a 90-minute 3D viewing session on distance phoria (a) and near phoria (b). An identity line is plotted in each panel ($X = Y$).

3.3.3. Negative Relative Accommodation (NRA). The negative relative accommodation of the observers decreased slightly after 3D viewing; however, this decrease was not significant (2-tailed paired-samples t-test, $p > 0.05$). The results of the three modes were also not significantly different ($F(2,93) = 0.112$, $p = 0.894$; Figure 5(c)).

3.3.4. Accommodative Convergence/Accommodation Ratio (AC/A). A 90-minute 3D viewing session did not considerably alter the AC/A (2-tailed paired-samples t-test, $p > 0.05$), and no significant differences were indicated among the three modes ($F(2,93) = 1.138$, $p = 0.325$; Figure 5(d)).

3.4. Phoria. The phoria before and after a 90-minute 3D viewing session for a given measuring distance (distant: 5 m; near: 40 cm) is plotted in Figure 6 for the three illumination modes. Before 3D TV viewing, 17 observers had exophoria, while 11 observers had esophoria, and the other 4 observers were orthophoric. After 3D TV viewing, both near and distance phoria had a tendency to show more exophoria, although there was no significant difference between the phoria data before and after a 90-minute 3D viewing session ($p > 0.05$). In addition, the phoria was not significantly different among the three modes of illumination (distance: $F(2,93) = 0.442$, $p = 0.644$; Figure 5(a); near: $F(2,93) = 0.300$, $p = 0.741$; Figure 6(b)).

3.5. Fusional Vergence

3.5.1. Negative Fusional Vergence (BI). A 2-tailed paired-samples t-test showed that both near and distance negative fusional vergence were not significantly affected by the 3D viewing ($p > 0.05$); neither near nor distance negative fusional vergence was significantly different among the three modes (distance, $F(3,124) = 0.568$, $p = 0.637$; near, $F(3,124) = 1.060$, $p = 0.369$; Figure 7(a)).

3.5.2. Positive Fusional Vergence (BO). The near positive fusional vergence was significantly decreased after the 3D viewing (Mode A: $p = 0.006$; Mode B: $p = 0.034$; Mode C: $p = 0.005$). Neither the near nor distance positive fusional vergence was significantly different among the three modes (near: $F(2,93) = 0.19$, $p = 0.982$; distance: $F(2,93) = 0.842$, $p = 0.473$; Figure 7(b)).

In summary, after 3D TV viewing, the accommodative response was significantly changed under illumination Modes A, while accommodative microfluctuation was significantly changed under illumination Modes A and B; the near positive fusional vergence decreased significantly after a 90-minute 3D viewing session under each illumination mode, and this effect was not significantly different among the three modes. Other measures of ocular status, such as accommodative facility, relative accommodation, gradient AC/A, and phoria, exhibited no significant change between the pre- and postviewing data or among the three modes.

4. Discussion

In the present study, the observers watched 3D TV under three illumination modes. Before and after a 90-minute 3D

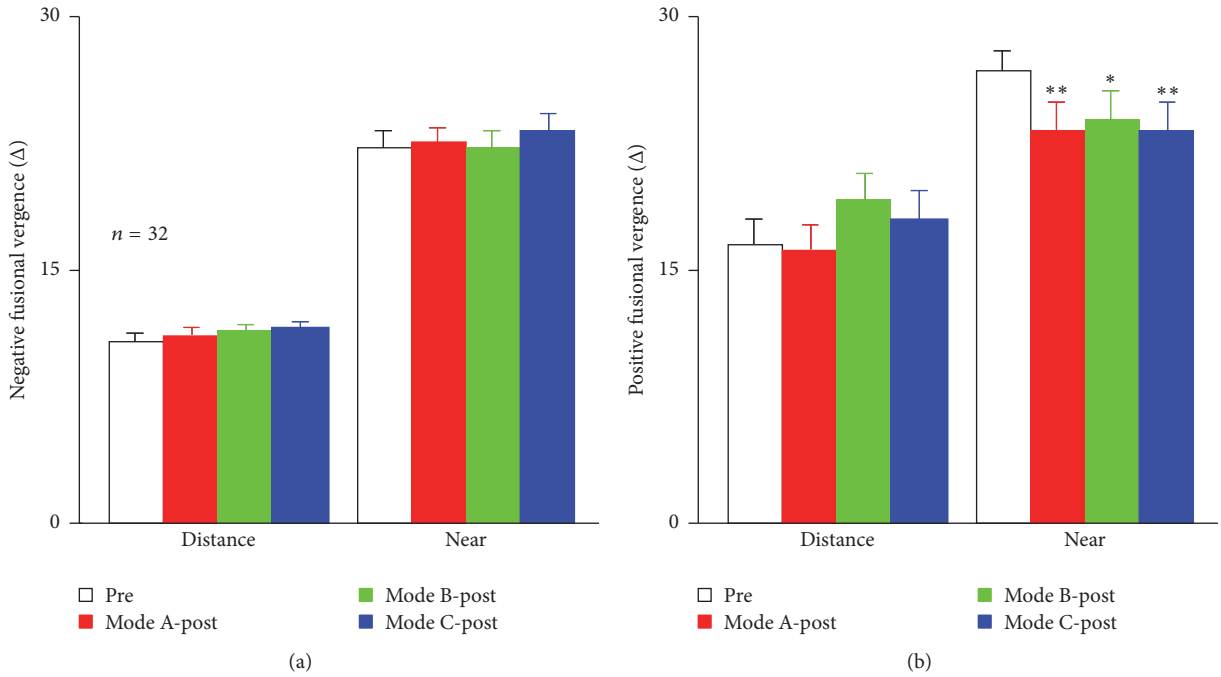

Figure 7: The effect of a 90-minute 3D viewing session on fusional vergence. The effect of a 90-minute 3D viewing on negative fusional vergence (a) and positive fusional vergence (b), which were measured at distant and near measuring conditions. Error bars indicate the standard error across 32 observers; $^{*}P < 0.05$; $0.05 < {}^{**}P < 0.01$.

viewing session under each mode, the ocular status, including accommodative facility, positive and negative relative accommodation, gradient AC/A, distance and near phoria, and positive and negative fusional vergence, was measured. Overall, we found that Mode B (the back illumination) and Mode C (the front illumination) produced the same effect on the different measures of ocular status; both modes were superior to Mode A (complete darkness) in terms of inducing less change after 3D viewing. Furthermore, Mode C produced the smallest change in accommodative microfluctuation. We conclude that the front illumination mode is much more appropriate for shutter 3D TV viewing when the change in ocular status is taken into account.

In previous research, Torii et al. [15] found that after viewing a 3D movie with film-patterned retarder glasses for 30 minutes, the amplitude of accommodation and vergence was decreased, while Fujikado [21] reported that subjects who viewed 3D video for 30 minutes experienced transient low-diopter myopia (0.2 D) due to excessive accommodation. Maeda et al. [6] found no significant difference between the accommodative microfluctuation data from before and after 90 or 60 minutes of 3D viewing in either the adult or child group; however, accommodative microfluctuation tended to increase after 3D viewing in some subjects. In the present study, we demonstrated that both the accommodative response and accommodative microfluctuation increased slightly after 3D viewing which was significantly under a certain mode of illumination (the accommodative response changed significantly under Mode A and the accommodative microfluctuation changed significantly under Mode A and Mode B). This result was consistent with the results of previous studies [6, 21]. The increased accommodative response and increased microfluctuation may occur when there is a convergence-accommodation conflict while viewing a 3D image. This conflict would increase accommodation and the burden on the accommodative system and result in incomplete relaxation of the visual system for a short time after viewing 3D TV [15].

As shown in Figure 7, the positive fusional vergence data of the viewers at a distance of 40 cm decreased significantly after 3D TV viewing under all three illumination modes, although no significant differences were found among these modes at a distance of 5 m. Previous studies have suggested that the change in reliance or fusional vergence could result in muscle and neural adaptation fatigue and lead to a series of visual symptoms [8, 16, 22, 23]. Wee et al. [24] found the increase of accommodative responses and the near point of convergence (decreased ability of convergence) after 30-minute 3D movies viewing with patterned retarder glasses, which did not occur after 30-minute 2D movies viewing. These results are very consistent with our study. In the present study, the distance and near phoria had a tendency to show more exophoria. Based on previous studies [25, 26], it would be logical to suggest that the decreased convergence and changed phoria after 3D TV viewing may be due to the adaptation of the vergence and accommodative controllers [27].

Apart from the above parameters (i.e., accommodative response and accommodative microfluctuation), the other measures of ocular status exhibited no significant differences after 3D viewing or among the three illumination modes. These no effect findings are somehow counterintuitive. As

we know, the natural relationship between binocular convergence and accommodation is disrupted to perceive a single clear image while watching 3D TV, inducing more adaptation and better visual plasticity. However, the adaptation can disappear, and the disrupted cross-linking interaction between accommodation and vergence can recover after taking a break in 3D TV viewing [15, 23]. Torii et al. indicated that accommodative overshoot had lasting less than 1 min while viewing stereoscopic images [15], while Emoto et al. found that decreased fusional amplitude, after viewing of stereoscopic images, recovered to previewing levels in ten minutes [23]. The recovery time was indeterminate and depended on many factors. Once stopped exposing in the 3D viewing, the ocular status might recover in less than 20 minutes, which was the postmeasurement time of the present study. This recovery could be the reason for some of our current findings. Spatial frequency components, the disparity of the images, and long-term and frequent exposure to the 3D display as well as individual differences may account for the discrepancies among different studies [3].

Altogether, we arrived at the conclusion that ocular status is modulated not only by 3D viewing but also by the illumination mode. This finding may be attributed to the difference in luminance at the position of the viewer, the direction of the light source, or the familiar viewing environment of the participants. We did not examine the mechanism in this study, but we demonstrated that front illumination is an appropriate illumination mode for watching 3D displays. There is much evidence suggesting that illumination of the environment is a modifying factor forocular status [2, 3, 6], visual asthenopia [25, 28], and the contrast modulation of visual cortical cells [29, 30]. Low luminance levels, as in Mode A (complete darkness), would create inadequate viewing conditions and notable variations in the eyes when moving the gaze intermittently between the bright display and darker surroundings and would potentially cause eye strain. Increasing the ambient illumination to minimize differences in eye adaptation would potentially reduce visual fatigue for workers using typical LCDs in medical image soft-copy reading rooms [31]. Zhou et al. found that the selective reduction of monocular mean luminance in one eye can significantly affect the interocular balance in binocular combination in both normal and amblyopic observers [29]. Our results together with these previous reports suggest that the environmental illumination is critical in modulating our visual system and that a higher luminance such as that in Mode C produces a smaller change in ocular status.

We demonstrated that according to the type of illumination, 3D viewing can modify the ocular status with regard to visual plasticity to maintain a relatively stable visual system and thereby ensure that the cerebral cortex perceives a single clear image. The entire process is associated with the ocular muscles, nerves, or local brain areas that are involved in 3D viewing; therefore, the modification of visual plasticity may lead to the modification of these components of the visual system to a certain extent. We believe that this study may yield evidence of visual plasticity and provide clues for scientists working on neural plasticity.

5. Conclusion

We conclude that luminance plays a modulating role in ocular modification induced by the shutter display viewing of 3D images. Subjective accommodative function exhibits greater stability when illumination is in front of a viewer. Front illumination using fluorescent lamps may be an appropriate illumination mode for shutter 3D TV viewing.

Competing Interests

The authors declare that they have no competing interests.

Authors' Contributions

Hao Chen and Yuwen Wang contributed equally to this study. The authors alone are responsible for the content and writing of this paper.

Acknowledgments

The study was supported by research grants from the Key Project of The Affiliated Eye Hospital of Wenzhou Medical University, Zhejiang, China (YNZD201004), Zhejiang Provincial Natural Science Foundation of China (LY14H120007), and National Key Research and Development Program of China (2016YFB0401203).

References

[1] Y. Suzuki, Y. Onda, S. Katada, S. Ino, and T. Ifukube, "Effects of an eyeglass-free 3-D display on the human visual system," *Japanese Journal of Ophthalmology*, vol. 48, no. 1, pp. 1–6, 2004.

[2] S.-H. Kim, Y.-W. Suh, C.-M. Yun, E.-J. Yoo, J.-H. Yeom, and Y. A. Cho, "3D asthenopia in horizontal deviation," *Current Eye Research*, vol. 38, no. 5, pp. 614–619, 2013.

[3] T. Fukushima, M. Torii, K. Ukai, J. S. Wolffsohn, and B. Gilmartin, "The relationship between CA/C ratio and individual differences in dynamic accommodative responses while viewing stereoscopic images," *Journal of Vision*, vol. 9, no. 13, pp. 1–13, 2009.

[4] S. Nishina, A. Wakayama, A. Miki et al., "[Viewing 3D stereoscopic images in children and adults with and without strabismus: multicenter study in Japan]," *Nippon Ganka Gakkai zasshi*, vol. 117, no. 12, pp. 971–982, 2013.

[5] Y. Lin, S. Fotios, M. Wei, Y. Liu, W. Guo, and Y. Sun, "Eye movement and pupil size constriction under discomfort glare," *Investigative Ophthalmology and Visual Science*, vol. 56, no. 3, pp. 1649–1656, 2015.

[6] F. Maeda, A. Tabuchi, K. Kani, K.-I. Kawamoto, T. Yoneda, and T. Yamashita, "Influence of three-dimensional image viewing on visual function," *Japanese Journal of Ophthalmology*, vol. 55, no. 3, pp. 175–182, 2011.

[7] J. E. Sheedy, J. Hayes, and J. Engle, "Is all asthenopia the same?" *Optometry and Vision Science*, vol. 80, no. 11, pp. 732–739, 2003.

[8] R. Jones and G. L. Stephens, "Horizontal fusional amplitudes. Evidence for disparity tuning," *Investigative Ophthalmology & Visual Science*, vol. 30, no. 7, pp. 1638–1642, 1989.

[9] M. Michaelides, A. J. Hardcastle, D. M. Hunt, and A. T. Moore, "Progressive cone and cone-rod dystrophies: phenotypes and

underlying molecular genetic basis," *Survey of Ophthalmology*, vol. 51, no. 3, pp. 232–258, 2006.

[10] Y.-J. Yao, Y.-M. Chang, X.-P. Xie, X.-S. Cao, X.-Q. Sun, and Y.-H. Wu, "Heart rate and respiration responses to real traffic pattern flight," *Applied Psychophysiology Biofeedback*, vol. 33, no. 4, pp. 203–209, 2008.

[11] G. Carozzi, "Illumination of the work environment," *Rivista Italiana Degli Odontotecnici*, vol. 19, pp. 41–51, 1983.

[12] C. J. Lin, W.-Y. Feng, C.-J. Chao, and F.-Y. Tseng, "Effects of VDT workstation lighting conditions on operator visual workload," *Industrial Health*, vol. 46, no. 2, pp. 105–111, 2008.

[13] S. Taptagaporn, M. Sotoyama, S. Saito, T. Suzuki, and S. Saito, "Visual comfort in VDT workstation design," *Journal of Human Ergology*, vol. 24, no. 1, pp. 84–88, 1995.

[14] K.-K. Shieh and Y.-R. Lai, "Effects of ambient illumination, luminance contrast, and stimulus type on subjective preference of vdt target and background color combinations," *Perceptual and Motor Skills*, vol. 107, no. 2, pp. 336–352, 2008.

[15] M. Torii, Y. Okada, K. Ukai, J. S. Wolffsohn, and B. Gilmartin, "Dynamic measurement of accommodative responses while viewing stereoscopic images," *Journal of Modern Optics*, vol. 55, no. 4-5, pp. 557–567, 2008.

[16] L. Zhang, Y.-Q. Zhang, J.-S. Zhang, L. Xu, and J. B. Jonas, "Visual fatigue and discomfort after stereoscopic display viewing," *Acta Ophthalmologica*, vol. 91, no. 2, pp. e149–e153, 2013.

[17] L. S. Gray, B. Winn, and B. Gilmartin, "Effect of target luminance on microfluctuations of accommodation," *Ophthalmic and Physiological Optics*, vol. 13, no. 3, pp. 258–265, 1993.

[18] M. Day, D. Seidel, L. S. Gray, and N. C. Strang, "The effect of modulating ocular depth of focus upon accommodation microfluctuations in myopic and emmetropic subjects," *Vision Research*, vol. 49, no. 2, pp. 211–218, 2009.

[19] M. Day, L. S. Gray, D. Seidel, and N. C. Strang, "The relationship between object spatial profile and accommodation microfluctuations in emmetropes and myopes," *Journal of Vision*, vol. 9, no. 5, pp. 1–13, 2009.

[20] A. L. Sheppard and L. N. Davies, "Clinical evaluation of the Grand Seiko Auto Ref/Keratometer WAM-5500," *Ophthalmic and Physiological Optics*, vol. 30, no. 2, pp. 143–151, 2010.

[21] T. Fujikado, "Asthenopia from the viewpoint of visual information processing-effect of watching 3D images," *Journal of the Eye*, vol. 14, pp. 1295–1300, 1997.

[22] M. Emoto, T. Niida, and F. Okano, "Repeated vergence adaptation causes the decline of visual functions in watching stereoscopic television," *Journal of Display Technology*, vol. 1, no. 2, pp. 328–340, 2005.

[23] M. Emoto, Y. Nojiri, and F. Okano, "Changes in fusional vergence limit and its hysteresis after viewing stereoscopic TV," *Displays*, vol. 25, no. 2-3, pp. 67–76, 2004.

[24] S. W. Wee, N. J. Moon, W. K. Lee, and S. Jeon, "Ophthalmological factors influencing visual asthenopia as a result of viewing 3D displays," *British Journal of Ophthalmology*, vol. 96, no. 11, pp. 1391–1394, 2012.

[25] E. Karpicka and P. A. Howarth, "Heterophoria adaptation during the viewing of 3D stereoscopic stimuli," *Ophthalmic and Physiological Optics*, vol. 33, no. 5, pp. 604–610, 2013.

[26] V. Sreenivasan, W. R. Bobier, E. Irving, and V. Lakshminarayanan, "Effect of vergence adaptation on convergence accommodation: model simulations," *IEEE Transactions on Bio-Medical Engineering*, vol. 57, no. 11, 2010.

[27] C. Costa Lança and F. J. Rowe, "Variability of fusion vergence measurements in heterophoria," *Strabismus*, vol. 24, no. 2, pp. 63–69, 2016.

[28] P. A. Howarth, "Potential hazards of viewing 3-D stereoscopic television, cinema and computer games: a review," *Ophthalmic and Physiological Optics*, vol. 31, no. 2, pp. 111–122, 2011.

[29] J. Zhou, W. Jia, C.-B. Huang, and R. F. Hess, "The effect of unilateral mean luminance on binocular combination in normal and amblyopic vision," *Scientific Reports*, vol. 3, article 2012, 2013.

[30] J. Zhou, R. Liu, L. Feng, Y. Zhou, and R. F. Hess, "Deficient binocular combination of second-order stimuli in amblyopia," *Investigative Ophthalmology and Visual Science*, vol. 57, no. 4, pp. 1635–1642, 2016.

[31] A. S. Chawla and E. Samei, "Ambient illumination revisited: a new adaptation-based approach for optimizing medical imaging reading environments," *Medical Physics*, vol. 34, no. 1, pp. 81–90, 2007.

Hindawi
Neural Plasticity
Volume 2017, Article ID 3478742, 12 pages
https://doi.org/10.1155/2017/3478742

Research Article

The Impact of Feedback on the Different Time Courses of Multisensory Temporal Recalibration

Matthew A. De Niear,[1,2] Jean-Paul Noel,[2,3] and Mark T. Wallace[2,4,5,6]

[1] *Medical Scientist Training Program, Vanderbilt University Medical School, Vanderbilt University, Nashville, TN 37235, USA*
[2] *Vanderbilt Brain Institute, Vanderbilt University Medical School, Vanderbilt University, Nashville, TN 37235, USA*
[3] *Neuroscience Graduate Program, Vanderbilt Brain Institute, Vanderbilt University Medical School, Vanderbilt University, Nashville, TN 37235, USA*
[4] *Department of Hearing and Speech Sciences, Vanderbilt University Medical Center, Nashville, TN 37235, USA*
[5] *Department of Psychology, Vanderbilt University, Nashville, TN 37235, USA*
[6] *Department of Psychiatry, Vanderbilt University Medical Center, Nashville, TN 37235, USA*

Correspondence should be addressed to Matthew A. De Niear; matthew.a.de.niear@vanderbilt.edu

Received 26 October 2016; Revised 14 January 2017; Accepted 26 January 2017; Published 21 February 2017

Academic Editor: Zili Liu

The capacity to rapidly adjust perceptual representations confers a fundamental advantage when confronted with a constantly changing world. Unexplored is how feedback regarding sensory judgments (top-down factors) interacts with sensory statistics (bottom-up factors) to drive long- and short-term recalibration of multisensory perceptual representations. Here, we examined the time course of both cumulative and rapid temporal perceptual recalibration for individuals completing an audiovisual simultaneity judgment task in which they were provided with varying degrees of feedback. We find that in the presence of feedback (as opposed to simple sensory exposure) temporal recalibration is more robust. Additionally, differential time courses are seen for cumulative and rapid recalibration dependent upon the nature of the feedback provided. Whereas cumulative recalibration effects relied more heavily on feedback that informs (i.e., negative feedback) rather than confirms (i.e., positive feedback) the judgment, rapid recalibration shows the opposite tendency. Furthermore, differential effects on rapid and cumulative recalibration were seen when the reliability of feedback was altered. Collectively, our findings illustrate that feedback signals promote and sustain audiovisual recalibration over the course of cumulative learning and enhance rapid trial-to-trial learning. Furthermore, given the differential effects seen for cumulative and rapid recalibration, these processes may function via distinct mechanisms.

1. Introduction

In order to accurately perceive the world, individuals must adjust their perceptual representations to meet the changing nature of the sensory world and changing task contingencies [1]. Given this, the capacity to rapidly adjust perceptual representations confers a fundamental advantage [2, 3]. Such perceptual plasticity often leads to an improved representation of the sensory environment, a process termed perceptual learning [4, 5]. Changes in perceptual representations resulting from perceptual learning have been observed to occur within both rapid [6, 7] and more gradual time courses [8, 9]. Furthermore, the contribution of feedback signals, in conjunction with sensory experience, is known to alter the rate of perceptual learning or enable perceptual learning to occur when sensory experience is insufficient [10].

Although initial investigations of perceptual plasticity tended to focus on changes in perception for a single sensory modality, there has been an increasing interest in examining the plasticity of multisensory perceptual representations [4, 11]. One such area of investigation has focused on how the temporal processing of multisensory stimuli (particularly audiovisual stimuli [12–15]; for other modalities see [16–18]) can be altered via changes in sensory experience. The temporal structure of sensory stimuli from the different modalities is a fundamental feature determining whether these stimuli should be associated or perceived as a single multisensory

event [19–21]. One critical aspect of this process must take into account the differences in neural and physical transmission times for the respective sensory stimuli (e.g., light and sound energy propagate through the environment at very different rates). In order to circumvent this challenge and ultimately achieve perceptual coherence, there exists an epoch of time spanning several hundred milliseconds within which stimuli from vision and audition are likely to be associated. This construct has been collectively referred to as the temporal binding window (TBW). Similarly, the point of asynchrony at which the separate sensory stimuli are most likely to be perceived as occurring synchronously has been termed the point of subjective simultaneity (PSS). These two metrics, the TBW and PSS, are thus important tools in evaluating the nature of audiovisual temporal representations.

Prior work has shown both the TBW and PSS to be malleable. These dynamic changes in the TBW and PSS, termed temporal recalibration, were initially hypothesized as a means to resolve asynchronous sensory signals reflective of the statistics of the environment [19]. Thus, initial studies showed that it was possible to shift an individual's PSS by providing extensive experience that overrepresented certain asynchronies [12, 13]. More recent evidence suggests that these changes not only occur after extensive experience, but can also be seen on a moment-to-moment basis (i.e., based on the characteristics of the previous trial, t-1) [7, 15, 22–27]. Thus, changes in multisensory temporal representations happen on both rapid and cumulative time scales. Such observations raise fundamental mechanistic questions about these short- and longer-term changes, most immediately in regard to whether one (short-term) represents the substrate upon which the other (longer-term) is built. One can envision a scenario in which rapid temporal recalibration may be needed in order to properly represent immediate changes in the sensory environment whereas cumulative temporal recalibration may result in more durable changes in perceptual representations [24, 28].

While sensory experience is undoubtedly an important element that influences perceptual plasticity, feedback signals that inform an individual regarding the accuracy of their perceptual judgments are likely to interact with sensory experience to influence temporal recalibration of the TBW and PSS. Early studies of visual perceptual learning suggest that feedback signals enhance perceptual learning [9, 29] and are capable of eliciting perceptual learning even in the absence of awareness in regard to the changing nature of the sensory environment [30]. Increasingly, changes on top-down processing regions have been observed to parallel perceptual learning [31, 32] and are likely to be activated by a feedback signal. Collectively, the evidence suggests that the dynamics of perceptual learning are likely dependent upon coordinated interactions between sensory statistics primarily represented in low-level cortical areas and the brain areas that initially represent them and higher-order factors and their neural substrates [33]. Recent studies have observed that feedback signals also produce rapid improvements in multisensory temporal acuity [34–36] and elicit changes in connectivity between primary sensory cortices and multisensory cortex [37]. Despite the independent evidence for the importance of these bottom-up and top-down factors in perceptual plasticity, few studies have looked at the interdependence between them. Here, we sought the interaction of bottom-up and top-down factors in perceptual plasticity by altering top-down factors (i.e., presence of a feedback signal and/or feedback reliability) and examining its impact on temporal recalibration across both immediate and longer-term time scales.

2. Materials and Methods

2.1. Participants. Sixty-five young adults partook in this study (36 females; age, $M = 20.48$ years; range = 18–28 years). All participants had self-reported normal hearing and normal or corrected to normal vision. Written informed consent was obtained from all individuals participating in this study. All participant recruitment and experimental procedures were approved by the Vanderbilt University Institutional Review Board and were in accordance with the ethical standards of the 1964 Helsinki Declaration and its later amendments or comparable ethical standards.

2.2. Assessment of Temporal Acuity by Simultaneity Judgment Task. We employed simultaneity judgment (SJ) task to measure audiovisual temporal acuity as prior studies assessing temporal recalibration have utilized similar SJ tasks [12, 15, 22, 38, 39]. Participants were seated in a light and sound attenuating WhisperRoom™ (SE 2000 Series, Whisper Room Inc.) room for all tasks. All visual stimuli were presented at approximately 60 cm from the seated participants. A fixation marker (1 cm × 1 cm) on a black background was present on the screen both between trials and throughout the duration of a trial including presentation of the visual stimulus. Participants were asked to maintain fixation on the fixation marker throughout the experiment. For the SJ task, participants were instructed to judge whether the visual stimulus and auditory stimulus "were synchronous, at the same time" or "were asynchronous, at different times" by pressing either 1 or 2, respectively, using a keyboard (see Figure 1(a)). The visual stimulus consisted of a white ring on a black background that subtended 7.2° of visual space with an outer diameter of 6.0 cm and an inner diameter of 3.0 cm. Visual stimuli were presented for 8.3 ms (the duration of a single screen refresh cycle) on a monitor (Samsung syncmaster 22-inch 2233 RZ LCD) with a refresh-rate of 120 Hz. The auditory stimulus consisted of 1800 Hz tone that was presented biaurally via headphones (Sennheiser HD 558) with no interaural time or level differences. Auditory stimuli were 10 ms in duration (1.3 ms onset and offset ramp) and were presented at 83 dB and were calibrated using a sound level meter (Larson Davis SoundTrack® LxT2). For each trial, visual and auditory stimuli were presented in synchrony (0 ms of asynchrony between onset of visual stimuli and onset of maximal auditory amplitude) or with a stimulus onset asynchrony (SOA) ranging ±400–50 ms (negative values indicate that the auditory stimulus was the leading stimulus while positive values indicate that visual stimulus was the leading stimulus). To ensure accurate presentation of auditory and visual stimuli, SOAs were verified externally using an oscilloscope. A response screen was

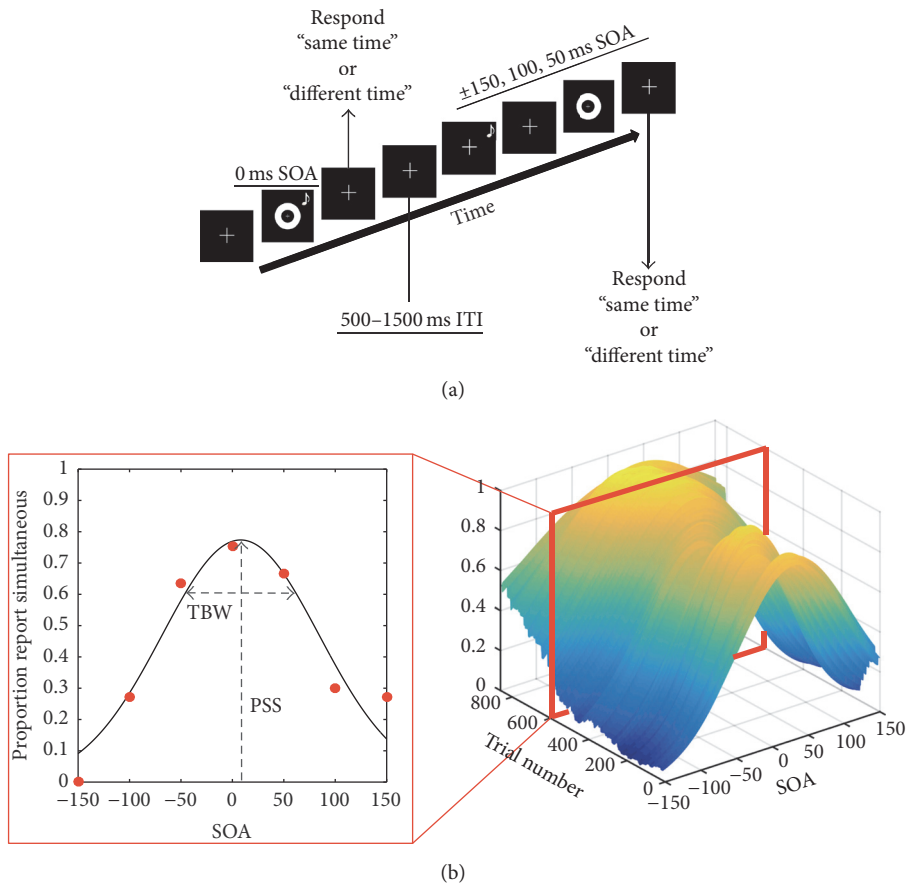

Figure 1: (a) Representation of a trial sequence for the simultaneity judgment (SJ) task. Participants were asked to judge if stimuli occurred at the same time or different times. (b) Individual fittings for a single participant using the sliding-window approach across Trials 1–860. The inset on the left shows a single fitting at one time-point along the time course with the PSS (mean of distribution) and TBW (standard deviation of distribution) at that particular moment in time. The TBW, PSS (cumulative) and ΔTBW, ΔPSS (rapid) were normalized on a within-subject basis, and in order to correct for multiple comparisons we consider an effect significant at $\alpha < 0.01$ for at least 10 consecutive trials. Trial 0 was defined as the 140 trials utilized to establish initial estimates of the PSS and TBW. The time course analysis was conducted on the following 860 trials. From Trials 1–720, participants were assigned to one of four groups that received varying amounts of feedback following a response. From Trials 721–860, no feedback was presented following a response for all participants.

presented following each audiovisual pair at which time subjects could make a response. The intertrial interval (ITI) was randomly jittered from 500 to 1500 ms (uniform distribution). MATLAB (The MathWorks, Inc.) with Psychophysics Toolbox extensions [40, 41] was used to create and present the SJ task.

2.3. General Experimental Procedure for the Assessment of Temporal Recalibration. The estimates put forward on Trial 0 were defined as the values derived from the trials comprising the first phase of the experiment (Trials 0 to 300). The time course analysis was conducted on the following 860 trials. From Trials 1–720 of the second phase, participants were assigned to one of four groups that received varying amounts of feedback following a response (see below). From the next 140 trials, no feedback was presented following a response for all participants.

To derive initial estimates of the TBW and PSS (to assess cumulative recalibration) and trial-to-trial change in the PSS and TBW (to assess rapid recalibration), participants first completed an initial block of 300 trials (although only 140 of these were utilized, see below) of the SJ task comprising 20 trials at each of the following SOAs: ±400, 300, 250, 200, 150, 100, 50, and 0 ms. Performance over this block of trials was utilized to derive Trial 0 of the time course analysis (effects of feedback on the time course of recalibration will be tested against this Trial 0, see below). Participants subsequently completed a second block of 720 trials of the SJ task with stimuli presented at SOAs of ±150, 100, 50, and 0 ms. To avoid introducing a response bias for participants in groups receiving feedback, the number of trials at each SOA was not equally distributed in the second trial block. Instead true synchrony was overrepresented at a 6 : 1 ratio in comparison to the objectively asynchronous SOAs, such that the total number of simultaneous trials presented was equal to the total number of asynchronous trials presented (0 ms, 360 trials; ±150, 100, and 50 ms × 60 trials each). Participants next completed a third block of 300 additional trials of the SJ task

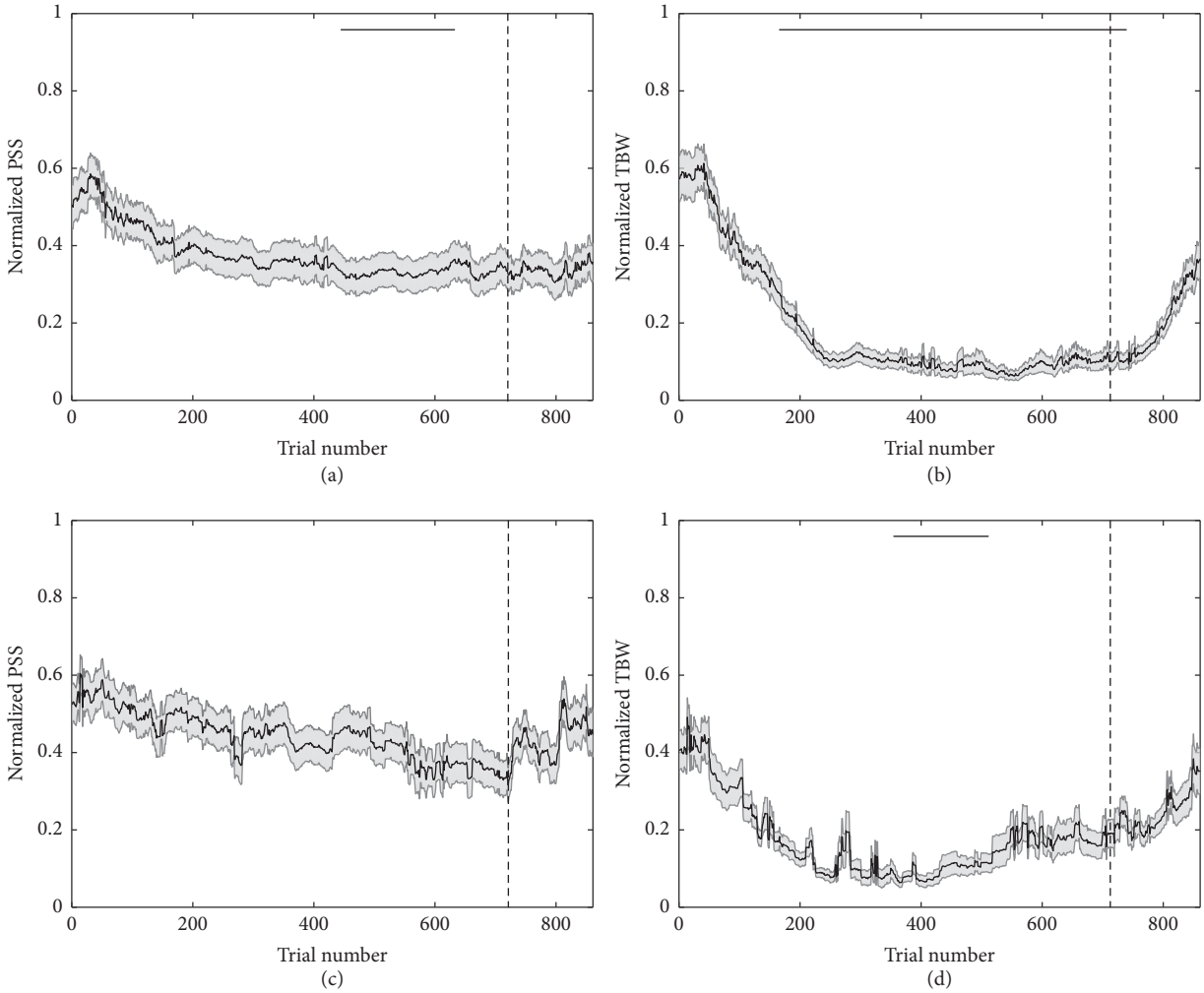

Figure 2: The time course of cumulative (grayscale) multisensory temporal recalibration of the PSS ((a) and (c)) and TBW ((b) and (d)) with ((a) and (b)) and without feedback ((c) and (d)). Solid bars shown above the time course are indicative of at least 10 consecutive trials at which the PSS or TBW (cumulative recalibration) significantly differed from Trial 0 ($\alpha < 0.01$ for all trials). Shaded region illustrates SEM at each trial across the time course analysis. The post-feedback period beginning at Trial 721 is denoted by the gray, dashed vertical line.

identical to the first block of 300 trials (20 trials × 15 SOAs; ±400, 300, 250, 200, 150, 100, 50, and 0 ms). The time course analysis was performed using the responses in the second and third blocks. During only the second block was feedback presented for groups receiving a form of feedback. No feedback was presented during the first or third blocks. Total duration of the experiment was under 1 h30 min, and participants were given an opportunity to rest after every 100 trials in each experimental trial block.

2.4. Presentation of Feedback Signal. For all participants, feedback was not provided during the presentation of trials in the first trial block. Participants were randomly assigned to one of four experimental groups characterized by the nature of the feedback presented during the second block. For the first group ($n = 15$), participants did not have access to any explicit feedback. Participants in the second group ($n = 25$) had access to reliable visual feedback in the form of a blue-green check mark or red X following objectively correct and incorrect responses. Reliable feedback was defined as feedback that accurately reflected the objective relationship of the audiovisual stimuli. The third ($n = 13$) and fourth ($n = 12$) groups were, respectively, presented with reliable feedback on only 80% and 50% of trials (i.e., false or erroneous feedback on 20% and 50% of the remaining trials). False feedback (i.e., feedback that was not reliable) was defined as the presentation of the incorrect feedback for each SOA-response pair (i.e., a response of synchronous for a trial in which the SOA presented was 0 ms yielded the presentation of a red X, the exact opposite of the objectively accurate feedback). Reliable and false feedback were distributed equally between synchronous and asynchronous trials for all participants. All feedback was presented for 500 ms immediately following the participant's response. No feedback was presented for the third trial block for all participants (post-feedback period as denoted by dashed line at Trial 721 in Figures 2, 3, and 4 and Figures S1 and S2 in Supplementary Material available online at https://doi.org/10.1155/2017/3478742).

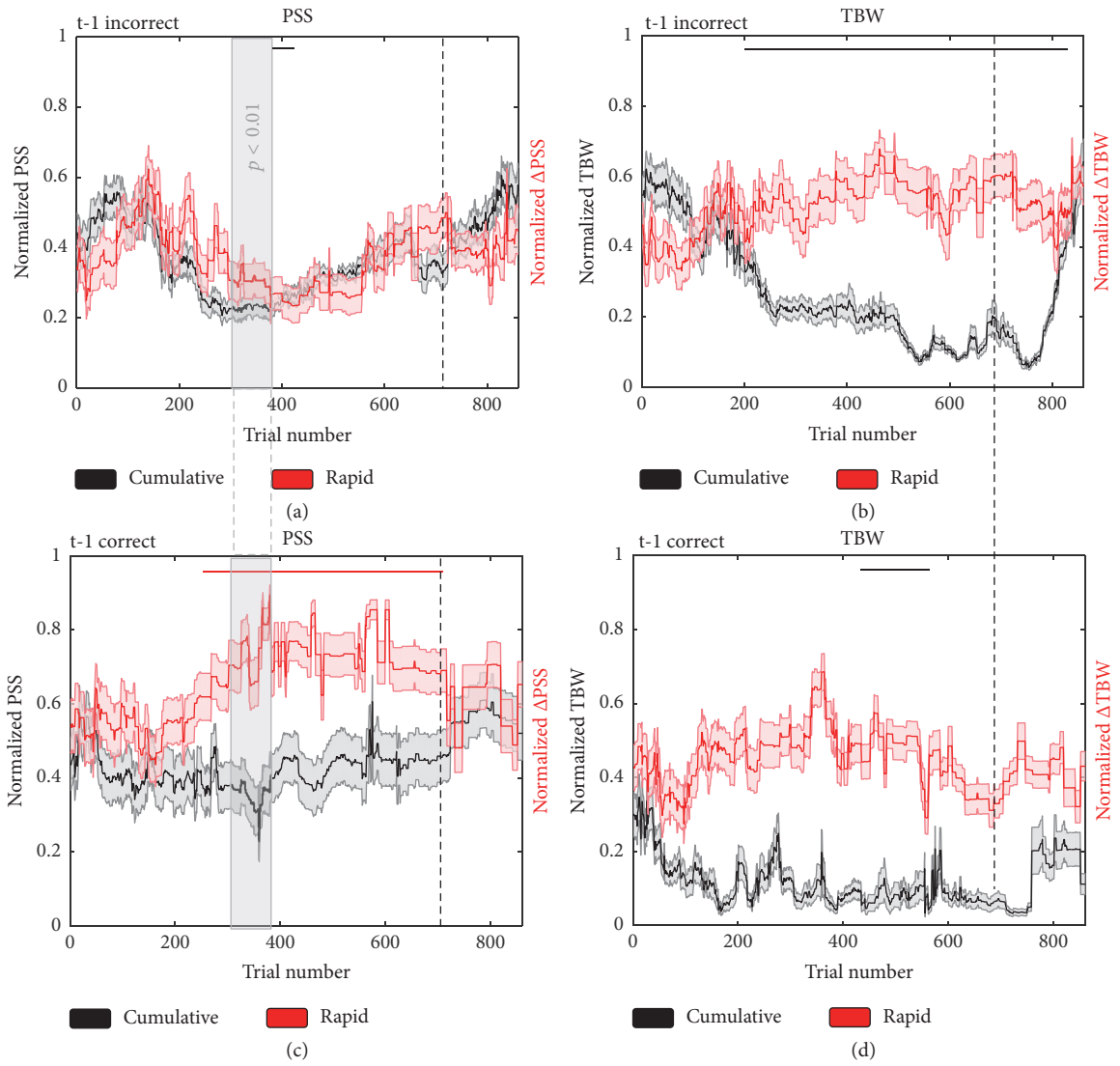

Figure 3: The time course of multisensory rapid (color) and cumulative (grayscale) temporal recalibration as a function of prior negative ((a) and (b)) and positive ((c) and (d)) feedback on trial t-1. Shaded region illustrates SEM at each trial across the time course analysis. Solid bars shown above the time course are indicative of at least 10 consecutive trials at which the PSS or TBW (cumulative) or ΔPSS or ΔTBW (rapid) significantly differed from Trial 0 ($\alpha < 0.01$ for all trials). The trials for which we observed a significant interaction of temporal recalibration (cumulative versus rapid) × feedback (t-1 correct versus t-1 incorrect) is indicated by the vertical solid gray shading ($\alpha < 0.01$ for all trials).

2.5. Analysis of the Time Course of Multisensory Temporal Recalibration. Two distinct multisensory temporal recalibration time courses are of interest here. The first, denominated "cumulative" recalibration, refers to the degree to which participants consider accumulating feedback when executing audiovisual simultaneity judgments. This recalibration, thus, requires the conscious acknowledgment of received feedback. The second, referred to as "rapid" recalibration, denotes the degree to which the nature of the immediately preceding trial (t-1)—audio- or visual-leading—influences the perception of simultaneity at the given trial (t). The examination of rapid audiovisual temporal recalibration effects, thus, is taken to index an implicit sensory phenomenon, perceptual learning, and involves a one-back analysis (analysis of trial t as a conditional of trial t-1).

PSS and TBW for the different conditions and time courses were contrasted. In order to examine the effect of feedback, we compared the mean initial estimate of PSS, ΔPSS (i.e., rapid change in PSS), TBW, and ΔTBW (i.e., the estimates based on block 1: no feedback) to estimates derived from subsequent time period with feedback (a sliding time window of 140 trials, see below). To maintain a consistent estimate of the different parameters exposed above across all blocks, only SOAs of ±150, 100, 50, and 0 ms were utilized to fit distributions of reports of synchrony as a function of SOA for the entire time course. Although we employed wider ranging SOAs in the first trial block to ensure an accurate estimate of the PSS and TBW, further analysis revealed that fitting these distributions with the entire course of SOAs and those present across all trial blocks did not result in any significant

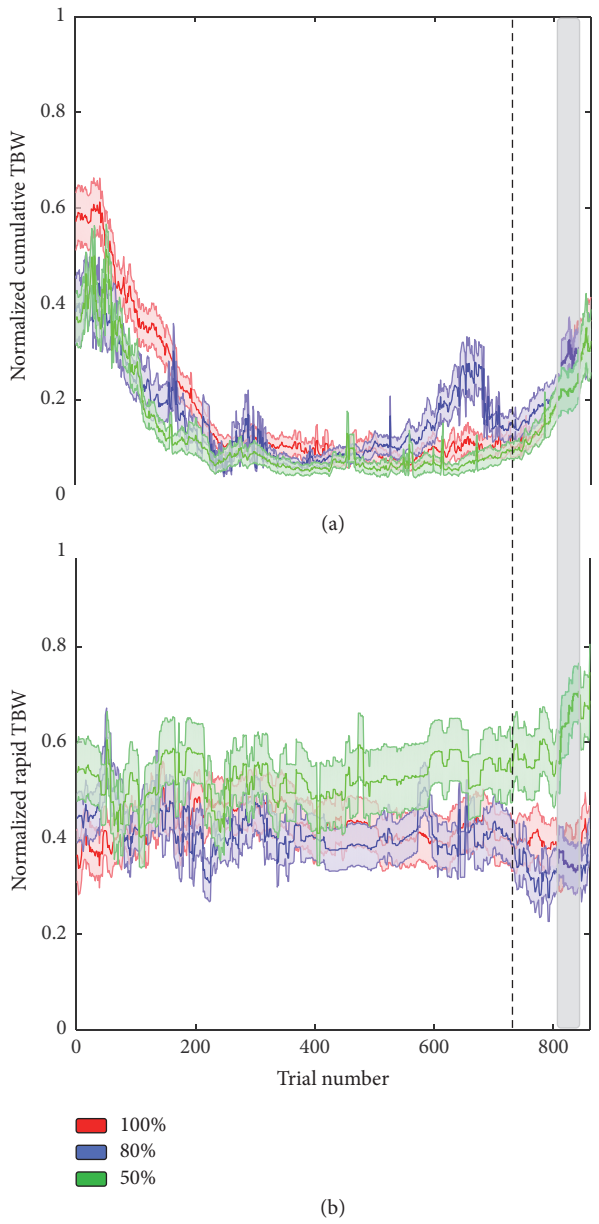

Figure 4: The time course of cumulative (a) and rapid (b) temporal recalibration of the TBW for feedback that was 100% (red), 80% (blue), and 50% (green) reliable. Shaded region illustrates SEM at each trial across the time course analysis. We observe that the time course of rapid recalibration of the TBW for the group receiving uncorrelated feedback signals (50% reliable) diverges from the other group in the post-feedback trial block such that there is greater trial-to-trial readjustment of the TBW (the area of vertical gray shading indicates interaction).

differences in our initial estimates for all measures ($p > 0.21$ for all measures). Thus, initial distributions of reports of synchrony as a function of SOA (Trial 0 in the time course analysis) were drawn based on the 140 trials comprising the first trial block (no feedback). These distributions of responses were fitted with a Gaussian distribution whose amplitude, mean, and standard deviation were free to vary (see (1)).

$$P(\text{response} \mid \text{SOA}) = \text{amp} \times \exp^{-((\text{SOA}-\text{PSS})^2/2\text{SD}^2)}. \quad (1)$$

The normal distribution proved to be overall a good fit (mean $R^2 = 85.6$, SD = 2.45). The mean of the best fitting distribution is taken as the PSS and the standard deviation as a measure of the TBW. That is, PSS is the point (i.e., SOA) at which participants are most likely to categorize a presentation as synchronous and the TBW is the temporal interval over which participants are highly likely to categorize the presentation as synchronous.

In order to index rapid recalibration, the amount of change in these values (PSS and TBW) is computed (e.g., ΔPSS = PSS audio-leading − PSS visual leading) as a function of the prior trial. Further, in order to examine the time courses of rapid versus slow multisensory temporal recalibration effects, we adopt a sliding-window approach (Figure 1(b)). That is, after the first estimation of the mean and standard deviation of the Gaussian describing reports of synchrony, a window of 140 trials—initially placed between Trials 0 and 140—is moved trial-per-trial across the entire span of the second trial block (Trials 1–720) as well as during the third trial block post-feedback (Trials 721–860). A window of 140 trials is chosen in order to mimic the initial estimates based on the first block of 140 trials. At each subsequent step the new distribution is fitted again, and estimates of the mean and standard deviation are calculated. Similarly, at each step rapid recalibration values are recomputed. Upon completion of the protocol (~5000 fittings per subject), PSS and TBW values were normalized from 0 to 1 within-subjects. That is, in order to appropriately compare across time scales of recalibration (cumulative versus rapid), with vastly different values and ranges, the data were normalized. For every participant and for each of their parameters (PSS, ΔPSS, TBW, and ΔTBW), their time-series was normalized such that their most extreme absolute values, minimum and maximum, respectively, corresponded to a value of 0 and 1, respectively. Absolute values were taken in order to assure interpretability of the PSS estimates. That is, for the TBW, there is no possibility of negative values; thus the smaller the window is, the closer our normalized estimate is to 0, whether absolute values are taken or not. For the PSS, however, negative values are possible. Here, however, we are interested in determining the relationship of a particular individual's PSS to true synchrony, SOA = 0 ms. Hence, we take the absolute value. Deriving these normalized values allows for comparison across time scales and participants but undoubtedly obfuscates interpretation. To be clear, this data is normalized within subjects, and hence, when PSS approaches 0, it does not mean that the group's PSS was equal to zero, but that at this instance all or most participants were at their smallest PSS (in absolute value). Similarly, a TBW of or close to zero indicates the smallest TBW reached for each individual—a normalized TBW of 0.1 is more precise than a TBW of 0.2 but delineates no absolute measure of "preciseness."

The effects of feedback on recalibration (i.e., analyses comprised in Figure 2; first section) are analyzed via a

one-sample t-test versus the initial estimate of the given parameter (i.e., estimate on Trial 0). The impact of the nature of the feedback (positive versus negative; second section) on recalibration is analyzed via one-sample t-test (as above) and via within-subjects ANOVAs where appropriate (see below). Similarly, for the analyses regarding the reliability of feedback (i.e., third section), results are analyzed with both one-sample t-test and within- and between-subjects ANOVAs, where appropriate. Given the inherent multiple comparisons problem in utilizing a sliding-window approach, we correct for false positives by considering an effect significant by setting $\alpha < 0.01$ for at least 10 consecutive window positions (see [25] for a similar approach).

3. Results and Discussion

3.1. Feedback Accelerates and Maintains Cumulative Temporal Recalibration. Previous adaptation studies have shown that temporal recalibration occurs over slow time scales as extended periods of passive exposure to asynchronous stimuli (often biased in the direction of either an auditory or visual leading stimulus with a constant SOA) elicit changes in perceptual representations as indexed via the PSS and TBW (audiovisual, see [12, 13, 15, 22–24, 28, 42, 43]; for other modalities see [15]). Here, we sought to address if sensory experience for unbiased, asynchronous stimuli elicited changes in time course of the PSS or TBW based on immediately prior (rapid calibration) or cumulative (cumulative recalibration) sensory history. We first sought to assess the cumulative time course of temporal recalibration in the presence or absence of feedback as participants completed the SJ task (i.e., feedback, in this initial comparison, was reliable on 100% of trials). In the presence of feedback, the PSS, as illustrated in Figure 2(a), decreased in absolute value over time. This shift in the PSS toward objective synchrony (i.e., an SOA of 0 ms) became significant for the interval between Trials 413 and 623 (black bar denotes period of significant difference, one-sample t test; $t(24) => 2.49$, $p < 0.01$, partial eta-squared => 0.09). In contrast, the absence of feedback (Figure 2(c)) failed to result in any significant changes in the PSS over the course of the experiment (all $p \geq 0.04$). These results illustrate that feedback coupled to the presentation of sensory information, but not sensory statistics alone, was responsible for the shift in the PSS toward objective synchrony.

With regard to the TBW, as illustrated in Figures 2(b) and 2(d), there was significant narrowing for groups receiving feedback ((a) and (b), significant at $p < 0.01$ between Trials 170 and 720, one-sample t test, $t(24) => 2.49$, partial eta-squared => 0.09) as well as for those who did not ((c) and (d), significant between Trials 370 and 540, $t(24) => 2.49$, partial eta-squared => 0.09). These results highlight a cumulative recalibration of audiovisual temporal acuity, even under circumstances of more passive sensory stimulation. However, the dynamics of these changes differed between the feedback and no-feedback conditions, with the narrowing arising more rapidly in the presence of feedback and persisting until the end of the feedback epoch (as opposed to the transient effect observed in the case of no feedback).

In addition to examining the effects during the training interval (i.e., the period in which feedback was given, Trials 1–720), we also sought to examine the durability of these effects following the removal of feedback. This assessment was carried out over Trials 721–860. For individuals previously given feedback, the earlier effect of cumulative recalibration of the TBW persisted over Trials 721–744 ($t(24) => 2.49$, $p < 0.01$) but dissipated with time. For the group that did not receive feedback, no change in the time course of cumulative recalibration was observed during this period (Trials 721–860, all $p \geq 0.29$). For the PSS, not surprisingly we did not observe any additional changes in the time course of cumulative recalibration during this period for both the group receiving feedback and the group that did not receive feedback (all $p \geq 0.20$).

In contrast to these cumulative recalibration effects on both the PSS and TBW, little was seen in regard to a change in the time course of rapid recalibration with regard to the initial estimate of rapid recalibration at Trial 0 (see Figure S1). Thus, when the data were analyzed on the basis of the immediately preceding trial (audio- versus video-leading), there were no apparent changes in the time course of recalibration effects for either the PSS or the TBW, or for the feedback and no-feedback groups (all $p \geq 0.34$). We did, however, observe that, for the mean of all trials, the PSS (Feedback M (mean) = 14.8 ms, one-sample t-test to zero; $t(24) =< 3.46$, $p < 0.001$, partial eta-squared => 0.17; No Feedback $M = 11.1$ ms, $t(14) =< 3.78$, $p < 0.001$, partial eta-squared => 0.35) and TBW (Feedback $M = 5.1$ ms, $t(24) =< 3.46$, partial eta-squared => 0.17, $p < 0.001$; No Feedback $M = 5.1$ ms, $t(14) =< 3.78$, partial eta-squared => 0.35, $p < 0.001$) were significantly shifted on a trial-to-trial basis. Thus, while a significant effect of rapid recalibration is present between individual trials, the magnitude of the recalibration does not change when analyzed as a time course. Hence, we conclude that while immediately prior sensory experience (i.e., bottom-up factors) shifted the PSS and TBW on a trial-to-trial basis, sensory experience alone is not sufficient to influence a change in the time course of rapid recalibration.

Collectively, the results illustrate that change in sensory statistics alone is enough to drive perceptual learning, as defined by the cumulative narrowing of the TBW in the no-feedback group. However, the time course of this plasticity is accelerated when feedback was provided. Further, changes in the PSS, which took place over a slower time scale and were more transient when compared to the TBW, indicated that this measure is more stable as compared to the TBW (a finding reinforced by the lack of change for the PSS in the no-feedback conditions). Although prior work has shown perceptual learning in the absence of a reinforcement signal [12, 13], the enhanced temporal recalibration observed when a feedback signal is present resembles the enhancing effect of feedback for other forms of perceptual learning [16, 17]. Thus, while perceptual learning may occur over time, feedback accelerates perceptual learning. The capacity for feedback to elicit more rapid temporal recalibration in response to feedback is likely adaptive as it would allow for faster changes in perception that would allow for more accurate responses to the salient aspects of the sensory environment. For other

indices of temporal perception, as we observe for the PSS, feedback may be essential for perceptual learning to occur [33, 44], although our data does not preclude temporal recalibration of the PSS with increasing sensory exposure.

3.2. Positive and Negative Feedback Differentially Impact the Time Course of Temporal Recalibration. As illustrated above, feedback strongly influences the time course of cumulative audiovisual temporal recalibration. However, how this feedback is driving these changes remains an open question. Stated differently, individuals received two forms of feedback in the context of this task—positive feedback when they were correct in their judgment and negative feedback when they were incorrect in their judgment. Do these two types of feedback differentially impact the time course of temporal recalibration? That such a distinction might exist is grounded in evidence from studies of reward system circuitry, which show that this system is differentially activated by positive and negative feedback and is underpinned by distinct neural networks [10]. Additionally, although no change was seen in rapid recalibration in the presence of feedback, this initial analysis lumped together positive and negative feedback, which may have masked differential effects based on prior feedback history. Hence, we analyzed both cumulative and rapid recalibration effects of the PSS and TBW as a function of whether individuals were correct (i.e., received positive feedback) or incorrect (i.e., received negative feedback) on the previous trial. That is, in order to assess if the time course of temporal recalibration was affected by positive or negative feedback, distributions of perceived simultaneity (i.e., report of synchrony) as a function of SOA were compiled for each participant separately for the cases in which on the precedent trial (t-1) participants were informed that their answer had been correct (t-1 correct; prior positive feedback) or incorrect (t-1 incorrect; prior negative feedback). Additionally, in order to compute rapid recalibration effects, reports of synchrony were further bifurcated into those in which trial t-1 had either a negative (i.e., audition led) or positive SOA (i.e., vision led).

Findings revealed a relatively small effect of feedback type on the dynamics of PSS cumulative recalibration. Negative feedback drove a very transient change in the PSS toward true synchrony (i.e., smaller absolute value; significant at $p < 0.01$, $t(24) => 2.49$, partial eta-squared => 0.11, between Trials 392–409; Figure 3(a)). Positive feedback did not elicit significant cumulative recalibration of the PSS (Figure 3(c), black lines). In contrast, for the TBW, cumulative recalibration was greatly impacted by feedback. Following prior incorrect responses (i.e., negative feedback), narrowing of the cumulative TBW was evident earlier and sustained over a longer time course (Trials 200–720, $p < 0.01$, $t(24) => 2.49$, partial eta-squared => 0.11) than changes to the TBW observed following prior correct responses (i.e., positive feedback) (Trials 418–551; Figures 3(b) and 3(d)). Collectively, these results support the conclusion that feedback that informs (i.e., incorrect feedback), rather than confirms (i.e., correct feedback), a perceptual decision accelerates and sustains perceptual learning.

For rapid recalibration, immediately preceding positive feedback elicited a significant change in PSS that began relatively early and lasted for the duration of the feedback (i.e., significant, $p < 0.01$, $t(24) => 2.49$, partial eta-squared => 0.11, change in PSS between Trials 239 and 720 for t-1 correct trials; Figure 3(c), red lines). Thus, it appears that, following a signal confirming a perceptual decision, individuals exhibited a greater propensity for adjusting their PSS on a trial-by-trial basis. In contrast, no significant change in the PSS was seen after negative feedback (all $p \geq 0.39$). No change in rapid recalibration of the TBW was observed as a function of positive or negative feedback (all $p > 0.52$).

In order to examine the interaction between cumulative and rapid recalibration effects as a function of feedback type, separate 2 (cumulative versus rapid) × 2 (previous trial correct versus incorrect) within-subjects ANOVAs for the PSS and TBW were conducted. As illustrated in Figure 3, a significant interaction was observed for the PSS (Trials 301–399, $p < 0.01$, $F(1, 96) => 6.91$, partial eta-squared => 0.06, as illustrated by the gray shaded area). This effect was driven by the finding that when on the previous trial participants had been informed of an incorrect response, the time courses of cumulative and rapid recalibration followed one another. This was not the case when the participant had been informed of a correct response on the previous trial. Hence, when participants were informed of a correct response on the preceding trial, they appear to more readily incorporate recent sensory evidence into their judgments. Summarizing these results, under conditions of informative (i.e., negative) feedback, the time courses of rapid and cumulative recalibration appear to be yoked, while, under conditions of confirmative (i.e., positive) feedback, rapid and cumulative recalibration effects appear to uncouple. This uncoupling may be adaptive in that only corrective signals are able to drive rapid plasticity.

3.3. Time Course of Rapid Recalibration of the TBW Diverges as a Function of Prior Feedback Reliability. To better understand the contribution of feedback to recalibration processes and the interrelationship between rapid and cumulative recalibration effects, we tested whether changing the reliability of the feedback would differentially alter rapid versus cumulative temporal recalibration. Prior studies of visual perceptual learning have demonstrated that while feedback enhances perceptual learning, presenting feedback that is uncorrelated to responses (i.e., unreliable feedback) impairs perceptual learning [45]. Feedback was provided to different groups of participants and was reliable on 100%, 80%, or 50% of trials (for this comparison, the group receiving 100% reliable feedback was the same group of participants that was previously compared to the no-feedback condition; see Section 3.1). We hypothesized that if the time course of temporal recalibration was dependent on external reinforcement, we would see progressively less temporal recalibration as feedback reliability decreased. Indeed, unlike the group receiving 100% reliable feedback (described above), we did not observe cumulative recalibration of the PSS for the groups receiving 80% or 50% reliable feedback (see Figure S2). In contrast, however, we did observe cumulative recalibration of the TBW for all groups, although these changes were seen over a shorter extent of trials when compared with the 100% reliable feedback group (see Figure S2). Specifically, when participants were 100% reliably informed of their performance, TBWs were

significantly smaller during and after feedback than before feedback between Trials 170 and 744 (all $p < 0.01$). In the cases of 80% and 50% reliable feedback, the feedback effects were somewhat more short-lived (resp., between Trials 305 and 541, $p < 0.01$, and between Trials 219 and 430, $p < 0.01$), nonetheless apparent. These findings are similar to the transient change in the TBW without any changes in the PSS that was observed in the absence of feedback (see Section 3.1).

In order to examine the different time courses of multisensory temporal recalibration as a function of feedback reliability, we conducted separate 2 (type of recalibration: cumulative versus rapid) × 3 (feedback reliability: 100%, 80%, 50%) between-subjects ANOVAs for the PSS and TBW along the time-series of trials such that an effect was interpreted as significant at $\alpha < 0.01$ for at least 10 consecutive trials. For the PSS, we did not observe a main effect of type of recalibration, feedback reliability, or an interaction (see Figure S2, all $p \geq 0.24$). When this analysis was expanded to include the no-feedback group, conducting a 2 (type of recalibration: cumulative versus rapid) × 4 (feedback reliability: 100%, 80%, 50%, no feedback) mixed model ANOVA on PSS values did not alter the above-mentioned findings (all $p > 0.18$). In contrast, for the TBW, we observed a significant main effect of type of recalibration between Trials 103 and 841 (all $p < 0.01$, $F(1, 294) => 6.72$, partial eta-squared => 0.04) and a significant type of recalibration × feedback reliability interaction between Trials 816 and 844 (Figure 4; $F(2, 294) => 4.68$, all $p < 0.01$, partial eta-squared => 0.03; indicated by the gray shading). Thus, and as is evident in Figure 4, although the dynamics of cumulative temporal recalibration of the TBW failed to differ dependent upon feedback reliability ((a); one-way between-subjects ANOVA, all $p > 0.06$), the dynamics of rapid temporal recalibration of the TBW did diverge (b). Specifically, a one-way between-subject ANOVA on the rapid recalibration values demonstrated a significant effect between Trials 806 and 851 ($F(2, 47) => 5.09$, all $p < 0.01$, partial eta-squared => 0.17). Subsequent post hoc t-tests performed on the rapid recalibration patterns as a function of feedback reliability demonstrated that the 50% reliable feedback elicited a higher degree of rapid recalibration (variability on a trial-by-trial basis, weighting more heavily immediately preceding sensory experience) than the 80% reliable feedback (between Trials 780 and 861, $t(23) => 2.50$, $p < 0.01$, partial eta-squared => 0.21) and the 100% reliable feedback (between Trials 801 and 827, $t(35) => 2.43$, $p < 0.01$, partial eta-squared => 0.14). The 100% and 80% reliable feedback conditions did not differ from one other (all $p > 0.33$). Additionally, when performing one-sample t-test to their respective departing values after the no-feedback phase (e.g., Trial 0) the 50% reliable group demonstrated a significant increase in TBW rapid recalibration (Trial 556 onward, $t(11) => 2.71$, $p < 0.01$, partial eta-squared => 0.4), while the 80% and 100% reliable groups showed no change (all $p > 0.03$).

Enlarging this analysis in order to include the no-feedback group and conducting a 2 (type of recalibration: cumulative versus rapid) × 4 (feedback reliability: 100%, 80%, 50%, no feedback) mixed model ANOVA on TBW values conserved the presence of a main effect of type of recalibration between Trials 117 and 841 (all $p < 0.01$, $F(3, 294) \geq 5.12$, partial eta-squared ≥ 0.06) and a significant type of recalibration × feedback reliability interaction between Trials 816 and 844 ($F(4, 294) \geq 3.18$, all $p < 0.01$). Feedback reliability groups did not differ from one another with regard to the time course of cumulative recalibration (between-subjects one-way ANOVA; all $p > 0.03$) but did regarding the time course of rapid recalibration (between-subjects one-way ANOVA, $p < 0.01$) between Trials 806 and 851 (as mentioned above). Subsequent post hoc t-test showed that the no-feedback group differed from the 100% ($p < 0.01$, more trial-to-trial recalibration in the no-feedback group between Trials 825 and 860), the 80% ($p < 0.01$, more trial-to-trial recalibration in the no-feedback group between Trials 818 and 860), and the 50% reliability groups ($p < 0.01$, less trial-to-trial recalibration in the no-feedback group between Trials 809 and 827).

The increase in rapid recalibration when feedback is not present during the post-feedback trial block for the group that had previously been presented with the 50% reliable feedback signal may represent an increased tendency for the subjects to disregard feedback and more heavily weigh sensory statistics when prior feedback has been unreliable in signaling the correctness of their judgments.

This finding represents the second example in our data of an uncoupling between cumulative and rapid recalibration (the first being that brought about by the correct versus incorrect nature of the feedback). Namely, we observe that when feedback reliability is reduced, perceptual learning occurs, but with differing dynamics for cumulative and rapid recalibration, again suggesting differing mechanistic processes. We hypothesize that, as a result of the conflict between sensory evidence and feedback signals, those individuals presented with the least reliable feedback (50%) were more likely to rely on immediate sensory information to recalibrate their audiovisual temporal representation. This may be due to a decreased reliance on top-down signals generated by sensory feedback and an increased reliance on bottom-up sensory information. In the groups receiving unreliable feedback, as some of the feedback was misinformative, increased reliance on sensory statistics would be adaptive in that sensory driven recalibration would produce a more accurate perceptual representation.

4. General Discussion

Here we show that top-down factors (i.e., feedback signals) can interact with bottom-up signals in order to change the dynamic time course of temporal recalibration for two measures of audiovisual temporal perception (PSS and TBW). By employing a sliding-window analysis for this study, we were able to characterize, for the first time, how rapid and cumulative temporal recalibration occur in both the presence and absence of feedback and to characterize the differing temporal dynamics for these two time scales of perceptual learning. Our findings illustrate that while sensory experience alone is sufficient to elicit some degree of temporal recalibration, feedback signals can work in conjunction with sensory experience to produce greater perceptual plasticity.

That feedback signals alter the dynamics of temporal recalibration is not surprising as enhanced plasticity would

be adaptive in response to changing environmental statistics or task demands. Despite this assumption, it is interesting that feedback is sufficient, if only transiently, to alter perceptual representations for which a strong history of sensory experience exists. The PSS, a measure that is reflective of an individual's internal representation of the temporal statistical structure of the external world, is rarely at true synchrony (i.e., 0 ms). Rather, this measure is typically biased toward an asynchrony in which the visual stimulus leads the auditory stimulus—reflective of the typical statistical structure of audiovisual stimuli within our world [30, 32, 34, 46]. Although adaptation studies have shown that repeated presentation of asynchronous audiovisual stimuli (i.e., toward either a visual or auditory leading stimulus set) can shift the PSS in the direction of the experienced asynchrony [47–49], we report a shift in the PSS in the absence of any changes in the temporal structure of the stimuli and based solely on the presence of feedback. Indeed, the changes elicited under such circumstances are invariably in the direction of true synchrony. As we did not introduce a change in the temporal structure of the stimuli that would favor a directional shift in the PSS, we conclude that this change is driven largely by top-down factors linked to the delivery of feedback.

That the changes in TBW and PSS in response to feedback are quick to develop is also not surprising as this too may be adaptive. Interestingly, it also appears that, over the course of a single session, both sensory and feedback-induced changes in the PSS and TBW can be quick to dissipate as, with the exception of the group receiving 100% reliable feedback, the time course returns to the level of the initial estimate within a relatively small number of trials after feedback is removed. As studies of perceptual training have reported changes in temporal acuity between training sessions [50, 51], it is possible that by extending our analysis across multiple sessions we might observe further changes in the time course of recalibration. Future investigations will be necessary to determine if sensory experience or feedback elicits durable changes in the PSS and TBW or whether the plasticity we observe is simply reflective of fast adaptation.

Future studies may also explore if unreliable feedback elicits lasting changes beyond the post-feedback period measured in this study and if such changes differ from any changes elicited by sensory experience in the absence of feedback. Although we observed similarities in the time course of recalibration of the TBW and PSS in the absence of feedback and with unreliable feedback, the mechanism by which these changes occur may be different. It is possible that the return to original levels in performance we observed may be due to a change in criteria when unreliable feedback was present (i.e., Trials 1–720) rather than perceptual learning that results in a lasting change in the perceptual representation [52]. Changing perceptual decision criteria in response to erroneous (i.e., unreliable) feedback has been suggested to be adaptive as such a transient change in criteria would minimize error signals while protecting prior representations of the stimuli [53]. Thus, when the unreliable feedback signal is removed, the criterion can be rapidly adjusted to criterion prior to exposure to unreliable feedback. Although changes in criterion are usually limited to a perceptual training session, changes in criterion are typically not observed during a second session a day later whereas changes in sensitivity are maintained after at least a day [54]. By extending the time course analysis of temporal recalibration beyond a single day, we would hypothesize that if unreliable feedback elicited any durable change in the PSS or TBW, we would observe a change in the PSS or TBW relative to the final estimate of the TBW or PSS on the first day.

Increasing evidence suggests that the mechanisms supporting unisensory (i.e., within-modality) perceptual learning are evident at higher cortical levels [33, 55] and that enhanced perception of amodal sensory properties due to perceptual training in modality can exhibit transfer across sensory modalities to an untrained sensory modality [56, 57]. Stimulus exposure that is more passive in nature appears to drive changes at lower cortical levels while increasingly the relevance of the stimulus properties elicits changes at both higher and lower cortical levels [8]. Multisensory stimuli, which engage a larger cortical network than unisensory stimuli, may facilitate perceptual learning by increasing activity of primary sensory regions as well as higher-level sensory cortex. Recent evidence suggests that multisensory interactions, while present across different levels of the cortical hierarchy, may differ in their computational functions across higher-order and sensory regions [12, 13]. Accordingly, a feedback signal may also serve to engage a larger cortical network, which in turn enables a greater capacity for perceptual learning to occur.

A possible explanation for why greater temporal recalibration occurs with feedback, provided it is reliable, is that sensory readout is improved for higher-order cortical areas involved in sensory decision-making due to the feedback signal. At the neural level, this is in line with studies of visual perceptual learning that observed changes in activity patterns in the anterior cingulate cortex to track changes in decision-making during visual perceptual learning [34, 37]. Furthermore, neural evidence suggests that prediction error signals during perceptual learning refine and strengthen neural connectivity between sensory neurons and those neurons required for the perceptual response and thus may support changes in higher-order regions [58]. Thus, in the absence of an informative reinforcement signal, rapid but transient changes in perceptual plasticity are likely due to changes in low-level sensory areas. Future investigations will be necessary to determine if changes in the connectivity of higher-order cortical areas and low-level sensory processes underlie the observed changes in temporal recalibration and if these changes are durable or transient (see [58] for a helpful review in this regard).

5. Conclusions

We report that sensory experience and feedback signal interact to drive both rapid and cumulative temporal recalibration of the TBW and PSS for audiovisual stimuli. While rapid and cumulative temporal recalibration often follow similar time courses, these time courses may diverge dependent upon prior feedback signals. Our findings support the fact that prior sensory history feedback signals influence subsequent

perceptual plasticity to elicit both rapid and cumulative temporal recalibration.

Data Access

Data from this study can be viewed at https://vanderbilt.box.com/s/a04pr5dbsjrhrnquz5lrcvv5i6buafdp.

Competing Interests

The authors have no competing interests.

Authors' Contributions

Matthew A. De Niear, Jean-Paul Noel, and Mark T. Wallace designed the study; Matthew A. De Niear collected the data; Jean-Paul Noel and Matthew A. De Niear analyzed the data; Matthew A. De Niear, Jean-Paul Noel, and Mark T. Wallace wrote the manuscript. Matthew A. De Niear and Jean-Paul Noel contributed equally to this work.

Acknowledgments

The project was supported by NIH Grants CA183492 and HD083211, the Simons Foundation Autism Research Initiative, and the Wallace Foundation. Jean-Paul Noel was additionally supported by a NSF GRF (NSF-14-590).

References

[1] G. M. Ghose, "Learning in mammalian sensory cortex," *Current Opinion in Neurobiology*, vol. 14, no. 4, pp. 513–518, 2004.

[2] J. Medina and B. Rapp, "Rapid experience-dependent plasticity following somatosensory damage," *Current Biology*, vol. 24, no. 6, pp. 677–680, 2014.

[3] L. Yu, B. E. Stein, and B. A. Rowland, "Adult plasticity in multisensory neurons: short-term experience-dependent changes in the superior colliculus," *The Journal of Neuroscience*, vol. 29, no. 50, pp. 15910–15922, 2009.

[4] L. Shams and A. R. Seitz, "Benefits of multisensory learning," *Trends in Cognitive Sciences*, vol. 12, no. 11, pp. 411–417, 2008.

[5] M. Fahle, "Perceptual learning: specificity versus generalization," *Current Opinion in Neurobiology*, vol. 15, no. 2, pp. 154–160, 2005.

[6] M. Fahle, S. Edelman, and T. Poggio, "Fast perceptual learning in hyperacuity," *Vision Research*, vol. 35, no. 21, pp. 3003–3013, 1995.

[7] D. R. Wozny and L. Shams, "Recalibration of auditory space following milliseconds of cross-modal discrepancy," *The Journal of Neuroscience*, vol. 31, no. 12, pp. 4607–4612, 2011.

[8] T. Watanabe, J. E. Náñez Sr., S. Koyama, I. Mukai, J. Liederman, and Y. Sasaki, "Greater plasticity in lower-level than higher-level visual motion processing in a passive perceptual learning task," *Nature Neuroscience*, vol. 5, no. 10, pp. 1003–1009, 2002.

[9] M. Fahle and S. Edelman, "Long-term learning in vernier acuity: effects of stimulus orientation, range and of feedback," *Vision Research*, vol. 33, no. 3, pp. 397–412, 1993.

[10] A. R. Seitz and H. R. Dinse, "A common framework for perceptual learning," *Current Opinion in Neurobiology*, vol. 17, no. 2, pp. 148–153, 2007.

[11] M. T. Wallace and R. A. Stevenson, "The construct of the multisensory temporal binding window and its dysregulation in developmental disabilities," *Neuropsychologia*, vol. 64, pp. 105–123, 2014.

[12] W. Fujisaki, S. Shimojo, M. Kashino, and S. Nishida, "Recalibration of audiovisual simultaneity," *Nature Neuroscience*, vol. 7, no. 7, pp. 773–778, 2004.

[13] J. Vroomen, M. Keetels, B. De Gelder, and P. Bertelson, "Recalibration of temporal order perception by exposure to audio-visual asynchrony," *Cognitive Brain Research*, vol. 22, no. 1, pp. 32–35, 2004.

[14] M. Keetels and J. Vroomen, "No effect of auditory–visual spatial disparity on temporal recalibration," *Experimental Brain Research*, vol. 182, no. 4, pp. 559–565, 2007.

[15] E. Van der Burg, D. Alais, and J. Cass, "Rapid recalibration to audiovisual asynchrony," *Journal of Neuroscience*, vol. 33, no. 37, pp. 14633–14637, 2013.

[16] J. Navarra, S. Soto-Faraco, and C. Spence, "Adaptation to audiotactile asynchrony," *Neuroscience Letters*, vol. 413, no. 1, pp. 72–76, 2007.

[17] M. Keetels and J. Vroomen, "Temporal recalibration to tactile-visual asynchronous stimuli," *Neuroscience Letters*, vol. 430, no. 2, pp. 130–134, 2008.

[18] J.-P. Noel and M. Wallace, "Relative contributions of visual and auditory spatial representations to tactile localization," *Neuropsychologia*, vol. 82, pp. 84–90, 2016.

[19] J. Vroomen and M. Keetels, "Perception of intersensory synchrony: a tutorial review," *Attention, Perception, and Psychophysics*, vol. 72, no. 4, pp. 871–884, 2010.

[20] B. E. Stein, T. R. Stanford, and B. A. Rowland, "Development of multisensory integration from the perspective of the individual neuron," *Nature Reviews Neuroscience*, vol. 15, no. 8, pp. 520–535, 2014.

[21] J.-P. Noel, M. Łukowska, M. Wallace, and A. Serino, "Multisensory simultaneity judgment and proximity to the body," *Journal of Vision*, vol. 16, no. 3, article no. 21, 2016.

[22] C. Harvey, E. Van Der Burg, and D. Alais, "Rapid temporal recalibration occurs crossmodally without stimulus specificity but is absent unimodally," *Brain Research*, vol. 1585, pp. 120–130, 2014.

[23] E. Van der Burg and P. T. Goodbourn, "Rapid, generalized adaptation to asynchronous audiovisual speech," *Proceedings of the Royal Society B: Biological Sciences*, vol. 282, no. 1804, 2015.

[24] P. Bruns and B. Röder, "Sensory recalibration integrates information from the immediate and the cumulative past," *Scientific Reports*, vol. 5, Article ID 12739, 2015.

[25] J.-P. Noel, M. A. De Niear, R. Stevenson, D. Alais, and M. T. Wallace, "Atypical rapid audio-visual temporal recalibration in autism spectrum disorders," *Autism Research*, vol. 10, no. 1, pp. 121–129, 2017.

[26] J. Noel, M. De Niear, E. Van der Burg, M. T. Wallace, and J. Ahveninen, "Audiovisual simultaneity judgment and rapid recalibration throughout the lifespan," *PLOS ONE*, vol. 11, no. 8, Article ID e0161698, 2016.

[27] D. M. Simon, J. P. Noel, and M. Wallace, "Evoked related potentials index rapid recalibration to audiovisual temporal asynchrony," *Frontiers in Integrative Neuroscience*, In press.

[28] E. Van Der Burg, D. Alais, and J. Cass, "Audiovisual temporal recalibration occurs independently at two different time scales," *Scientific Reports*, vol. 5, Article ID 14526, 2015.

[29] A. R. Seitz, J. E. Nanez Sr., S. Holloway, Y. Tsushima, and T. Watanabe, "Two cases requiring external reinforcement in

perceptual learning," *Journal of Vision*, vol. 6, no. 9, pp. 966–973, 2006.

[30] A. R. Seitz, D. Kim, and T. Watanabe, "Rewards evoke learning of unconsciously processed visual stimuli in adult humans," *Neuron*, vol. 61, no. 5, pp. 700–707, 2009.

[31] C.-T. Law and J. I. Gold, "Neural correlates of perceptual learning in a sensory-motor, but not a sensory, cortical area," *Nature Neuroscience*, vol. 11, pp. 505–513, 2008.

[32] C.-T. Law and J. I. Gold, "Reinforcement learning can account for associative and perceptual learning on a visual-decision task," *Nature Neuroscience*, vol. 12, pp. 655–663, 2009.

[33] T. Watanabe and Y. Sasaki, "Perceptual learning: toward a comprehensive theory," *Annual Review of Psychology*, vol. 66, pp. 197–221, 2015.

[34] A. R. Powers III, A. R. Hillock, and M. T. Wallace, "Perceptual training narrows the temporal window of multisensory binding," *Journal of Neuroscience*, vol. 29, no. 39, pp. 12265–12274, 2009.

[35] A. R. Powers, A. Hillock-Dunn, and M. T. Wallace, "Generalization of multisensory perceptual learning," *Scientific Reports*, vol. 6, Article ID 23374, 2016.

[36] M. A. de Niear, B. Koo, and M. T. Wallace, "Multisensory perceptual learning is dependent upon task difficulty," *Experimental Brain Research*, pp. 1–9, 2016.

[37] A. R. Powers, M. A. Hevey, and M. T. Wallace, "Neural correlates of multisensory perceptual learning," *Journal of Neuroscience*, vol. 32, no. 18, pp. 6263–6274, 2012.

[38] R. A. Stevenson and M. T. Wallace, "Multisensory temporal integration: task and stimulus dependencies," *Experimental Brain Research*, vol. 227, no. 2, pp. 249–261, 2013.

[39] R. A. Stevenson, S. Park, C. Cochran et al., "The associations between multisensory temporal processing and symptoms of schizophrenia," *Schizophrenia Research*, vol. 179, pp. 97–103, 2017.

[40] D. H. Brainard, "The psychophysics toolbox," *Spatial Vision*, vol. 10, no. 4, pp. 433–436, 1997.

[41] D. G. Pelli, "The VideoToolbox software for visual psychophysics: transforming numbers into movies," *Spatial Vision*, vol. 10, no. 4, pp. 437–442, 1997.

[42] E. Van der Burg, E. Orchard-Mills, and D. Alais, "Rapid temporal recalibration is unique to audiovisual stimuli," *Experimental Brain Research*, vol. 233, no. 1, pp. 53–59, 2014.

[43] J.-P. Noel, M. T. Wallace, E. Orchard-Mills, D. Alais, and E. Van Der Burg, "True and perceived synchrony are preferentially associated with particular sensory pairings," *Scientific Reports*, vol. 5, Article ID 17467, 2015.

[44] T. Watanabe, J. E. Náñez, and Y. Sasaki, "Perceptual learning without perception," *Nature*, vol. 413, no. 6858, pp. 844–848, 2001.

[45] M. H. Herzog and M. Fahle, "The role of feedback in learning a vernier discrimination task," *Vision Research*, vol. 37, no. 15, pp. 2133–2141, 1997.

[46] D. B. Polley, E. E. Steinberg, and M. M. Merzenich, "Perceptual learning directs auditory cortical map reorganization through top-down influences," *Journal of Neuroscience*, vol. 26, no. 18, pp. 4970–4982, 2006.

[47] X. Liu, J. Hairston, M. Schrier, and J. Fan, "Common and distinct networks underlying reward valence and processing stages: a meta-analysis of functional neuroimaging studies," *Neuroscience and Biobehavioral Reviews*, vol. 35, no. 5, pp. 1219–1236, 2011.

[48] K. M. Lempert and E. Tricomi, "The value of being wrong: intermittent feedback delivery alters the striatal response to negative feedback," *Journal of Cognitive Neuroscience*, vol. 28, no. 2, pp. 261–274, 2016.

[49] A. Bischoffgrethe, E. Hazeltine, L. Bergren, R. Ivry, and S. Grafton, "The influence of feedback valence in associative learning," *NeuroImage*, vol. 44, no. 1, pp. 243–251, 2009.

[50] N. F. Dixon and L. Spitz, "The detection of auditory visual desynchrony," *Perception*, vol. 9, no. 6, pp. 719–721, 1980.

[51] M. Zampini, D. I. Shore, and C. Spence, "Audiovisual temporal order judgments," *Experimental Brain Research*, vol. 152, no. 2, pp. 198–210, 2003.

[52] M. H. Herzog and M. Fahle, "Effects of biased feedback on learning and deciding in a vernier discrimination task," *Vision Research*, vol. 39, no. 25, pp. 4232–4243, 1999.

[53] M. H. Herzog, K. R. F. Ewald, F. Hermens, and M. Fahle, "Reverse feedback induces position and orientation specific changes," *Vision Research*, vol. 46, no. 22, pp. 3761–3770, 2006.

[54] K. C. Aberg and M. H. Herzog, "Different types of feedback change decision criterion and sensitivity differently in perceptual learning," *Journal of Vision*, vol. 12, no. 3, 2012.

[55] N. Zilber, P. Ciuciu, A. Gramfort, L. Azizi, and V. Van Wassenhove, "Supramodal processing optimizes visual perceptual learning and plasticity," *NeuroImage*, vol. 93, no. 1, pp. 32–46, 2014.

[56] D. P. McGovern, A. T. Astle, S. L. Clavin, and F. N. Newell, "Task-specific transfer of perceptual learning across sensory modalities," *Current Biology*, vol. 26, no. 1, pp. R20–R21, 2016.

[57] B. Barakat, A. R. Seitz, and L. Shams, "Visual rhythm perception improves through auditory but not visual training," *Current Biology*, vol. 25, no. 2, pp. R60–R61, 2015.

[58] T. Rohe and U. Noppeney, "Distinct computational principles govern multisensory integration in primary sensory and association cortices," *Current Biology*, vol. 26, no. 4, pp. 509–514, 2016.

Hindawi
Neural Plasticity
Volume 2017, Article ID 6724631, 10 pages
https://doi.org/10.1155/2017/6724631

Research Article

Short-Term Monocular Deprivation Enhances Physiological Pupillary Oscillations

Paola Binda[1,2] and Claudia Lunghi[1,2]

[1]*Department of Translational Research on New Technologies in Medicine and Surgery, University of Pisa, Pisa, Italy*
[2]*CNR Neuroscience Institute, Pisa, Italy*

Correspondence should be addressed to Claudia Lunghi; clalunghi@gmail.com

Received 28 October 2016; Accepted 18 December 2016; Published 9 January 2017

Academic Editor: Fang Hou

Short-term monocular deprivation alters visual perception in adult humans, increasing the dominance of the deprived eye, for example, as measured with binocular rivalry. This form of plasticity may depend upon the inhibition/excitation balance in the visual cortex. Recent work suggests that cortical excitability is reliably tracked by dilations and constrictions of the pupils of the eyes. Here, we ask whether monocular deprivation produces a systematic change of pupil behavior, as measured at rest, that is independent of the change of visual perception. During periods of minimal sensory stimulation (in the dark) and task requirements (minimizing body and gaze movements), slow pupil oscillations, "hippus," spontaneously appear. We find that hippus amplitude increases after monocular deprivation, with larger hippus changes in participants showing larger ocular dominance changes (measured by binocular rivalry). This tight correlation suggests that a single latent variable explains both the change of ocular dominance and hippus. We speculate that the neurotransmitter norepinephrine may be implicated in this phenomenon, given its important role in both plasticity and pupil control. On the practical side, our results indicate that measuring the pupil hippus (a simple and short procedure) provides a sensitive index of the change of ocular dominance induced by short-term monocular deprivation, hence a proxy for plasticity.

1. Introduction

Recent studies have shown that activity in early visual cortex can be altered by a short period of monocular deprivation (MD) in adult humans. Specifically, after a few hours of monocular deprivation, ocular dominance unexpectedly shifts in favor of the deprived eye [1–7]. For example, monocular deprivation has dramatic perceptual consequences on the dynamics of binocular rivalry (a particular form of bistable perception that engages strong competition between the monocular signals [8]): following deprivation, the deprived eye dominates rivalrous perception for twice as long as the nondeprived eye, indicating a strong shift of ocular dominance in favor of the deprived eye [2, 3]. This apparently counterintuitive effect reflects a compensatory reaction of the visual system to the transient impoverishment of monocular visual input that is likely mediated by an upregulation of contrast-gain control mechanisms of the deprived eye (this hypothesis is supported by evidence that short-term monocular deprivation increases apparent contrast of the deprived eye [2]). These results indicate that the adult human visual cortex retains a high degree of homeostatic plasticity that takes place in the early levels of visual processing, since short-term monocular deprivation modulates the earliest component of the Visual Evoked Potential [1].

Evidence from animal studies has suggested that a key determinant for adult visual cortical plasticity is the balance between intracortical excitation and inhibition [9]. For instance, the critical period for ocular dominance plasticity is regulated by the maturation of specific GABAergic circuits [10, 11], suggesting that the decreased plastic potential of the visual cortex observed in adulthood can be determined by an increase of inhibition [12]. Consistent with this hypothesis, ocular dominance plasticity can be reinstated in adult animals

by decreasing GABAergic inhibition (pharmacologically [13] or through environmental manipulations [14–16]). A recent study has shown that following 2.5 hours of monocular deprivation GABA concentration (measured by means of Magnetic Resonance Spectroscopy at 7-Tesla) drops in the adult primary visual cortex and across subjects the decrease in GABA levels highly correlates with the boost of deprived eye during binocular rivalry [4]. In agreement with the animal literature, these results strongly suggest that a release of GABAergic inhibition plays a crucial role in mediating homeostatic plasticity in adult humans.

Ocular dominance plasticity in adult animals can also be reinstated by increasing excitation. Specifically, three classes of excitatory neurotransmitters have been found to enhance visual cortical plasticity: serotonin [17], acetylcholine (Ach) [18], and norepinephrine (NE) [19, 20]. However, there is no evidence at present about a role of excitatory signaling modulating adult visual plasticity in humans.

The animal literature has recently highlighted how cortical excitability may be monitored through a simple, noninvasive, and yet sensitive measure: the diameter of the pupil [21]—resonating with a long tradition of studies in human participants [22].

It is well known that a range of stimuli can evoke pupil constrictions and dilations [23]: not only light increments and decrements, but also equiluminant stimuli [evoking a transient constriction [24]] and visual or nonvisual stimuli capable of evoking an orienting response [accompanied by pupil dilation, [25]]. Pupil dilations also accompany task effort, both physical work [e.g., [26]] and mental effort [27]. However, when stimulation is kept to a constant and minimal level and no task is assigned, the pupil still shows variations in size. These take the form of quasiperiodic slow oscillations, sometimes termed hippus [23, 28–30].

In the mouse, these alternations of pupil constriction and dilation effectively track the responsiveness of the cortex to sensory stimuli [21, 26, 31, 32]. Specifically, dilations are coupled with desynchronized activity across neural populations and increased sensitivity to visual/somatosensory stimulation, both time-locked to the change of activity in different classes of inhibitory interneurons [26] and to signaling in the norepinephrine and acetylcholine systems [33].

In primates, low-frequency oscillations of pupil size have been studied in diverse contexts and often linked to arousal levels, although the interpretation of such link and its relevance to cortical excitability are not straightforward. There is a large body of work associating very slow and very large pupil size changes with diminished arousal or sleepiness in humans [28, 30], yet pupil dilations are generally associated with increased arousal [22, 27, 34, 35] and prompt orienting to sensory stimuli [25]. Moreover, slow pupil waves can accompany epileptic seizures characterized by abnormally increased cortical excitability [36, 37]. In general, recent work has convincingly shown that the relationship between arousal levels and pupil size is well explained by a coupling of pupil diameter with activity in the Locus Coeruleus, the subcortical nucleus responsible for NE release [38, 39].

The importance of NE for adult cortical plasticity on the one hand and the tight relationship between NE tone and pupil diameter on the other inspired us to ask whether adult cortical plasticity is accompanied by a systematic change in the dynamics of pupil diameter.

As done in past experiments on adult MD, we assess the plasticity effect by means of binocular rivalry, comparing eye dominance before and after eye-patching. We choose not to measure pupil dynamics during binocular rivalry, but in a separate session with no visual stimulation. This choice is motivated by prior work showing that pupil size is sensitive to the dynamics of binocular rivalry [40, 41] and that pupil responses to visual stimuli may be larger/smaller when the stimulus representation in the visual cortex is enhanced/suppressed, for example, enhanced during focused attention [42–46] or suppressed during saccadic eye movements [47, 48]. Thus, it is expected that pupil behavior during binocular rivalry changes after MD, simply as a result of its modifying the rivalrous interplay between the eyes [2] and affecting cortical responses to the deprived eye [1]. We avoid this confound by measuring pupil dynamics at rest: in the dark, with participants staring straight-ahead while no visual or otherwise sensory stimulus is manipulated.

2. Methods

2.1. Subjects. 10 subjects (5 females, mean age ± standard deviation: 24.57 ± 2.06) participated in the study. All subjects were naïve to the experiment, had normal or corrected-to-normal visual acuity, and did not show strong eye dominance (ratio between the two eyes binocular rivalry mean phases durations ≤ 1.5). Experimental procedures were approved by the regional ethics committee [Comitato Etico Pediatrico Regionale—Azienda Ospedaliero-Universitaria Meyer—Firenze (FI)] and are in line with the Declaration of Helsinki; participants gave their written informed consent.

2.2. General Procedure. We measured binocular rivalry and pupil diameter before and after 2 hours of monocular deprivation. The measurements obtained before the deprivation were used as baseline (two 180 sec experimental blocks for binocular rivalry, one 120 sec block of pupillary measurement).

During the two hours of monocular deprivation, observers watched a movie while sitting in front of a TV screen at a distance of 80 cm. Immediately after eye-patch removal, we measured binocular rivalry for 18 minutes in four separate 180 sec blocks separated by a two-minute break to allow the subject to rest: this is the standard protocol used in the previous studies on MD from our laboratory [2, 3, 49]. Two minutes after the last binocular rivalry block (20 minutes after eye-patch removal), we measured the pupillary diameter in one 120 sec block. A diagram of the experimental procedure is shown in Figure 1. Binocular rivalry and pupil size were measured in different setups, both housed in dark and quiet experimental rooms. This protocol allowed for collecting a single measure of pupil size before and (20 minutes) after MD; future work is necessary to measure the changes of pupil behavior immediately after eye-patch removal (when the effect on binocular rivalry is maximum) and later on

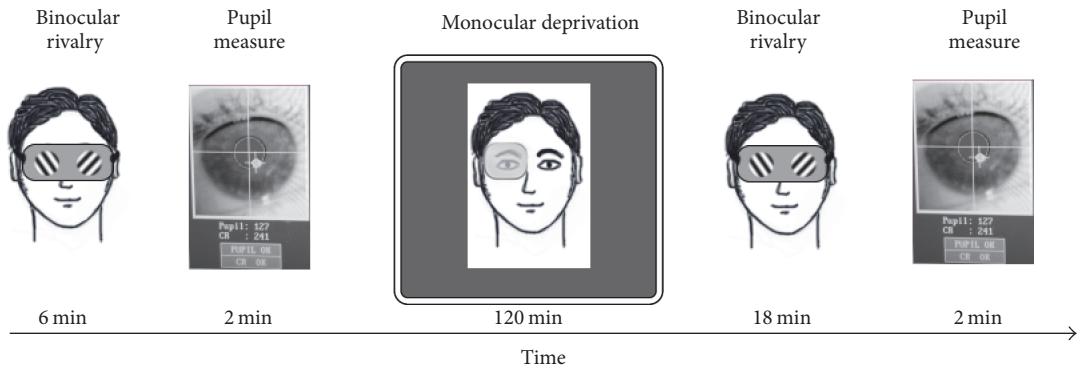

Figure 1: Diagram of the experimental procedure. Baseline binocular rivalry dynamics and pupillary measurements were obtained before deprivation (2 × 180 sec binocular rivalry blocks, 2 minutes of pupil measurement in total darkness). Short-term monocular deprivation was achieved by having observers wear a translucent eye-patch over the dominant eye for 2 hours. Immediately after eye-patch removal, 4 × 180 sec binocular rivalry blocks were acquired within a temporal interval of 18 minutes. Binocular rivalry tests were followed by 2 minutes of pupillary measurement in the dark.

(comparing the decay of the MD effect on pupil behavior versus binocular rivalry).

2.3. Monocular Deprivation. Previous reports [2, 3] have shown that monocular deprivation induces stronger shifts in eye-dominance when the dominant eye is patched compared to the nondominant eye. For this reason, in the current study monocular deprivation was performed by patching the dominant eye for 2 hours. Eye-dominance was assessed using binocular rivalry: the dominant eye was defined as the eye showing the longer mean phase duration in the baseline (predeprivation) measurements. The eye-patch was made of a translucent plastic material that allowed light to reach the retina (attenuation 15%) but completely prevented pattern vision, as assessed by the Fourier transform of a natural world image seen through the eye-patch.

2.4. Apparatus and Procedure: Binocular Rivalry. Visual stimuli were generated by the VSG 2/5 stimulus generator (CRS, Cambridge Research Systems), housed in a PC (Dell) controlled by Matlab (The Mathworks) scripts. Visual stimuli were two Gabor Patches (Gaussian-vignetted sinusoidal gratings), oriented either 45° clockwise or counterclockwise (size: $2\sigma = 2°$, spatial frequency: 2 cycles/degree of visual angle, and contrast: 50%), presented on a uniform background (luminance: 37.4 cd/m2, C.I.E.: 0.442 0.537) in central vision with a central black fixation point and a common squared frame to facilitate dichoptic fusion. Visual stimuli were displayed on a 20-inch Clinton Monoray (Richardson Electronics Ltd., LaFox, IL) monochrome monitor, driven at a resolution of 1024 × 600 pixels, with a refresh rate of 120 Hz. In order to achieve dichoptic stimulation, observers viewed the display at a distance of 57 cm through CRS ferromagnetic shutter goggles that occluded alternately one of the two eyes each frame.

Observers sat in front of the monitor wearing the shuttering goggles. After an acoustic signal (beep), the binocular rivalry stimuli appeared. Subjects reported their perception (clockwise, counterclockwise, or mixed) by continuously pressing with the right hand one of three keys (left, right, and down arrows) of the computer keyboard. Another acoustic signal (three beeps) signaled the end of each 180 sec experimental block. At each experimental block, the orientation associated to each eye was randomly varied so that neither subject nor experimenter knew which stimulus was associated with which eye until the end of the session, when it was verified visually.

2.5. Apparatus and Procedure: Pupillometry. An EyeLink 1000 system (SR Research, Canada) monitored two-dimensional eye position and pupil diameter with an infrared camera mounted below a monitor screen (Barco Calibrator, 40 × 30 cm), which was only used for calibrating the eye tracker (13-point calibration routine). The eye-monitor (and eye-camera) distance was maintained to 57 cm by means of a chin rest. Eye-tracking data were acquired at 1000 Hz and streamed from the EyeLink to a Mac Pro 4.1 through the EyeLink toolbox for Matlab [50]. The setup is hosted in an experimental room illuminated only by the monitor screen. Pupil diameter values were output online by the EyeLink system (computed with internal algorithms) and we only used Matlab to receive and store them together with gaze position estimates.

Recording sessions lasted 120 seconds, during which participants faced the monitor screen set to minimum luminance (<1 cd/m2) with no fixation point or other prominent features they might focus on. They were instructed to relax accommodation and stare straight-ahead, trying to avoid eye, head, and body movements and to keep blinking to a minimum.

Gaze position and pupil diameter were always recorded from the nondeprived eye (although both eyes were unpatched at the time of recording, that is, viewing was always binocular during eye-tracking). Note that pupillary responses are consensual, the two pupils reacting simultaneously and by the same amount in all but pathological cases. Therefore, we do not expect any change of the present results if the deprived eye pupil was recorded instead. Pupil diameter measures were

transformed from pixels to millimeters using an artificial 4 mm pupil, positioned at the approximate location of the subjects' left eye.

2.6. Analyses: Binocular Rivalry. The perceptual reports recorded through the computer keyboard were analyzed with custom Matlab scripts. During binocular rivalry, visual perception oscillates between the monocular images and periods of exclusive dominance of one of the two rivalrous stimuli are sometimes interleaved with periods in which the observer perceives a mixture of the two images, called mixed percepts. In order to quantify ocular dominance, for each subject and each experimental block, we computed the average duration of exclusive dominance of each stimulus, called mean phase duration, as well as the average duration of mixed percepts. The 180 sec blocks acquired after monocular deprivation were binned as follows: 0–8 min and 10–18 min. In order to obtain an index of the effect of deprivation, we computed the Deprivation Index (DI) described in [4], which summarizes the change in eye-dominance (defined as the ratio between the deprived and nondeprived eye mean phase durations) induced by monocular deprivation (see (1)). DI = 1 indicates no change in ocular dominance compared to predeprivation measurements, DI < 1 indicates increased dominance of the deprived eye, and DI > 1 indicates increased dominance of the nondeprived eye.

$$\text{Deprivation Index} = \frac{\text{DepEye}_{\text{pre}}}{\text{DepEye}_{\text{post}}} * \frac{\text{NonDepEye}_{\text{post}}}{\text{NonDepEye}_{\text{pre}}}. \quad (1)$$

The deprivation indexes obtained for each of the two experimental blocks measured after eye-patch removal were compared against the value of 1 using a one-sample, two-tailed t-test. Mean phase durations of each eye obtained before and after deprivation were compared using a two-tailed paired-samples t-test. The Bonferroni correction for multiple comparisons was applied.

2.7. Analyses: Pupillometry. Eye-tracking data were analyzed with custom Matlab scripts. Pupillometry data consisted of 120 × 1000 time points (120 seconds at 1000 Hz). These included signal losses, eye-blinks, and other artifacts, which we eliminated before assessing the oscillatory behavior of the pupil. The majority of these artifacts were excluded based on pupil size being 0 (e.g., during eye-blinks). However, this left time points with highly instable pupil size measures (e.g., disturbances from eye-lashes) as well as short intervals, typically preceding and following a blink, where the pupils acquired very small or very large values. We cleaned these out by means of custom software that identifies and excludes the changes of pupil size that are too fast to be physiologically meaningful. Specifically, the algorithm starts by identifying time points where the rate of change of pupil diameter (pupil difference in the unit of time) is larger than a threshold (set to the 90th percentile of pupil change rate of each participant). These time points are labeled as artifacts and temporarily replaced with the average pupil diameter; then the procedure is repeated ten times. The first round will exclude any time point where the pupil recording is unstable as well as the first time point where pupil size suddenly drops (a blink) or increases (disturbance from eye-lashes). Iterating the procedure allowed for further eliminating the short intervals where the pupil happens to stabilize at an artefactual value (which typically last few ms).

This custom procedure proved to be more effective than a standard blink removal algorithm, which eliminates 500 ms worth of data every time the pupil drops below 2 mm (see example in Figure 2(a)). We verified that the number of detected artifacts was indistinguishable before and after deprivation (paired t-test on the percentage of excluded data samples, $t(9) = 1.54$, $p = 0.1586$) and that the main results could be reproduced using either of the two algorithms (see caption of Figure 4).

We then used linear interpolation to replace data points labeled as artifacts and we proceeded to extract the low-frequency components of pupil oscillations by means of fast Fourier transform (applied after subtracting the mean pupil size). For each 120 sec trace we computed the energy in three contiguous frequency bands: hippus (0–0.8 Hz), delta (0.8–4 Hz), and theta (4–8 Hz). As an alternative quantification of the energy in the hippus range, we also computed the Pupillary Unrest Index or PUI [29]: the sum of absolute changes in pupil diameter based on a sample frequency of 1.5625 Hz (exactly the same definition used in [29]).

Horizontal and vertical gaze position data from time points where an artifact in pupil diameter was detected (see above) were excluded. Deviations from screen center were computed and the sign of horizontal gaze shifts was flipped for subjects where the right eye was recorded. In this way, a positive horizontal gaze shift implies a shift in the nasal direction and a negative shift implies a shift in the temporal direction. We took the average across time of horizontal and vertical gaze shifts as a measure of systematic gaze deviations and we estimated fixation instability by means of Bivariate Contour Ellipse analysis. This amounts to defining an ellipse around the x, y coordinates of gaze position samples. Its area is defined by

$$\text{BCEA} = 2k\sigma_H\sigma_V\left(1 - R^2\right)^{0.5}, \quad (2)$$

where the constant k relates to the percentage of data points that fall within the ellipse. As in previous studies, for example, [51], we set $k = 1.14$ so that 68.2% of the data points fall within the ellipse.

Using a series of paired t-tests we compared the average pupil diameter, the power in the hippus/delta/theta range, the PUI, the horizontal and vertical gaze shifts, and the fixation instability values obtained after deprivation versus before deprivation. We took the difference between the two values as an estimate of the deprivation effect, which we correlated with the effect of deprivation observed on binocular rivalry (quantified as the "Deprivation Index" defined in (1)).

3. Results

We measured the dynamics of binocular rivalry and the diameter of the pupil in a group of healthy adult volunteers before and after a short period (2 hours) of monocular

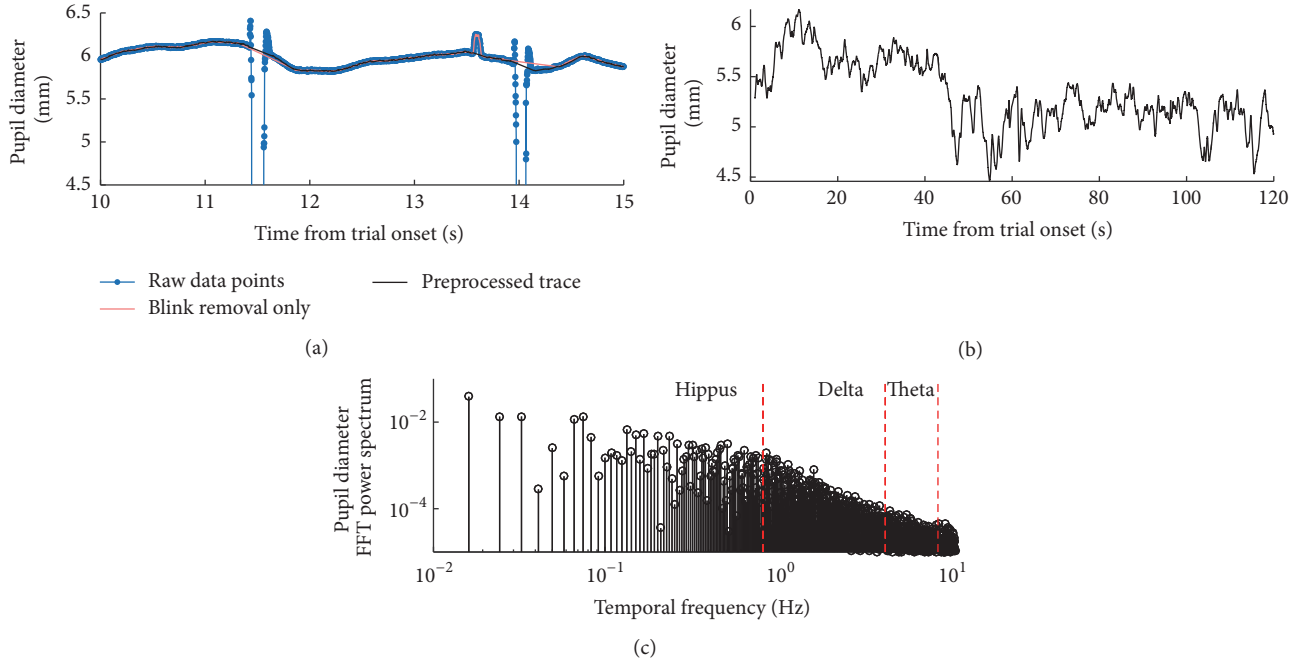

Figure 2: Preprocessing of pupillometry data. (a) Segment of pupil recording showing three artifacts: two typical blink artifacts and a short dilation artifact (eye-lashes disturbance). All three were removed by our preprocessing algorithm (black line). For comparison, the result of applying a more standard blink removal algorithm is shown by the red line. (b) Full preprocessed trace, same block from which the segment in (a) was extracted. (c) FFT spectrum of the pupil recording in (c), highlighting the frequency bands used in the main analysis. For this trace, the PUI value was 3.07.

deprivation during which observers wore a translucent eye-patch over the dominant eye.

3.1. Binocular Rivalry. Mean phase durations of the deprived and nondeprived eye measured before eye-patching and during the first 8 minutes after short-term monocular deprivation are reported in Figure 3(a). Consistently with previous reports [2, 3], two hours of monocular deprivation boosted the deprived eye signal, resulting in increased deprived eye-predominance on eye-patch removal. After deprivation, mean phase durations of the deprived eye increased significantly (baseline mean phase duration (mean ± 1 s.e.m.) = 3.99 ± 0.23 s, mean phase duration after deprivation = 5.43 ± 0.6 s, two-tailed paired-samples t-test: $t(9) = -2.87$, $\alpha = 0.025$, Bonferroni corrected $p = 0.036$), while mean phase durations of the nondeprived eye decreased (baseline mean phase duration (mean ± 1 s.e.m.) = 3.57 ± 0.19 s, mean phase duration after deprivation = 3.14 ± 0.24 s, two-tailed paired-samples t-test: $t(9) = 3.63$, $\alpha = 0.025$, Bonferroni corrected $p = 0.011$) compared to predeprivation measurements.

A direct measure of the deprived eye increase in perceptual predominance induced by monocular deprivation is summarized by the *Deprivation Index* (see (1) in Methods), and it is shown in Figure 3(b). The Deprivation Index was significantly lower than 1 in both measurements obtained during the first 8 minutes after deprivation offset (mean ± 1 s.e.m. = 0.67 ± 0.05, one-sample, two-tailed t-test, H_0: $X = 1$, $t(9) = -6.71$, $\alpha = 0.025$, Bonferroni corrected $p < 0.001$), indicating that monocular deprivation robustly shifted eye dominance in favor of the deprived eye compared to predeprivation levels. The effect of deprivation decayed after eye-patch removal and was significant, albeit smaller, for measurements obtained in the interval from 10 to 18 minutes after eye-patch removal (mean ± 1 s.e.m. = 0.82 ± 0.05, one-sample, two-tailed t-test, H_0: $X = 1$, $t(9) = -3.42$, $\alpha = 0.025$, Bonferroni corrected $p = 0.016$).

3.2. Pupil. Pupillary diameter was measured in the dark immediately before eye-patching and 20 minutes after eye-patch removal (after the binocular rivalry measurements). Pupillary oscillations in the low-frequency range (<0.8 Hz, known as the "hippus" range) are enhanced after monocular deprivation, compared to the baseline measure acquired before applying the eye-patch (Figure 4(a); paired t-test $t(9) = 6.278$, $p < 0.001$). Similar values are obtained using an alternative preprocessing algorithm (blink removal only: t-test $t(9) = 6.743$, $p < 0.001$).

This is also seen as an increase of the Pupillary Unrest Index, which provides an alternative measure of slow oscillations. The PUI goes from an average 1.10 ± 0.15 (mean and s.e.m. across subjects) before deprivation to 1.39 ± 0.14 after deprivation (paired t-test: $t(9) = 4.545$, $p < 0.01$).

On the other hand, oscillations in the delta (0.8–4 Hz) and theta ranges (4–8 Hz) are unaffected by deprivation (delta before: 0.30 ± 0.03, after: 0.31 ± 0.03, $t(9) = 0.583$, $p = 0.574$; theta before: 0.07 ± 0.01, after: 0.07 ± 0.01, $t(9) = 0.151$, $p =$

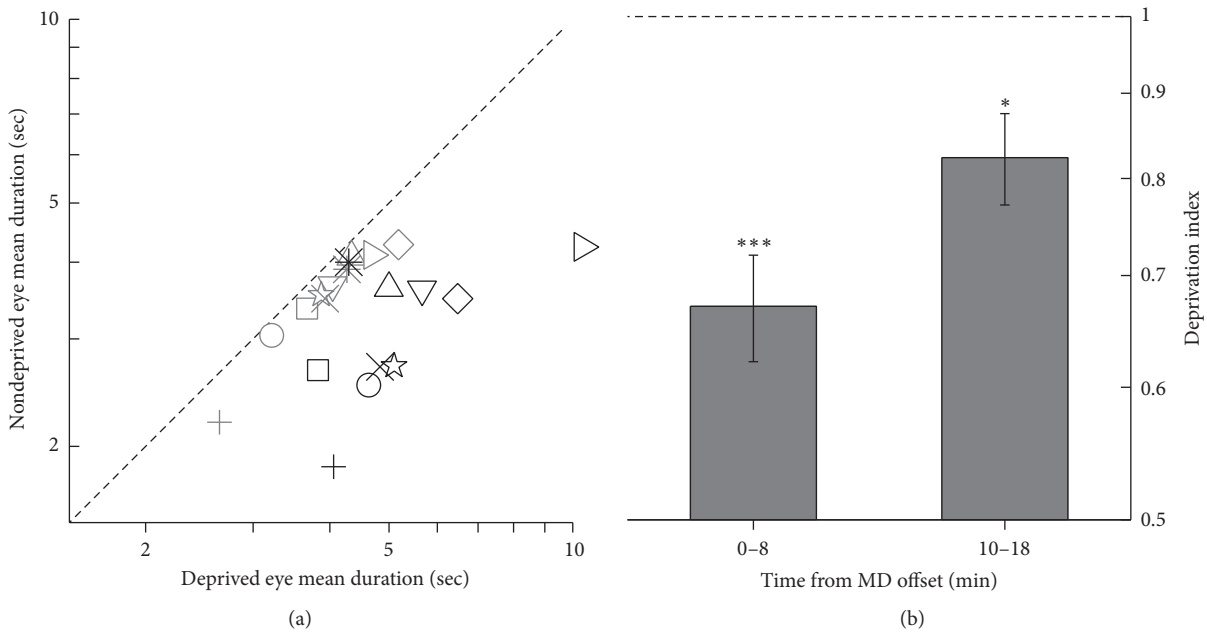

Figure 3: Binocular rivalry results. (a) Scatter plot of the individual subjects' mean phase durations for the deprived and nondeprived eye obtained before (light grey symbols) and during the first 8 minutes after monocular deprivation (black symbols). (b) Deprivation Index (see (1) in Methods) summarizing the increase in deprived eye-predominance for the first 8 minutes after eye-patch removal and for the interval between 10 and 18 minutes after deprivation. The Deprivation Index value of 1 (designated by the dashed line) would indicate no change in ocular dominance after deprivation; values smaller than one indicate increased deprived eye-predominance. Error bars represent 1 ± s.e.m.; asterisks represent statistical significance ($^{***}p < 0.001$, $^{*}p < 0.05$).

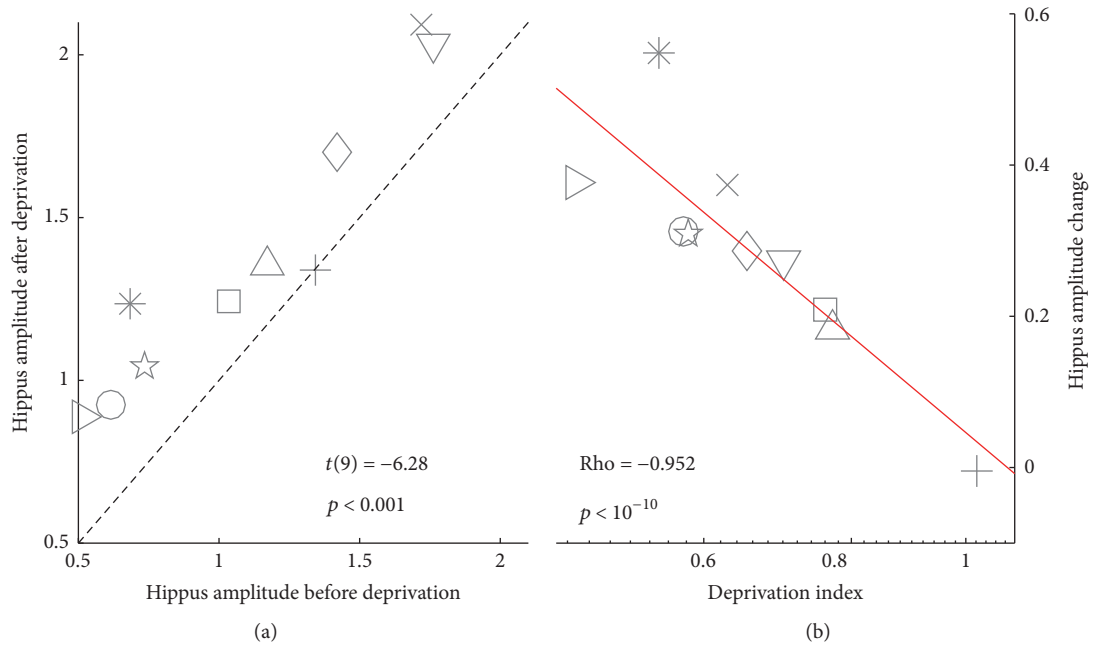

Figure 4: Pupillometry results and correlation with binocular rivalry. (a) Scatter plot of the FFT energy in the 0–0.8 Hz range, measuring the amplitude of the pupil hippus, before deprivation versus 20 minutes after deprivation. The text inset shows the result of a paired t-test comparing values on the x- and y-axis. Similar values are obtained using the alternative preprocessing algorithm (blink removal only: t-test comparing before/after hippus amplitude: $t(9) = 6.743$, $p < 0.001$). (b) Difference of FFT energy in the hippus range across deprivation, plotted against the binocular rivalry Deprivation Index (see (1)). The text inset shows Spearman's rank correlation coefficient Rho between values on the x- and y-axis (note that Spearman's Rho is insensitive to whether the axes are logarithmic or linear). The thick red line is the best-fit linear function through the data points. Each symbol is one subject, consistent across panels (a)-(b) and with Figure 3(a).

0.883). The average pupil diameter shows a nonsignificant tendency towards decreasing after deprivation (average pupil diameter before: 6.02 ± 0.21 mm, after 5.88 ± 0.16 mm, $t(9) = -1.657$, $p = 0.132$).

3.3. Gaze Stability. While vertical gaze position was indistinguishable before/after deprivation, there was a tendency for horizontal gaze position to shift inward (nasally) after deprivation, from -0.59 ± 0.42 deg before to 0.27 ± 0.49 deg after; the effect is only significant before correcting for multiple comparisons ($t(9) = 2.573$, $p = 0.030$). This marginally significant effect might be related to anomalies in the vergence eye movements occurring during the deprivation period, to be clarified by future studies.

More importantly, we find that the variability of gaze position (measured as the area of the Bivariate Contour Ellipse, BCEA) was not affected by deprivation, with similar BCEA values observed before and after MD (0.70 ± 0.24 deg^2 and 0.41 ± 0.08 deg^2, respectively, paired t-test $t(9) = 1.500$, $p = 0.168$).

3.4. Correlation between Deprivation Effects on Pupillary and Binocular Rivalry Behavior. To test whether the effects of deprivation on binocular rivalry and slow pupil oscillations are related, we measured Spearman's correlation coefficient (Rho) between the binocular rivalry Deprivation Index (see (1)) and the increased power in the hippus range (Figure 3(b)). The two measures show a tight correlation (Spearman's Rho $= -0.952$, $p < 10^{-10}$, 95% Confidence Intervals, CI = from -0.805 to -0.988); the correlation remains high and significant using the alternative algorithm for preprocessing pupil (blink removal only: Spearman's Rho $= -0.806$, $p = 0.008$, 95% CI = 0.359–0.952).

We also tested the correlation between the Deprivation Index and the other two indices of gaze behavior that showed at least a trend towards changing with deprivation: PUI, average pupil diameter, and shift of horizontal gaze (in the nasal direction). The correlation with PUI is weaker than with hippus power (Spearman's Rho $= -0.418$, $p = 0.232$), indicating that FFT power gives a more precise quantification of the pupillary behavior. There is no correlation with either average pupil diameter (Spearman's Rho = 0.297, $p = 0.407$) or horizontal gaze (Spearman's Rho $= -0.2$, $p = 0.584$).

4. Discussion

By testing binocular rivalry before and after monocular deprivation, we find that MD transiently shifts ocular dominance in favor of the deprived eye, in line with previous work from our and other laboratories [1–7]. Upon completion of the binocular rivalry tests, we measured pupil size during two minutes of rest: with no visual stimulation, with participants sitting in the dark and performing no task except minimizing body and gaze movements. We find that the dynamics of the pupil are altered after MD, with increased amplitude of low-frequency oscillations, that is, enhanced hippus. This effect is specific for oscillations in the "hippus" range (slower than about 1 Hz, a time scale that is very similar to the frequency of perceptual oscillations during binocular rivalry), whereas faster oscillations (in the delta or theta ranges) are indistinguishable before/after MD, and so is the average pupil diameter.

Testing conditions also allowed us to check for the statistics of gaze position. This is important given that eye movements are known to influence both pupil dynamics [52] and binocular rivalry [53] and that increased frequency of eye movements could enhance pupil size oscillations. Our finding that the variability of gaze position is unaffected by MD speaks directly against this possibility.

The most important aspect of our results is the tight correlation between the effects of MD on our two very different measures, obtained minutes apart with different apparatus: pupillary hippus and increased eye-dominance of the deprived eye during binocular rivalry. We interpret this by suggesting that the change of visual cortical excitability induced by monocular deprivation [1, 4, 5] results in behavioral changes both during visual stimulation (as measured by binocular rivalry) and during rest (as indexed by pupillary oscillations). The tight correlation between psychophysics and pupillometry agrees with a growing body of literature showing that changes of cortical excitability can be accurately tracked by the variations of pupil size over time [21, 22] and our findings specifically agree with the observation that the change of pupil size (i.e., the first derivative of pupil diameter over time) is a better predictor than the raw pupil diameter [26, 54]. One limitation of the current study is the relatively small sample size ($n = 10$); even though the correlation between the change in pupillary hippus and ocular dominance is strong (Rho = 0.95), further experimental work is needed to confirm this result in a larger sample of participants.

We speculate that the key to understanding this close relationship between pupillary hippus and plasticity lies within the complex neural circuits that regulate the balance between inhibition and excitation in the cortex, where the neuromodulator norepinephrine plays a key role. Hippus amplitude is thought to depend on the imbalance of noradrenergic (NE) and cholinergic (Ach) transmission [55], with pupil dilations correlating tightly with activity in the NE-releasing Locus Coeruleus [38, 39]; at the same time, animal studies have implicated NE transmission in ocular dominance plasticity in the visual cortex [19, 20], suggesting the possibility that a change of NE tone might be responsible for both of the effects we observe. The neural circuitry linking NE to cortical excitability and plasticity is still unclear but current work being performed in animal models (especially mice) holds great potential for unraveling these complexities. For example, it has been recently shown that the activity of Vasoactive Intestinal Peptide-Expressing (VIP+) GABAergic interneurons and Somatostatin-Expressing (SOM+) interneurons in the primary visual cortex of mice is modulated during slow spontaneous pupillary oscillations [26]. Specifically, VIP+ interneurons are more active during pupil dilation than during constriction, while SOM+ interneurons show the opposite behavior. Interestingly, the VIP+/SOM+ circuit is also implicated in activating visual cortical plasticity in

adult animals [16]. Moreover, ocular dominance plasticity is enhanced by physical exercise in both mice and humans [49, 56], and the effect in mice is linked to a selective modulation of VIP+ and SOM+ interneurons [56]. Taken together, these data indicate that there is partial overlap between neural circuits that are important for the regulation of ocular dominance plasticity and the regulation of slow pupil oscillations, and this overlap may help explain the correlation we observe between short-term plasticity and hippus. This is further supported by recent evidence that low-frequency pupil oscillations track changes in adrenergic and cholinergic activity in cortex [33]. Yet, the evidence to-date remains correlational, and any causal link might be sought for in future work.

The present work highlights how pupil behavior, a physiological parameter that can be continuously and noninvasively tracked with relatively simple apparatus, provides for a rich source of information. Not only does it provide objective and quantitative measures of responses to sensory stimuli [as we argued elsewhere, [46]], it also indicates the "internal state" of the individual [31]. Here we show that, by tracking pupil size during just two minutes while the participant is simply required to rest, one can obtain an index that is strongly correlated with ocular dominance plasticity, which, to be measured directly, requires substantial time and participants' collaboration. This could prove particularly important for probing visual cortical plasticity in clinical populations, where the patients' collaboration is difficult to obtain. One paradigmatic case would be the monitoring of neuroplasticity in young amblyopic children, as short-term homeostatic plasticity has been recently shown to be present in adult amblyopic patients [57] and to be predictive of the occlusion therapy outcome in anisometropic children [58].

Competing Interests

The authors declare that there is no conflict of interests regarding the publication of this paper.

Acknowledgments

The research leading to these results was funded by the European Projects ERA-NET Neuro-DREAM and ECSPLAIN (European Research Council under the Seventh Framework Programme, FPT/2007-2013, Grant Agreement no. 338866) and the Italian Ministry of University and Research under the Projects "Futuro in Ricerca," Grant Agreement no. RBFR1332DJ, and "PRIN 2015." The authors are grateful to Professors Morrone and Burr for their continual advice and for providing laboratory instruments and spaces.

References

[1] C. Lunghi, M. Berchicci, M. C. Morrone, and F. Di Russo, "Short-term monocular deprivation alters early components of visual evoked potentials," *The Journal of Physiology*, vol. 593, no. 19, pp. 4361–4372, 2015.

[2] C. Lunghi, D. C. Burr, and C. Morrone, "Brief periods of monocular deprivation disrupt ocular balance in human adult visual cortex," *Current Biology*, vol. 21, no. 14, pp. R538–R539, 2011.

[3] C. Lunghi, D. C. Burr, and M. Concetta Morrone, "Long-term effects of monocular deprivation revealed with binocular rivalry gratings modulated in luminance and in color," *Journal of Vision*, vol. 13, no. 6, article no. 1, 2013.

[4] C. Lunghi, U. E. Emir, M. C. Morrone, and H. Bridge, "Short-term monocular deprivation alters GABA in the adult human visual cortex," *Current Biology*, vol. 25, no. 11, pp. 1496–1501, 2015.

[5] J. Zhou, D. H. Baker, M. Simard, D. Saint-Amour, and R. F. Hess, "Short-term monocular patching boosts the patched eye's response in visual cortex," *Restorative Neurology and Neuroscience*, vol. 33, no. 3, pp. 381–387, 2015.

[6] J. Zhou, S. Clavagnier, and R. F. Hess, "Short-term monocular deprivation strengthens the patched eye's contribution to binocular combination," *Journal of Vision*, vol. 13, no. 5, article 12, 2013.

[7] J. Zhou, A. Reynaud, and R. F. Hess, "Real-time modulation of perceptual eye dominance in humans," *Proceedings of the Royal Society B: Biological Sciences*, vol. 281, no. 1795, 2014.

[8] D. Alais and R. Blake, *Binocular Rivalry*, MIT Press, Cambridge, Mass, USA, 2005.

[9] L. Baroncelli, L. Maffei, and A. Sale, "New perspectives in amblyopia therapy on adults: a critical role for the excitatory/inhibitory balance," *Frontiers in Cellular Neuroscience*, vol. 5, article 25, 2011.

[10] M. Fagiolini, J.-M. Fritschy, K. Löw, H. Möhler, U. Rudolph, and T. K. Hensch, "Specific GABAA circuits for visual cortical plasticity," *Science*, vol. 303, no. 5664, pp. 1681–1683, 2004.

[11] M. Fagiolini and T. K. Hensch, "Inhibitory threshold for critical-period activation in primary visual cortex," *Nature*, vol. 404, no. 6774, pp. 183–186, 2000.

[12] J. A. Heimel, D. van Versendaal, and C. N. Levelt, "The role of GABAergic inhibition in ocular dominance plasticity," *Neural Plasticity*, vol. 2011, Article ID 391763, 11 pages, 2011.

[13] A. Harauzov, M. Spolidoro, G. DiCristo et al., "Reducing intracortical inhibition in the adult visual cortex promotes ocular dominance plasticity," *Journal of Neuroscience*, vol. 30, no. 1, pp. 361–371, 2010.

[14] L. Baroncelli, J. Bonaccorsi, M. Milanese et al., "Enriched experience and recovery from amblyopia in adult rats: impact of motor, social and sensory components," *Neuropharmacology*, vol. 62, no. 7, pp. 2388–2397, 2012.

[15] A. Sale, J. F. M. Vetencourt, P. Medini et al., "Environmental enrichment in adulthood promotes amblyopia recovery through a reduction of intracortical inhibition," *Nature Neuroscience*, vol. 10, no. 6, pp. 679–681, 2007.

[16] Y. Fu, M. Kaneko, Y. Tang, A. Alvarez-Buylla, and M. P. Stryker, "A cortical disinhibitory circuit for enhancing adult plasticity," *eLife*, vol. 2015, no. 4, Article ID e05558, 2015.

[17] J. F. Maya Vetencourt, A. Sale, A. Viegi et al., "The antidepressant fluoxetine restores plasticity in the adult visual cortex," *Science*, vol. 320, no. 5874, pp. 385–388, 2008.

[18] H. Morishita, J. M. Miwa, N. Heintz, and T. K. Hensch, "Lynx1, a cholinergic brake, limits plasticity in adult visual cortex," *Science*, vol. 330, no. 6008, pp. 1238–1240, 2010.

[19] T. Kasamatsu, J. D. Pettigrew, and M. Ary, "Restoration of visual cortical plasticity by local microperfusion of norepinephrine," *Journal of Comparative Neurology*, vol. 185, no. 1, pp. 163–181, 1979.

[20] T. Kasamatsu, J. D. Pettigrew, and M. Ary, "Cortical recovery from effects of monocular deprivation: acceleration with norepinephrine and suppression with 6-hydroxydopamine," *Journal of Neurophysiology*, vol. 45, no. 2, pp. 254–266, 1981.

[21] M. J. McGinley, M. Vinck, J. Reimer et al., "Waking state: rapid variations modulate neural and behavioral responses," *Neuron*, vol. 87, no. 6, pp. 1143–1161, 2015.

[22] B. Laeng, S. Sirois, and G. Gredebäck, "Pupillometry: a window to the preconscious?" *Perspectives on Psychological Science*, vol. 7, no. 1, pp. 18–27, 2012.

[23] I. Loewenfeld, *The Pupil: Anatomy, Physiology, and Clinical Applications*, Wayne State University Press, Detroit, Miss, USA, 1993.

[24] J. L. Barbur, A. J. Harlow, and A. Sahraie, "Pupillary responses to stimulus structure, colour and movement," *Ophthalmic and Physiological Optics*, vol. 12, no. 2, pp. 137–141, 1992.

[25] C.-A. Wang and D. P. Munoz, "A circuit for pupil orienting responses: implications for cognitive modulation of pupil size," *Current Opinion in Neurobiology*, vol. 33, pp. 134–140, 2015.

[26] J. Reimer, E. Froudarakis, C. R. Cadwell, D. Yatsenko, G. H. Denfield, and A. S. Tolias, "Pupil fluctuations track fast switching of cortical states during quiet wakefulness," *Neuron*, vol. 84, no. 2, pp. 355–362, 2014.

[27] D. Kahneman and J. Beatty, "Pupil diameter and load on memory," *Science*, vol. 154, no. 3756, pp. 1583–1585, 1966.

[28] O. Lowenstein, R. Feinberg, and I. E. Loewenfeld, "Pupillary movements during acute and chronic fatigue a new test for the objective evaluation of tiredness," *Investigative Ophthalmology & Visual Science*, vol. 2, no. 2, pp. 138–157, 1963.

[29] H. Lüdtke, B. Wilhelm, M. Adler, F. Schaeffel, and H. Wilhelm, "Mathematical procedures in data recording and processing of pupillary fatigue waves," *Vision Research*, vol. 38, no. 19, pp. 2889–2896, 1998.

[30] B. Wilhelm, H. Wilhelm, H. Lüdtke, P. Streicher, and M. Adler, "Pupillographic assessment of sleepiness in sleep-deprived healthy subjects," *Sleep*, vol. 21, no. 3, pp. 258–265, 1998.

[31] M. J. McGinley, S. V. David, and D. A. McCormick, "Cortical membrane potential signature of optimal states for sensory signal detection," *Neuron*, vol. 87, no. 1, pp. 179–192, 2015.

[32] M. Vinck, R. Batista-Brito, U. Knoblich, and J. A. Cardin, "Arousal and locomotion make distinct contributions to cortical activity patterns and visual encoding," *Neuron*, vol. 86, no. 3, pp. 740–754, 2015.

[33] J. Reimer, M. J. McGinley, Y. Liu et al., "Pupil fluctuations track rapid changes in adrenergic and cholinergic activity in cortex," *Nature Communications*, vol. 7, Article ID 13289, 2016.

[34] E. H. Hess and J. M. Polt, "Pupil size as related to interest value of visual stimuli," *Science*, vol. 132, no. 3423, pp. 349–350, 1960.

[35] M. Allen, D. Frank, D. S. Schwarzkopf et al., "Unexpected arousal modulates the influence of sensory noise on confidence," *eLife*, vol. 5, Article ID e18103, 2016.

[36] D. Schnell, L. Arnaud, V. Lemiale, and S. Legriel, "Pupillary hippus in nonconvulsive status epilepticus," *Epileptic Disorders*, vol. 14, no. 3, pp. 310–312, 2012.

[37] M. Centeno, M. Feldmann, N. A. Harrison et al., "Epilepsy causing pupillary hippus: an unusual semiology," *Epilepsia*, vol. 52, no. 8, pp. e93–e96, 2011.

[38] S. Joshi, Y. Li, R. M. Kalwani, and J. I. Gold, "Relationships between pupil diameter and neuronal activity in the locus coeruleus, colliculi, and cingulate cortex," *Neuron*, vol. 89, no. 1, pp. 221–234, 2016.

[39] D. Alnæs, M. H. Sneve, T. Espeseth, T. Endestad, S. H. P. van de Pavert, and B. Laeng, "Pupil size signals mental effort deployed during multiple object tracking and predicts brain activity in the dorsal attention network and the locus coeruleus," *Journal of Vision*, vol. 14, no. 4, article 1, 2014.

[40] W. Einhäuser, J. Stout, C. Koch, and O. Carter, "Pupil dilation reflects perceptual selection and predicts subsequent stability in perceptual rivalry," *Proceedings of the National Academy of Sciences of the United States of America*, vol. 105, no. 5, pp. 1704–1709, 2008.

[41] J.-M. Hupé, C. Lamirel, and J. Lorenceau, "Pupil dynamics during bistable motion perception," *Journal of Vision*, vol. 9, no. 7, article 10, 2009.

[42] P. Binda, M. Pereverzeva, and S. O. Murray, "Attention to bright surfaces enhances the pupillary light reflex," *The Journal of Neuroscience*, vol. 33, no. 5, pp. 2199–2204, 2013.

[43] S. Mathôt, L. van der Linden, J. Grainger, and F. Vitu, "The pupillary light response reveals the focus of covert visual attention," *PLoS ONE*, vol. 8, no. 10, Article ID e78168, 2013.

[44] M. Naber, G. A. Alvarez, and K. Nakayama, "Tracking the allocation of attention using human pupillary oscillations," *Frontiers in Psychology*, vol. 4, article 919, 2013.

[45] P. Binda and S. O. Murray, "Spatial attention increases the pupillary response to light changes," *Journal of Vision*, vol. 15, no. 2, article 1, 2015.

[46] P. Binda and S. O. Murray, "Keeping a large-pupilled eye on high-level visual processing," *Trends in Cognitive Sciences*, vol. 19, no. 1, pp. 1–3, 2015.

[47] A. Benedetto and P. Binda, "Dissociable saccadic suppression of pupillary and perceptual responses to light," *Journal of Neurophysiology*, vol. 115, no. 3, pp. 1243–1251, 2016.

[48] M. Lorber, B. L. Zuber, and L. Stark, "Suppression of the pupillary light reflex in binocular rivalry and saccadic suppression," *Nature*, vol. 208, no. 5010, pp. 558–560, 1965.

[49] C. Lunghi and A. Sale, "A cycling lane for brain rewiring," *Current Biology*, vol. 25, no. 23, pp. R1122–R1123, 2015.

[50] F. W. Cornelissen, E. M. Peters, and J. Palmer, "The Eyelink Toolbox: eye tracking with MATLAB and the Psychophysics Toolbox," *Behavior Research Methods, Instruments, & Computers*, vol. 34, no. 4, pp. 613–617, 2002.

[51] R. N. Raveendran, R. J. Babu, R. F. Hess, and W. R. Bobier, "Transient improvements in fixational stability in strabismic amblyopes following bifoveal fixation and reduced interocular suppression," *Ophthalmic and Physiological Optics*, vol. 34, no. 2, pp. 214–225, 2014.

[52] C.-A. Wang, D. C. Brien, and D. P. Munoz, "Pupil size reveals preparatory processes in the generation of pro-saccades and anti-saccades," *European Journal of Neuroscience*, vol. 41, no. 8, pp. 1102–1110, 2015.

[53] J. Ross and A. Ma-Wyatt, "Saccades actively maintain perceptual continuity," *Nature Neuroscience*, vol. 7, no. 1, pp. 65–69, 2004.

[54] R. L. van den Brink, P. R. Murphy, and S. Nieuwenhuis, "Pupil diameter tracks lapses of attention," *PLoS ONE*, vol. 11, no. 10, Article ID e0165274, 2016.

[55] M. C. Koss, T. Gherezghiher, and A. Nomura, "CNS adrenergic inhibition of parasympathetic oculomotor tone," *Journal of the Autonomic Nervous System*, vol. 10, no. 1, pp. 55–68, 1984.

[56] M. Kaneko and M. P. Stryker, "Sensory experience during locomotion promotes recovery of function in adult visual cortex," *eLife*, vol. 3, Article ID e02798, 2014.

[57] J. Zhou, B. Thompson, and R. F. Hess, "A new form of rapid binocular plasticity in adult with amblyopia," *Scientific Reports*, vol. 3, article 2638, 2013.

[58] C. Lunghi, M. C. Morrone, J. Secci, and R. Caputo, "Binocular rivalry measured 2 hours after occlusion therapy predicts the recovery rate of the amblyopic eye in anisometropic children," *Investigative Ophthalmology & Visual Science*, vol. 57, no. 4, pp. 1537–1546, 2016.